OREGON HEALTH & SCIENCE UNIVERSITY
SCHOOL OF MEDICINE – GRADUATE STUDIES

Understanding the Role of Interleukin-15 in T Cell Homeostasis and Simian Immunodeficiency Virus Pathogenesis

A DISSERTATION
by

Maren Quinn DeGottardi

Presented to the Department of Molecular Microbiology and Immunology
and the Oregon Health & Science University School of Medicine
in partial fulfillment of the requirements for the degree of
Doctor of Philosophy

Advisor: Louis J Picker, MD

2013

School of Medicine
Oregon Health and Science University

CERTIFICATE OF APPROVAL

This certifies that the PhD thesis of

Maren Quinn DeGottardi

has been approved

Louis J. Picker, MD, *thesis advisor*

Scott Wong, PhD, *committee chair*

Eric Barklis, PhD, *committee member*

Mark Slifka, PhD, *committee member*

David Jacoby, MD, *committee member*

TABLE OF CONTENTS Page

Acknowledgements

I would like to express my gratitude to my mentor, Dr. Louis Picker, for all of his support and help over the past six years. Louis' attention to detail, demand for perfection, and skill conducting scientific research have made me develop both intellectually and personally. With his guidance, I have become a more independent and skilled scientist. Thank you for working with me; it was both an honor and a privilege to be in your lab.

I would also like to thank Dr. Afam Okoye and Dr. Scott Hansen. Afam managed the SIV pathogenesis projects in the Picker lab, and critically, helped me write my dissertation and manage my independent projects. Additionally, Afam and his team managed and performed the experiments administering anti-IL-15 Ab to RM during acute-phase SIV-infection. Scott greatly helped me design and complete all of my experiments in the Picker lab. Scott has technical expertise in a large number of assays, and his guidance allowed me to acquire high quality data. I could never have completed my graduate work without both Dr. Okoye's and Dr Hansen's assistance. I will be forever grateful for your support during these past six years.

I would like to thank all present and past members of the Picker lab. Thank you to Mukta Rohankhedkar, Audrie Konfe, and Matt Reyes for their friendship, support, and help in the lab. Additionally, Dicky Lum and Shoko Hagen were instrumental in helping with all lab matters. Thank you to Stan Shiigi for his many hours sorting cells for my project and training me. I would also like to especially thank Lori Boshears for all of her administrative support in helping manage my bureaucratic affairs as a student.

I appreciate the time and input of my thesis committee members including Dr. Scott Wong, Dr. Eric Barklis, Dr. Mark Slifka, and Dr. David Jacoby. Your interest in my work was very supportive and your suggestions have improved my research and my critical thinking skills. Thank you for your willingness to participate on my committee and your continued support throughout graduate school.

Thank you to our many collaborators as well, including Dr. Jake Estes, Dr. Rafick Sekaly, Dr. Francois Villinger, Dr. Keith Reimann, Dr. Mike Piatak, and Dr. George Pavlokis. Also, many thanks to Dr. Byung Park for his assistance with the statistical analysis of my experiments.

I would like to thank the Program in Molecular and Cell Biology for admissions and the ability to pursue my career in science. Additionally, I would like acknowledge financial support from the PMCB and Virology Training Grants.

Finally, I would like to thank my friends and family for their support throughout my graduate career.

Dedication

This work is dedicated to my family – Monica, Warren, and Wade DeGottardi – and to my grandparents – Guido and Minnie DeGottardi and Margaret Mary Campbell. You have all supported me unconditionally my entire life and without you this never would have been possible. Your belief in education and the pursuit of knowledge has inspired my work in basic science research. Thank you for everything.

List of Figures

List of Abbreviations

Ab: antibody

AIDS: acquired immunodeficiency syndrome

ART: antiretroviral therapy

ANOVA: analysis of variance

BAL: bronchial alveolar lavage

CCR5: C-C chemokine receptor type 5

CCR7: C-C chemokine receptor type 7

CTL: cytotoxic T lymphocyte

HAART: highly active antiretroviral therapy

HIV: human immunodeficiency virus

IL-15: interleukin-15

IL-7: interleukin-7

JAK: Janus kinase

KO: knockout

LN: lymph node

MHC: major histocompatability complex

NK: natural killer

pSTAT5: Phospho-STAT5

RAG: recombination activation gene

rANOVA: repeated measures analysis of variance

RM: rhesus macaque

SIV: simian immunodeficiency virus

STAT5: Signal transducer and activator of transcription 5

TCR: T cell receptor

TM: Total memory

TCM: Central memory T cell

TTM: Transitional memory T cell

TEM: Effector memory T cell

Treg: T regulatory cell

XSCID: X-linked severe combined immunodeficiency

γc: common gamma chain

Abstract

In this study we sought to understand both the role of interleukin-15 (IL-15) in normal lymphocyte homeostasis in rhesus macaques and also how increased IL-15 levels during simian immunodeficiency virus (SIV) infection contribute to lymphocyte homeostatic dysregulation and SIV pathogenesis. The common gamma chain (γc) cytokine IL-15 regulates the homeostasis and differentiation of CD8 and CD4 memory T cells (TM) and is required for the generation and maintenance of the major innate immune effector population, natural killer (NK) cells. However, the role of IL-15 maintaining these lymphocyte populations *in vivo* has not been fully characterized. To clarify the role of IL-15 in normal lymphocyte homeostasis, we administered healthy rhesus macaques (RM) doses of anti-IL-15 antibody (Ab) (N=15) or an IgG1 control Ab (N=10). Significantly, we observed that NK cells were almost completely depleted following anti-IL-15 Ab administration. Anti-IL-15 Ab treatment had no effect on central memory T cells (TCM) but resulted in an initial decline of CD4 and CD8 effector memory T cell (TEM) absolute numbers, but this decline was countered by the onset of TEM homeostatic proliferation, potentially induced by an increased sensitivity to IL-7 in the absence of IL-15 mediated signaling. Although the TEM homeostatic proliferative burst was associated with stabilization of absolute numbers in WB, TEM levels in the colon remained depleted and tissue expression of active caspase-3 was increased following anti-IL-15 Ab compared to IgG control Ab treatment. Moreover, microarray revealed that TEM expression profiles were dysregulated, with a signature indicating they were pre-apoptotic and turning over at an increased rate. Our studies thus reveal that IL-

15 is necessary to maintain normal RM NK cell and effector memory T cell homeostasis *in vivo*.

IL-15 has been implicated in the pathogenic hyperimmune activation that characterizes HIV/SIV infection, and its administration during acute SIV infection is associated with enhanced activation of CD4 memory T cells and higher post-peak viral replication. Thus, IL-15 activity might provide benefit to an HIV/SIV infected host by support of anti-viral T and NK cell effectors, and/or contribute to HIV/SIV pathogenesis by support of hyperimmune activation. To better understand the role of IL-15 in pathogenic SIV-infection, we treated 18 chronically SIVmac239 infected RM with 6 doses of the rhesusized anti-IL15 Ab, M111, (N=9) or IgG1 isotype control Ab (N=9) biweekly over a 10-week period. We next investigated the effect of anti-IL-15 Ab dosing on acute SIV-infection by administering 23 RM anti-IL-15 M111 Ab (N=15) or IgG1 isotype control Ab (N=8) before and up to 8 weeks post SIVmac239 infection. In both cohorts, anti-IL15 Ab was highly efficient at neutralizing IL-15 signaling *in vivo* and caused a near complete depletion of NK cells in the blood and tissues. Throughout anti-IL-15 Ab dosing, CD4 and CD8 TEM exhibited a high-turnover homeostasis, but long-term CD4 TEM absolute counts in blood and tissues remained unchanged compared to IgG control Ab treatment during both chronic and acute SIV-infection. Despite these notable changes to immune cell populations, viral replication rates and disease progression during chronic and acute SIV infection were comparable to those of control animals. These studies suggest that increased IL-15 levels during SIV-infection are not

primary drivers of disease progression and that NK cells do not play a significant role in either controlling SIV replication or promoting SIV pathogenesis.

Chapter 1 – Introduction

Acquired immunodeficiency syndrome (AIDS) is still a global pandemic

AIDS has caused the deaths of over 30 million people worldwide since the epidemic's start in 1981, and over 34 million more people are currently infected with human immunodeficiency virus (HIV). Each year nearly two million people die from AIDS and almost three million more people become newly infected with HIV (1). Although overall infection rates have declined in recent years due to effective global health initiatives, AIDS remains a devastating pandemic, with HIV infection rates still rising in some areas of Eastern Europe and Asia. In the hardest hit nations of sub-Saharan Africa, almost 25% of the population is infected with HIV. In these developing countries, AIDS has lowered the mean age of death and has devastated the working-aged population. The consequence of a shrinking work force and the increased financial burden of caring for a rising number of HIV-infected individuals has set back economic development and social progress many years to decades in these areas (2). These nations show the devastation HIV and AIDS can cause if the pandemic is not effectively addressed.

Effective vaccines are not currently available for human populations, and although there have been great strides in anti-retroviral therapy (ART), health concerns still persist regarding HIV-infected individuals. The development of highly effective ART (HAART) has enabled many HIV-infected people to live normal, healthy lives, but HIV-infected individuals on ART have a shorter life expectancy and more health problems than uninfected peers (3). A significant barrier to the development of alternate

effective therapies to HIV disease has been a lack in understanding the mechanisms of AIDS pathogenesis, despite nearly 30 years of intensive research.

HIV/SIV pathogenesis

A model whereby HIV causes disease by simply killing CD4 T cells by direct infection does not explain the complicated mechanisms of AIDS pathogenesis (4). Notably, HIV rapidly and continuously replicates throughout the entire course of infection, killing target cells within hours or days, but the onset of AIDS only occurs many years or decades after initial HIV infection (5-7). Interestingly, although viral replication largely correlates with disease tempo, non-viral host parameters, specifically immune activation is a stronger predictor of disease outcome (8-12). Pathogenic CCR5-tropic HIV-infection is characterized by high, chronic immune activation. Chronic inflammation and disease progression has been associated with mucosal abnormalities that lead to translocation of microbial products from the intestinal lumen to systemic circulation (13).

Because of the complexity of AIDS and limitations when studying human subjects, HIV pathogenesis can best be studied using SIV infection of Indian-origin rhesus macaques as a non-human primate model of AIDS (14-16). Like HIV infection of humans, SIV infection of macaques represents a cross species transmission of the virus to an unnatural host. CCR5-tropic SIVs such as SIVmac239 exhibit similar patterns of viral replication, target cell depletion, and immune activation as HIV-1 infection (17, 18). The most significant difference between SIV infection of macaques and HIV infection of

humans is that SIV viral loads are higher and the pace of disease progression is accelerated; most macaques die of AIDS within two years after primary infection whereas untreated HIV infected humans do not develop AIDS until an average of eleven years after initial infection (17). Despite this difference in the rate of disease progression, SIV disease course is chronic and most animals survive acute infection and maintain a disease-free plateau phase before exhibiting immune degradation and AIDS. At the onset of AIDS, rhesus macaques will even develop opportunistic infections that are observed in humans with AIDS (17, 19, 20). Because of its unique relevance to understanding HIV infection and AIDS progression in humans, our studies were conducted using SIVmac239 infection of Indian-origin rhesus macaques as a non-human primate model, which may have parallels with HIV infection.

HIV/SIV and CD4 memory T cell biology

Major effectors of adaptive immunity are CD4 and CD8 T lymphocytes (T cells). CD4 and CD8 T cells use a method called V(D)J recombination whereby rearranged gene segments create a huge repertoire of T cell receptors (TCR) that recognize a diverse range of potential antigens (21-23). Upon specific antigen encounter, the T cell response is generally considered to go through three stages including activation/expansion, death, and stability/memory. Stability and memory of antigens mediated by T cells is achieved through the retention of long-lived memory T cells (TM) specific for previously encountered antigen. Upon antigen re-exposure, TM are able to respond more quickly

and robustly than antigen naive T cells (TN) and provide an immune response specific to that antigen.

The antigen experienced memory T cell compartment is composed of a heterogeneous population of cells that exist along a differentiation sequence that includes a stable "reserve" population with limited effector potential, so- called "central memory T cells" (TCM), and a more specialized and differentiated "hunter/killer" population, so-called "effector memory T cells" (TEM) (24-28). In the healthy immune system, the TCM population serves as a reservoir of cells that helps maintain the TEM population by proliferating and differentiating to TEM in response to antigen, cytokines or MHC II interactions (29). In contrast to TCM, TEM are programmed to migrate into effector sites and once there exhibit high effector cytokine production, high cytotoxicity, and little recirculatory potential. TCM and TEM differentiation status can be distinguished by their expression of the homing C-C chemokine receptors type 5 (CCR5) and type 7 (CCR7); CCR7 is expressed on TCM and causes these cells to circulate through the blood and lymph, whereas CCR5 is expressed on TEM and directs their migration to effector sites (24, 30).

CD4 TEM are the most efficiently targeted cells by most SIV/HIV because they constitutively express CCR5, the SIV/HIV co-recteptor. Pathogenic CCR5-tropic SIV-infection of RM results in the rapid depletion of most CCR5+ CD4 TEM in effector sites such as the lung and gut lamina propria within days of initial infection (31). Antigen-stimulated systemic immune activation causes TCM proliferation and differentiation to TEM in order to supply the peripheral effector sites with adequate TEM to fight local

infection. It was shown that SIV infection initiates a persistent hyper-proliferative state among CD4 (and CD8) memory T cells (32). However, despite lacking detectable CCR5 co-receptor expression and being relatively (albeit not absolutely) resistant to lytic HIV infection, CD4 TCM populations are not maintained during chronic SIV infection, and it is this instability that appears to be responsible for progressive failure of CD4 TEM production. A progressive decline in CD4 TCM leads to an insufficient supply of CD4 TEM to effector sites, and ultimately to immune failure and the onset of AIDS. Given that most strains of SIV only efficiently replicate in CD4 TEM and continuously replicate throughout the course of chronic infection, the mechanism by which the CD4 TCM population is slowly, yet progressively depleted, is unknown (32). The slow depletion of the CD4 TCM population without increased evidence of direct viral-mediated killing implicates homeostatic failure of this population during HIV disease. Further suggesting a homeostatic dysregulation, it has been observed that the cellular response of CD4 TEM to homeostatic regulators is abnormal in animals with uncontrolled SIV infection "normal progressors" (25).

To understand the homeostatic failure of CD4 TCM during HIV/SIV disease, it is first necessary to understand T cell homeostasis in the healthy immune system. Indeed, a significant barrier to understanding HIV pathogenesis has been a lack in understanding T cell homeostasis during normal conditions. Whereas antigen-naïve T cells are dependent on peptide/MHC interactions *in vivo*, memory T (TM) cells can survive in the body for the lifetime of the individual, even in the absence of antigen stimulation (33-38). Several signals *in vivo* are required for the homeostatic maintenance of these long-lived TM cells.

Common gamma chain (γc) cytokines are considered major regulators of TM cell homeostasis.

Common gamma chain (γc) cytokine regulation of lymphocyte homeostasis

Cytokines are small signaling molecules that play a key role regulating immune cell development, function, and homeostasis throughout the body (39). A group of Type I cytokines, γc cytokines, share not only common structural features but also a common receptor component, the γc. The importance of the γc to the immune system is revealed in γc- deficient humans and mice. Mice lacking γc expression have severe lymphopenia, with T cell and B cell numbers drastically reduced and NK cells completely absent (40, 41). Humans with X-linked severe combined immunodeficiency (XSCID) have mutations in γc-encoding gene IL2RG and these patients fail to develop T cells or NK cells, originally implicating the γc in T cell and NK cell development and maturation (42). The cytokines sharing the γc include IL-2, IL-4, IL-7, IL-9, IL-15, and IL-21 (43-49). γc cytokine specificity and affinity is mediated by private receptors for each cytokine, designated their α-chains. Because γc cytokines share common receptors, some of their biologic functions are overlapping and redundant. However, unique, non-redundant functions of cytokines are elicited by expression of cytokines and their specific receptors at various times and places throughout the body.

It is generally recognized that the common gamma chain cytokines IL-7 and IL-15 are major regulators of T cell homeostasis (26, 29, 50-52). IL-7 has been fairly well characterized and functions to promote the proliferation and survival of both naïve and

memory T cells in the thymus and the periphery (50, 53-56). Although evidence suggests that IL-15 promotes lymphocyte effector function, the role of IL-15 *in vivo* is still not clearly defined (57-60).

IL-15

IL-15 is a pleiotropic cytokine that is involved in homeostasis and activation of both the innate and adaptive immune system. IL-15 has an extremely diverse set of functions on many cell types throughout the body including memory T cells, natural killer (NK) cells, invariant NKT cells, intestinal intraepithelial lymphocytes (IELs), activated B lymphocytes (B cells), dendritic cells (DCs), macrophage, mast cells and neutrophils (61-71). The IL-15 protein is expressed throughout the body by monocytes, macrophages, dendritic cells, and stromal cells (72, 73). To mediate signals, IL-15 binds to its heterotrimeric receptor composed of IL-15Rα, IL-2/15Rβ, and γc (65, 74-77). Binding the receptor initiates a signal cascade whereby Janus kinase 3 (JAK3) phosphorylation induces Signal transducer and activator of transcription 5 (STAT5) phosphorylation, which causes STAT5 translocation to the nucleus and binding to specific DNA sequences (78). Via STAT5 activation, IL-15 favors pro-survival signals by up-regulating anti-apoptotic proteins such as Bcl-2 and downregulating pro-apoptotic proteins such as Bim in T cells and NK cells (53, 79-83). Additionally, IL-15 can trigger several other signaling pathways including phosphorylation of Src-family kinases Lck and Syk, stimulation of phasphatidylinositol-3-kinase (PI3-K)/AKT pathway and stimulation of the Ras/Raf/MAPK pathway (84).

IL-15 is unique among cytokines because it has been shown to mediate signals via trans-presentation (85-90). During trans-presentation, a cell expressing IL-15Rα bound to IL-15 at the cell surface signals adjacent cells expressing only IL-2/IL-15Rβ and γc (88). It was demonstrated that both monocytes and dendritic cells are able to present IL-15 *in trans* to support lymphocyte survival and function (87, 91-94). However, there is also evidence that IL-15 signals via cis-presentation, where soluble, free IL-15 binds a cell expressing IL-15Rα, IL-2/IL15Rβ, and γc. Alternatively, studies also indicate IL-15 signaling may occur by soluble IL-15 complexes bound to IL-15Rα (95, 96).

IL-15 and T cell homeostasis

IL-15 is important in the generation and maintenance of memory T cells in vivo (97, 98). IL15Rα-/- knockout (KO) mice exhibited smaller lymph nodes with less cells due to defective lymphocyte homing and reduced proliferation. In these IL15Rα-/-mice, CD8 T cell numbers were reduced and so were activated memory phenotype CD8 T cells (99). Consistently, IL15-/- KO mice also show reduced numbers of CD8 T memory cells. Because CD8 TM numbers are reduced but still present, this suggests that IL-15 controls proliferation and or survival of these cells. Further supporting this idea, IL-15-/- KO mice have normal numbers of CD8 T cells in the thymus, but reduced numbers in the periphery, showing IL-15 is not necessary for CD8 T cell development (100, 101). The preferential support of memory phenotype cells by IL-15 may be due to the fact that memory phenotype T cells are more responsive to IL-15 than naïve T cells (102). IL-15-/- KO also results in a lack of antigen specific CD8 TM cells during infection. During the

contraction phase of the T cell response and the transition of effector to memory T cells, the absence of IL-15 signaling results in a much more drastic contraction phase and much higher death rate of CD8 effector T cells (103-107). Increased CD8 T cell loss during contraction is likely due to increased death resulting from a decrease in IL-15-mediated expression of pro-survival protein Bcl-2 (108, 109).

Early studies in mice deficient for IL-15 and IL-15Rα showed a normal sized CD4 memory T cell population suggesting that IL-15 had a negligible role in CD4 TM homeostasis. However, further studies provide evidence that IL-15 is indeed a significant regulator of CD4 TM cells as well as CD8 TM cells (32, 60, 99, 110). There are additional studies showing that IL-15 can induce CD4 TCM and CD4 TEM proliferation (110-113). Moreover, IL-15 can generally upregulate CCR5, a ligand that mediates T cell effector site migration and a marker of effector memory on CD4 T cells *in vitro* (110).

Several studies have investigated the effect of IL-15 in a nonhuman primate model by administering doses of exogenous rhesus recombinant IL-15 (rIL-15) to healthy rhesus macaques. The literature is quite consistent and several effects were routinely observed. After IL-15 administration, there is a brief lymphopenia followed by lymphocytosis (114-116). T lymphocytes are significantly affected by IL-15 administration, which causes an increase in CD4 and CD8 TM proliferation and absolute numbers. TEM populations have the highest increase in proliferation and absolute numbers, with TCM exhibiting lower increases in Ki-67 and absolute numbers. Additionally, CD8 T cells are more reactive to IL-15 than CD4 T cell counterparts (25,

114-116). IL-15 has been shown to induce cell migration causing a redistribution of long-lived cells from circulation to tissues (25, 115). Alternatively, overstimulation with IL-15 and or spikes of exogenous IL-15 do not always lead to long-lived accumulation of cells in tissues, but rather these proliferating cells have been associated with increased death or annexin V staining (114, 117). IL-15 treatment increases the production of long-lived antigen specific CD4 and CD8 T cells (118, 119).

IL-15 and NK cell homeostasis

In addition to regulating lymphocyte homeostasis of the adaptive immune system, IL-15 also regulates NK cell homeostasis. NK cells are typically considered to be part of the innate immune system, primarily protecting the body against viral pathogens, especially viruses that down regulate major histocompatibility complex (MHC) class I molecules to escape cytotoxic T lymphocytes (CTL). NK cells express relatively invariant inhibitory and activating receptors that recognize target cells through interaction with MHC class I molecules. NK cells function not only to directly kill infected target cells and mediate antibody dependent cellular cytotoxicity, but also are an important source of cytokines that help trigger the antigen-specific responses of the adaptive immune system (53, 120). NK cells have been shown to be dependent on IL-15-mediated signals for generation and maintenance *in vivo*. IL-15 supports NK cell development in the bone marrow and mature NK cell numbers are maintained by IL-15 controlled proliferation and survival (87, 121-124). IL-15 has also been shown to be important for NK cell activation and function (94, 125, 126). Clearly demonstrating NK cell reliance

on IL-15, IL15/Rα-/- KO mice had reduced innate cell numbers and function including a lack of NK cells and reduced NK T cell numbers (99). Similarly, in IL15-/- KO mice, NK cells were practically absent and no NK cell function could be observed, indicating that NK cells require IL-15 for development and function. Interestingly, observed phenotypes could be reversed by addition of exogenous IL-15 treatment, which increased NK cell number and functionality *in vivo* (101). The similar phenotypes of IL15-/- and IL15Rα-/- KO mice confirm that IL-15 primarily signals via the IL15Ra in NK cells *in vivo*. Furthermore, STAT5, which is known to mediate IL-15 signaling, was shown to be essential for NK cell proliferation and cytolytic activity in mice. Indeed, NK cell populations were diminished and lacked effector function in different STAT5 knockout mice (127).

The dependency of NK cells on IL-15 is a highly conserved feature in the immune systems of mammalian species studied. When cynomolgus monkeys or RM were dosed with a JAK3 inhibitor that is an essential component of several γc cytokine receptors including IL-15, NK cells were depleted compared to vehicle treated animals. Only after stopping of inhibitor dosing did NK cell numbers rebound (128, 129). Additionally, studies in RM show that IL-15 administration causes an increase in NK cell proliferation and absolute numbers over the course of treatment, preferentially expanding the CD16+ NK cell population (114-116). Very recently, a study showed that an anti-IL-15 antibody caused NK cell depletion in rhesus macaques (130). Interestingly, two groups have observed that anti-IL-15 Ab administration to humans does not cause NK cell depletion

(130, 131). Still, in humans NK cells are dependent on γc mediated signals as NK cells are largely absent in XSCID humans (42).

IL-15 in health and disease

As an important regulator of lymphocyte function and homeostasis, either a lack of IL-15 or an overabundance of IL-15 *in vivo* has been associated with various pathologies. Although patients with mutations in IL-15 or IL-15Rα have not been identified, mutations that lead to defective IL-15 signal transduction lead to severe immunodeficiency. Most notably, mutations in components of the γc cytokine signaling pathway, such as the γc or JAK3, leads to severe combined immunodeficiency, the result of a severe depletion or absence in T cell and NK cell numbers and functions (132, 133). Additionally IL-15 over-expression has been implicated in exacerbating a number of diseases including rheumatoid arthritis (RA), Staphylococcus aureus arthritis, celiac disease, virus-induced chronic obstructive pulmonary disease (COPD), HIV-infection, and SIV-infection of RM (111, 131, 134-137).

Recently, there was a clinical trial of blockade of IL2/IL-15Rβ by humanized mAb. This antibody also blocks trans presentation of IL-15. The study found cells expressing IL-15Rα along with IL2/IL15Rβ could still be signaled by IL-15. The blockade of IL-15 signaling did not improve the clinical outcome of patients with T-cell large granular lymphocytic leukemia (T-LGL). The antibody was not toxic after a dose although one patient did develop antibodies against the antibody. Moreover, T cells from peripheral blood taken *ex-vivo* from patients were inhibited from responding to IL-2 and

IL-15 signals, which they showed was due to blocking. This study confirmed and further validated the use of this antibody in cases where IL-15 is the cause of pathogenesis, such as celiac disease (138).

Separate studies have administered a human anti-IL-15 Ab, HuMax-IL15, to patients with RA. The antibody was well tolerated with no adverse side effects and results showed that patients had moderately improved clinical outcome following anti-IL-15 Ab administration. Interestingly, HuMax-IL15 caused no changes to T cell or NK cell numbers (131).

IL-15 and HIV/SIV infection

In response to systemic immune activation during pathogenic HIV/SIV infection, IL-15 levels become dysregulated. IL-15 levels have been shown to significantly increase during acute HIV and SIV infection (111, 135, 139, 140). It is unclear, however, whether increased IL-15 levels play a role in promoting immunity and T cell homeostasis or exacerbating HIV disease. Supporting a role for IL-15 in promoting immunity during HIV/SIV infection, IL-15 stimulates the expansion of virus-specific T cell responses (25, 111, 112, 118, 119, 141). Many recent studies administering IL-15 as an adjuvant during HIV/SIV vaccination protocols have demonstrated that IL-15 increased viral-specific T cell responses during T cell priming as well (142-152). Additionally, it was shown that short term IL-15 treatment did not change the SIV plasma viral load of either ART treated or untreated SIV-infected RM (25). Administration of IL-15 to chronically SIV-infected macaques did not result in changes to viral loads either (141, 153). Similarly, a

JAK/STAT inhibitor administered to chronically infected RM induced modest, transient increase to viral load (128). It therefore remains uncertain whether increased IL-15 levels protect against HIV/SIV disease progression through support of anti-viral effectors such as CD8 T cells and NK cells and through support of CD4 TEM populations numbers by inducing CD4 T cell differentiation. Alternatively, IL-15 may play a role driving HIV/SIV pathogenesis by causing an over-differentiation of CD4 TEM and exhausting the CD4 T cell population and by contributing to the chronic hyper immune activation. Certainly, multiple studies have suggested that IL-15 may in fact aggravate HIV/SIV disease. Administration of IL-15 to chronically SIV-infected rhesus monkeys on ART delayed viral suppression and did not reconstitute CD4 T cells at mucosal sights (153). Moreover, administration of IL-15 to rhesus macaques during acute SIV infection increased viral set point and accelerated disease progression despite higher SIV-specific CD8 T cell responses (112). Increased IL-15 cytokine concentrations have been correlated to increased viral loads (111, 135, 139). One study measures significantly higher plasma IL-15 levels during acute SIV infection, which correlated with increased immune activation and increased susceptibility of CD4 TM to SIV infection (111). Indeed, incubation of CD4 T cells with IL-15 increased the infection rate of CD4 T cells by SIV *in vitro* (111). It should be noted that despite the observed correlation between IL-15 and disease outcome, Okoye et al. documented that CD8 depletion of SIV infected RM results in a spike of IL-15 that causes dramatic CD4 TEM expansion. While the CD8 depleted monkeys succumb to rapid disease progression, blockade of IL-15 inhibits the CD4 TEM proliferation, but does not prevent rapid disease progression (154).

The goal of my work was to further elucidate the role of IL-15 regulating T cell and NK cell homeostasis *in vivo*. We first characterized the responses of individual lymphocyte populations to different γc cytokines *in vitro*. We then developed and administered an anti-IL15 Ab to mediate an IL-15 signaling blockade to healthy RM to assess how IL-15 controls lymphocyte homeostasis in the normal immune system. Subsequently, we used the anti-IL-15 Ab to understand how increased IL-15 levels during pathogenic SIV infection contribute to SIV pathogenesis.

Chapter 2 – *In vitro* effects of IL-15

Contribution

I planned and executed all experiments included in this chapter under the guidance of Afam Okoye and Louis Picker (Figures 2-1, 2-2, 2-3, 2-4, 2-5, 2-6, 2-7, 2-8, 2-9, 2-10, 2-11). Stan Shiigi and Nate Whizin often aided in cell sort-purification by operating the ARIA II.

Abstract

IL-15 is a pleiotropic cytokine with diverse functions on many cell types, but its non-redundant role regulating lymphocyte homeostasis *in vivo* has not yet been fully characterized. Because of the complex nature of IL-15, we used *in vitro* studies to understand the effect of IL-15 versus IL-7 on RM lymphocyte phenotypes. We observed that IL-15 is able to induce phosphorylation of STAT5 in NK cells and T cell subsets. Interestingly, the majority of NK cells were only able to phosyphorylate STAT5 in response to IL-15 but not IL-7 *ex vivo*. In contrast, all T cells subsets could be signaled to induce phosphorylation of STAT5 by both IL-15 and IL-7, but responsiveness to IL-15 versus IL-7 varied with T cell differentiation status. TN and TCM populations were highly responsive to IL-7, but only slightly responsive to IL-15. TEM and TTM populations, on the other hand, were very responsive to IL-15 but only a small percent were responsive to IL-7. The ability to be signaled by γc cytokines likely underlies the varying dependence of each lymphocyte population's reliance on distinct γc cytokines *in vivo*. Additionally, we observed that IL-15 could drive the *in vitro* proliferation of TEM and the differentiation of TCM to TEM. Our *in vitro* studies suggest that IL-15 supports effector cell populations through survival, proliferation, and differentiation.

Introduction

IL-15 is a γc cytokine that is involved in the homeostasis and activation of many cell types throughout the body, including memory T cells and NK cells (61-71). To mediate signals, IL-15 binds to its hetero-trimeric receptor composed of IL-15Rα, IL-2/15Rβ, and γc (65, 74-77). Binding the receptor initiates a signal cascade whereby JAK3 phosphorylation induces STAT5 phosphorylation, which causes STAT5 translocation to the nucleus and binding to specific DNA sequences (78). Via STAT5 activation, IL-15 favors pro-survival signals by up-regulating anti-apoptotic proteins such as Bcl-2 and downregulating pro-apoptotic proteins such as Bim in T cells and NK cells (53, 79-83). Because γc cytokines share common receptors, some of their biologic functions are overlapping and redundant, which has made it difficult to clarify the specific, non-redundant role of each γc cytokine *in vivo*.

A non-redundant role for IL-15 in lymphocyte homeostasis was demonstrated in IL-15/Rα-/- KO mice, which had reduced immune cell numbers and function. These mice had no NK cells and reduced numbers of CD8 T cells and activated CD8 memory T cells. Additionally, IL-15Rα-/- KO mice had smaller lymph nodes with less cells due to defective lymphocyte homing and reduced proliferation (99). Likewise, IL-15-/- KO mice also had practically no NK cells and reduced numbers of NK T cells, and CD8 T memory cells (101). Both of these KO studies in mice demonstrated that without IL-15 mediated signals, NK cells were practically absent and no NK cell function could be observed, indicating that NK cells require IL-15 for development and function. The reduced number of memory CD8 T cells in the periphery but normal CD8 T cell numbers

in the thymus of IL-15 pathway KO mice suggested that IL-15 controls proliferation and/or survival of these cells, but not their development (100, 101). Later studies investigating the role of IL-15 by administering doses of exogenous IL-15 to RM *in vivo* indicated that the role of IL-15 regulating lymphocyte homeostasis is highly conserved throughout mammalian species. IL-15 caused an increase in NK cell and T cell proliferation and absolute numbers over the course of treatment (114-116). TEM populations demonstrated the highest increase in proliferation and absolute numbers, with TCM exhibiting lower increases in Ki-67 expression and absolute numbers. More recently, studies that administered anti-IL-15 Ab to humans showed that IL-15 plays a role in T cell homeostasis but showed no effect on NK cell populations (130).

These previous studies clearly demonstrate a role for IL-15 in lymphocyte homeostasis, but the exact role that IL-15 plays maintaining each lymphocyte population *in vivo* has not been described in RM. To understand the complex nature of IL-15 in vivo, we first started our studies with in vitro experiments to understand how IL-15 signals each population and perhaps find underlying mechanisms of IL-15 mediated homeostasis *in vivo*.

Materials and Methods

Flow Cytometric Analysis

Polychromatic (8-12 parameter) flow cytometric analysis was performed on an LSR II instrument (BD) using Pacific Blue, AmCyan, FITC, PE, PE-Texas red, PE-Cy7, PerCP-Cy5.5, allophycocyanin (APC), APC-Cy7, and AlexaFlour 700 as the available fluorescent parameters. Instrument set up and data acquisition procedures were performed as previously described (155). List mode multiparameter data files were analyzed using FlowJo software. Criteria for delineating cell subsets: TN (live small lymphocytes, CD3+, CD28mid, CD95low, CCR7+, CCR5-); TCM (live small lymphocytes, CD3+, CD28high, CD95high, CCR7+, CCR5-); TTM (live small lymphocytes, CD3+ CD28high, CD95high, CCR7- and or CCR5+); TEM (live small lymphocytes, CD3+, CD28-, CD95high, CCR7-); NK cells (live small lymphocytes, CD3-, CD20-, CD8bright, NKG2a+, CD14-); monocytes (live large cells, CD14+, CD3-).

Antibodies

CD3 (SP34-2 BD Pharmingen), CD4 (L200 BD Pharmingen), CD8 (SKI BD Pharmingen, eBiosciences, BDIS), CD28 (CD28.2 Beckman Coulter, BD Pharmingen), CD95 (DX2 BD Pharmingen, eBiosciences), CCR5 (3A9 BD Pharmingen), CCR7 (15053 RandD Sysyems), Ki-67 (B56 BD Pharmingen), SA (BD Pharmingen), CD56 (MEM-188 Invitrogen), CD16 (3G8 BD Pharmingen, Biolegend), NKG2A (Z199 Beckman Coulter), NKp46 (195314 RandD Systems), CD14 (M5E2 BD Pharmingen,

RandD Systems), HLA-DR (TU36 Invitrogen, Immu357 Beckman Coulter), STAT5 (47/Stat5(pY6) BD Pharmingen),

Reagents

R10 media (RPMI (HyClone), 10% Fetal Bovine Serum (FBS), 100units/mL Penicillin 10mg/mL Streptomycin (PenStrep) (Sigma), 200μM L-glutamine (Sigma))

1X PAB (DPBS w 0.1% BSA and sodium azide)

Cytokines – rIL-15, rIL-7, rIL-21, rIL-2 were all generous gifts from Francois Villinger, TNFa (RandD Systems), IL-6 (RandD Systems), IL-8 (RandD Systems)

pIL-15 pIL-15-IL15Ra supernatants were generous gifts from George Pavlokis.

Peripheral blood mononuclear cell (PBMC) isolation from whole blood

Whole blood was collected in ACD tubes (BD). Whole blood was spun down for 15 minutes at 1800rpm to separate plasma. Plasma was collected and modified Hanks buffered saline solution (HBSS) (HyClone) was added back to the blood to a total volume of no more than 30mL and mixed well. 14mL Ficoll was layered under the blood and tubes were spun at 3000rpm for 20 minutes. PBMCs were removed from the buffy coat with a transfer pipette and placed in a new 50mL conical (no more than 15mL). Cells were then washed with 35mL HBSS and spun for 15 minutes at 1800rpm. For cell sorting, cells were then re-suspended in 5mL 1X ACK Lysing Buffer (Biossource International) for less than 5 minutes, and 45mL HBSS was then added to stop lysis.

Cells were spun for 8 minutes at 1800rpm. Cells were then washed 1X in R10 and re-suspended in fresh R10.

Sort Purification of Cells

Whole blood was collected in ACD vacutainers and lymphocytes were isolated by density gradient separation as described above. Live lymphocytes were stained extracellularly in R10, on ice in the dark for 30 minutes. After incubation, cells were washed 1X with cold R10 and spun at 1500rpm for 10 minutes at 4˚C. Cells were resuspended in cold R10 and kept on ice prior to sort and after purification. Cells were sorted using an ARIA II (BD).

Cellular Staining

Whole blood (150ul) was added to polystyrene flow tubes. For staining previously isolated tissue lymphocytes, $1x10^6$ cells were added to polystyrene flow tubes and washed 1X with IX PAB. Extracellular antibodies were added to appropriate tubes and tubes were lightly vortexed and incubated in the dark for 30 minutes. In the case that biotin was used, the appropriate SA conjugated antibody was added and incubated for an additional 20 minutes. After incubation, 1mL lyse solution (BD) was added and tubes were vortexed, and incubated at room temperature in the dark for 10 minutes. After 10 minutes, 3mL 1X PAB was added to each tube and tubes spun 5min at1800rpm. Supernatant was decanted and 0.5mL 2X Perm buffer (BD) was added to each tube, vortexed and incubated 10 minutes at room temperature in the dark. Following

incubation, cells were washed with 3mL 1X PAB, spun and decanted. Cells were permed one additional time then washed twice with 3mL 1X PAB. Extracellular antibodies were added and tubes were incubated at room temperature in the dark for 45 minutes. Cells were then washed with 3mL 1X PAB and were subsequently collected on an LSR II.

PhosFlow

Whole blood (100μL) was added to polystyrene flow tubes. Extracellular antibody stains were added and incubated in the dark at RT for 30 minutes. During last 15 minutes of surface stain, cytokine was spiked in (0-32ng/mL (final concentration) diluted in 2μL 1X PBS) to blood. Samples were incubated for 15 minutes at 37˚C. After 15 minutes, add 2mL 1X BD PhosFLow Lyse/Fix (BD) diluted in water. Mix well and incubate 5min at RT. After incubation, spin tubes for 5 minutes at 1800rpm. Discard supernatant and wash cells 1X with 2mL 1XPBS. Mix well and spin tubes for 5 minutes at 1800rpm. Decant supernatant. Add 1mL ice-cold 1X BD PhosFlow perm buffer IV (BD) diluted in PBS. Mix well and incubate exactly 5min at RT. After 5 minutes add 3mL 1XPAB and spin tubes 5 minutes at 1800rpm. Decant supernatant and wash 1X with 1X PAB. Add intracellular antibody and incubate 45 minutes at RT in the dark. Wash 1X with 1X PAB. Run on LSRII.

Proliferation and Differentiation Cultures

PBMCs from whole blood were sort purified based on phenotype. Purified cells were plated in a 48-well plate in 1mL R10 at a cell density of 150,000 to 300,000 cells per mL.

Cytokine and antibodies were spiked into the culture at the concentration described, and cultures were gently mixed. Cells were then placed in culture at 37˚C for two weeks. At day 7, the culture was resuspended and half the culture (0.5mL) was removed for phenotype analysis by flow cytometry. An equal amount of fresh R10 was added back to the remaining culture, which was placed back at 37˚C for the remaining 7 days. At day 14, the entire culture was resuspended and taken for phenotype analysis.

Luminex

Plasma cytokine concentrations (excluding IL-7) were measured using the Cytokine Monkey Magnetic 29-Plex Panel Kit (Life Technologies) according to the manufacturers' instructions. This panel allowed for the quantitative determination of EGF, Eotaxin, FGF-basic, G-CSF, GM-CSF, HGF, IFN-γ, IL-1B, IL-1Ra, IL-2, IL-4, IL-6, IL-8, IL-10, IL-12, IL-15, IL-17, IP-10, I-TAC, MCP-1, MDC, MIF, MIG, MIP-1a, MIP-1b, RANTES, TNF-a, and VEGF. Briefly, previously collected plasma was thawed on ice. Once thawed, plasma was spun for 10 minutes at 10,000g at 4˚C. Plasma and standards were incubated with provided beads overnight at 4˚C. After incubation, detection antibody was added and incubated for 1 hour and subsequently washed. Streptavidin-RPE was added next and incubated for 30 minutes at RT. Finally, beads were washed and resuspended in wash buffer for acquisition using a Luminex 200 machine. Data was analyzed using MasterPlex QT and MasterPlex CT Software.

Results

It was our first goal to determine the responsiveness of RM T cell subsets and NK cell subsets to IL-15 versus IL-7. As the γc cytokines IL-15 and IL-7 signal via the Jak3-Stat5 cascade, we used phosflow to assay for STAT5 phosphorylation as an indicator of the immediate early cell signaling by IL-15 and IL-7 (78). In the first experiment, we stimulated whole blood *ex vivo* with increasing concentrations of IL-15 and IL-7 and then stained for cell phenotypic markers and intracellular phospho-STAT5. We observed that soluble IL-15 is capable of signaling NK cells and TM as well as TN cell subsets. NK, TEM and TTM cells were found to be highly responsive to IL-15, with over 80% of cells from these populations inducing STAT5 phosphorylation in response to 8ng/mL IL-15 (Figure 2-1, 2-2). Although less responsive than NK cells, TEM and TTM cell populations, TCM and TN cells were reactive to IL-15, with at least half of these populations' cells inducing STAT5 phosphorylation after IL-15 stimulation. In contrast to their high responsiveness to IL-15, most NK cell subsets did not respond at all to stimulation with IL-7. Only the CD56+ CD16- NK cells were able to respond to high concentrations of IL-7 by phosphorylating STAT5. Whereas TCM, TTM, and TN were highly reactive to IL-7, TEM were relatively unresponsive to IL-7, with only approximately 20% of CD8 TEM and 40% of CD4 TEM inducing STAT5 phosphorylation after IL-7 stimulation. Taken together, NK cell, TEM cell, and TTM cell populations are most responsive to IL-15, whereas TCM and TN cell populations are more responsive to IL-7. Although TN and TM subsets can respond to both IL-15 and IL-7 to varying degrees, NK cells show little responsiveness to IL-7.

Clearly, IL-15 and IL-7 have differing abilities to signal distinct lymphocyte populations. In an effort to understand how IL-15 and IL-7 signaling affects downstream gene changes in the distinct T cell populations, we cultured sort-purified cells with cytokines and monitored cells for proliferation and phenotypic changes. When CD4 and CD8 TEM populations were cultured with IL-15 they were induced to proliferate, but not when they were cultured with IL-7 (Figure 2-3). When TCM and TN populations were cultured with IL-15 they had very little response, but were induced to proliferate at extremely low levels. In response to IL-7, TCM and TN also proliferated at low levels (Figure 2-4, 2-5).

Because we showed that IL-15 does induce STAT5 phosphorylation in TN and TCM, we hypothesized that IL-15 may require additional signals to induce phenotypic changes in TN and TCM. To that end, we next cultured sort-purified TN and TCM with IL-15 and purified CD14+ monocytes (91, 92). In this context, IL-15 induced high levels of proliferation and differentiation as measured by increased Ki-67 levels and a change in phenotype losing CD28 expression and CCR7 expression and gaining CCR5 expression of both TN and TCM populations (Figures 2-4A,B, 2-5). Monocytes also moderately enhanced proliferation of TN and TCM cultured with IL-7, though not nearly to the same extent as IL-15. Our results suggest that in some circumstances IL-15 is able to drive differentiation of T cells to an effector phenotype (156). We next sought to further characterize how monocytes were augmenting proliferation and differentiation of CD4 TN and TCM to TEM.

In vivo, IL-15 is capable of signaling via transpresentation, which was shown can be mediated by monocytes (88, 91). To determine whether IL-15 was being *trans*-presented to CD4 TCM by monocytes in our system, we cultured sort-purified CD14+ monocytes with IL-15 for two days. The cell-free supernatant of monocytes cultured with IL-15 was incubated with sort-purified CD4 TCM. This cell-free supernatant induced CD4 TCM to proliferate and differentiate to CD4 TEM, though less robustly than when CD4 TCM and monocytes were cultured in direct contact, indicating that IL-15 transpresentation by monocytes was not required in our system (Figure 2-6). It is possible, however, that IL-15 trans-presentation by monocytes augments the observed proliferation and differentiation of CD4 TCM to TEM, thus explaining the less robust induction of phenotypic changes caused by the cell-free supernatant of monocytes incubated with IL-15. Notably, differentiation induced by the cell-free supernatant from monocytes incubated with IL-15 could be specifically blocked by antibodies against IL-15. This suggested that IL-15 does in fact directly interact with CD4 TCM to induce the observed proliferation and differentiation.

To further confirm that cell contact was not necessary for the observed CD4 TCM proliferation and differentiation to TEM, we cultured monocytes with IL-15 together in one compartment of a transwell and cultured the purified CD4 TCM in a separate compartment of the transwell. Although the membrane of the transwell allowed passage of media and small molecules such as IL-15, cells were too large to pass through the membrane, thereby keeping the monocytes and CD4 TCM out of direct contact. Again, we observed that monocytes and IL-15 cultured in the same well but separate from the

CD4 TCM was sufficient to induce some CD4 TCM proliferation and differentiation to TEM (Figure 2-7).

We next hypothesized that monocytes could be secreting/cleaving a complex of IL-15/IL-15Rα in response to IL-15 and that this complex was inducing CD4 TCM differentiation to TEM. To test this hypothesis, George Pavlakis, through collaboration, kindly sent us transfection supernatant containing pIL-15/IL-15Rα, as confirmed by bioassay and western blot analysis (data not shown). The complex of pIL-15/IL-15Rα did not induce proliferation and differentiation of CD4 TCM to TEM (Figure 2-8). This data, taken together, suggests that IL-15 is inducing monocytes to produce a factor or factors that, along with IL-15, directly induce CD4 TCM proliferation and differentiation to TEM.

To identify factors that monocytes produce in response to IL-15, we cultured sort-purified monocytes with IL-15 for two days. After two days, the supernatant was analyzed by luminex for a panel of rhesus, immune-modulating cytokines. In response to IL-15, the monocytes of three separate rhesus monkeys produced extremely high levels of IL-8 and IL-6 (Figure 2-9). Other cytokines released, although to a lesser extent included TNFα, MCP-1 and MIP1α. A review of the literature showed that IL-15 together with TNFα and IL-6 could induce proliferation and differentiation of CD4 TCM to TEM *in vitro* (110). As both IL-6 and TNFα were factors that rhesus monocytes had produced in response to IL-15 *in vitro*, we tested whether TNFα and IL-6 along with IL-15 could induce CD4 TCM to TEM proliferation and differentiation in our system. Indeed, culture of CD4 TCM with IL-15, TNFα, and IL-6 induced proliferation and some

differentiation of CD4 TCM to TEM, though the effect did not recapitulate the entire effect of CD4 TCM cultured with IL-15 and monocytes (Figure 2-10). To test the possibility that another factor besides TNFα and IL-6 may be involved in the monocyte-induced proliferation of CD4 TCM in the presence of IL-15, we tested IL-8 as it was up-regulated in monocyte-IL-15 supernatant. It was found, however, that IL-8 did not induce any additional proliferation or differentiation of CD4 TCM cultured with TNFα, IL-6, and IL-15 (Figure 2-11).

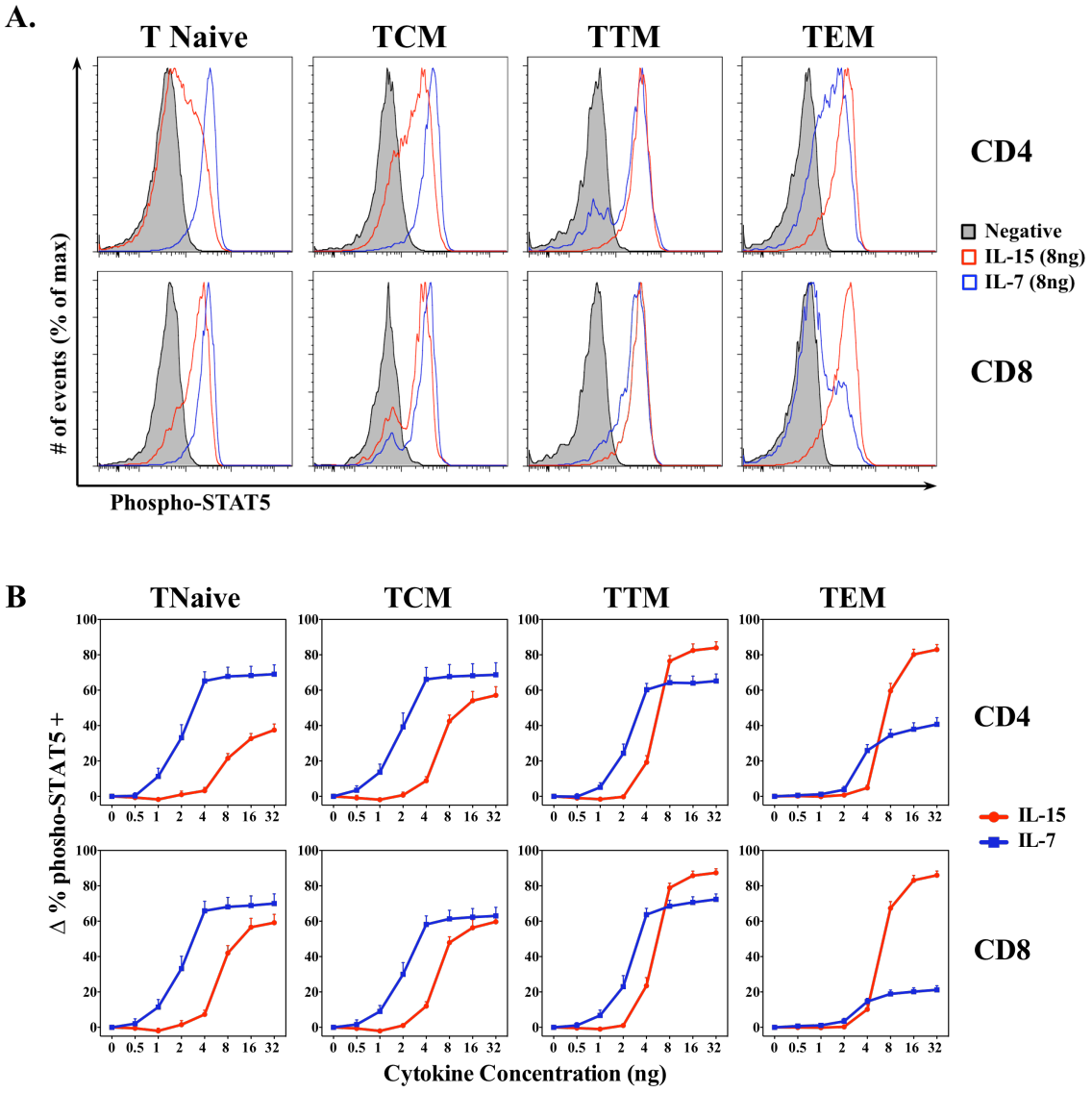

Figure 2-1 – IL-15 signals both CD4 and CD8 T cell populations via STAT5 phosphorylation – Shown in A are histograms of T cell populations' induction of phospho-STAT5 in response to 8ng/mL IL-15 (red) or 8ng/mL IL-7 (blue) from a representative RM. B. Mean T cell population dose response curves to increasing concentrations (0, 0.5, 1, 2, 4, 8, 16, 32ng/mL) of IL-15 (red) or IL-7 (blue), N=14. WB was stimulated *ex vivo* with IL-15 or IL-7 and then stained for T cell phenotype markers (CD3, CD4, CD8, CD28, CD95, CCR7, CCR5) and phosph-STAT5 and analyzed by flow cytometry.

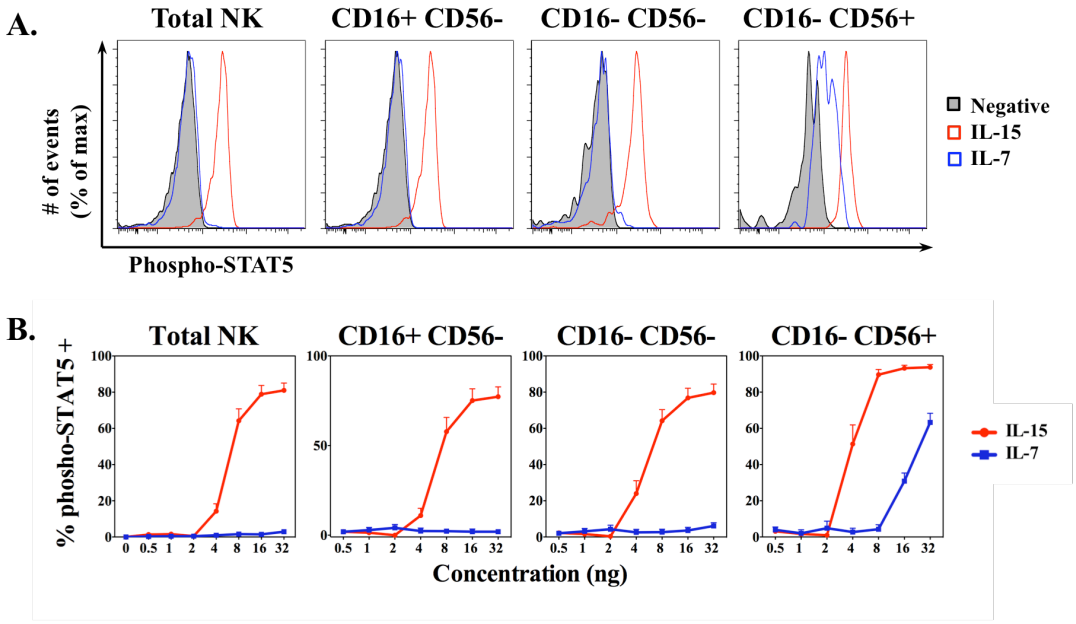

Figure 2-2 – IL-15 signals NK cell populations via STAT5 phosphorylation – Shown in A are histograms of NK cell subsets induction of phospho-STAT5 in response to 16ng/mL IL-15 (red) or 16ng/mL IL-7 (blue) from a representative RM. (B) Mean NK cell population dose response curves to increasing concentrations (0, 0.5, 1, 2, 4, 8, 16, 32ng/mL) of IL-15 (red) or IL-7 (blue), N=8. WB was stimulated *ex vivo* with IL-15 or IL-7 and then stained for cell phenotype markers (NKG2A, CD8, CD16, CD56) and phosph-STAT5 and analyzed by flow cytometry.

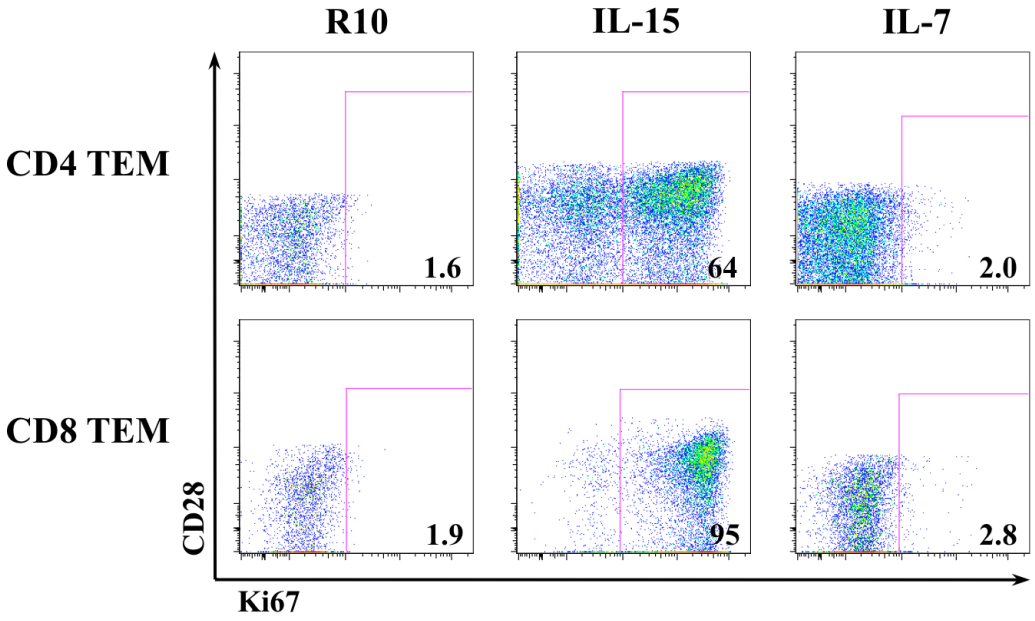

Figure 2-3 – TEM proliferate when cultured with IL-15 but not IL-7 *in vitro* – Shown is the proliferative response of sort-purified CD4 and CD8 TEM that were cultured in R10 with 50ng/mL IL-15 or IL-7 for 7 days. Cultures were then stained for CD3, CD4, CD8, CD28, CD95, CCR7, CCR5 and Ki-67 expression and analyzed via flow cytometry. Shown are dot plots of a representative RM, demonstrative of eight separate experiments.

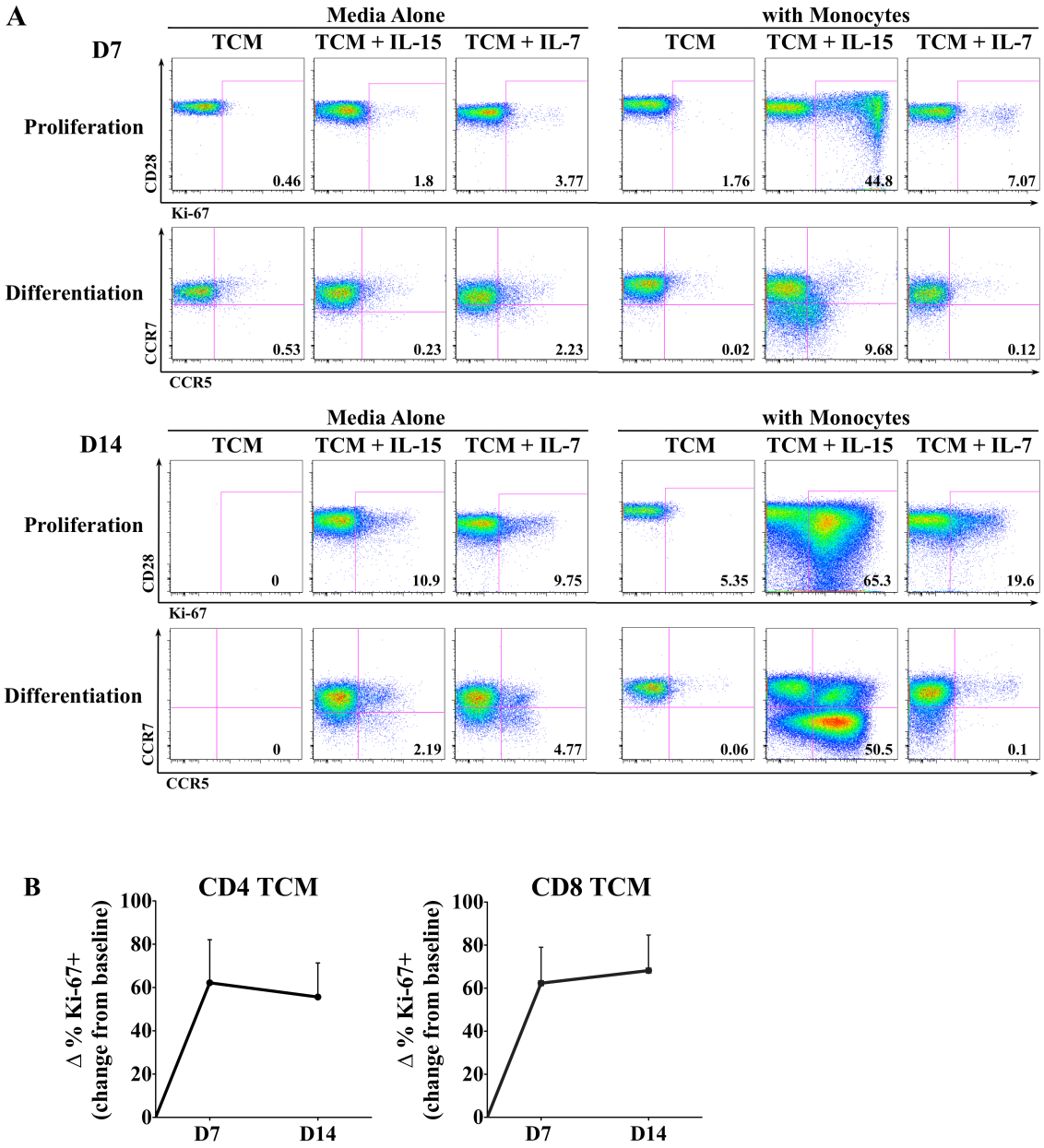

Figure 2-4 – CD4 and CD8 TCM cultured with IL-15 and monocytes are induced to proliferate and differentiate to TEM – Sort-purified CD4 TCM or CD8 TCM were cultured alone or with sort-purified CD14+ monocytes and 50ng/mL IL-15 or IL-7 for 14 days. At days 7 and 14, cells were stained for CD28, Ki-67, CCR7 and CCR5 expression and analyzed by flow cytometry. A. Representative dot plots of RM CD4 TCM response to 50ng/mL IL-15 or IL-7. B. Mean CD4 TCM (N=19) and CD8 TCM (N=11) percent increase in Ki-67 expression when cultured with monocytes and 50ng/mL IL-15 as compared to culture with monocytes alone.

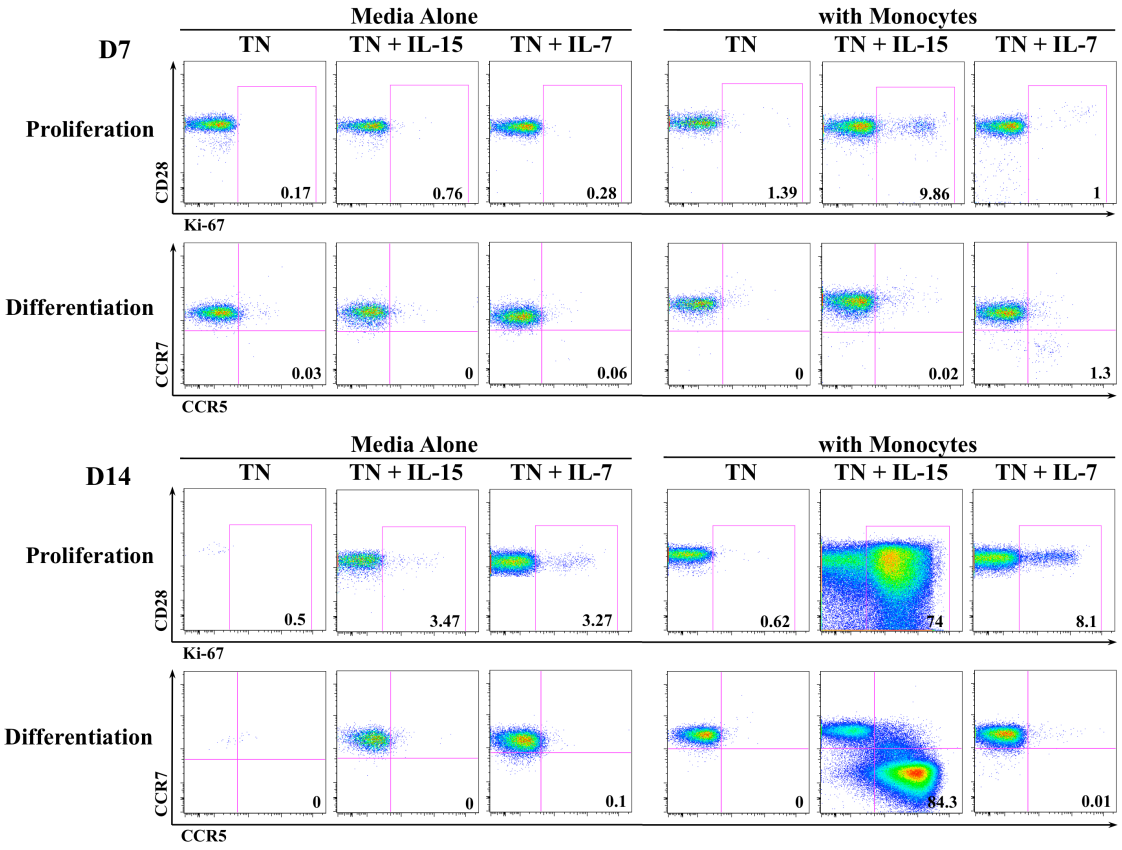

Figure 2-5 – CD4 TN cultured with IL-15 and monocytes are induced to proliferate and differentiate to TEM – Sort-purified CD4 TN were cultured alone or with sort-purified CD14+ monocytes along with 50ng/mL IL-15 or IL-7 for 14 days. At day 7 and day 14, cultured cells were stained for CD28, Ki-67, CCR7, and CCR5 and analyzed by flow cytometry. Shown are dots plot from a representative RM of four separate experiments.

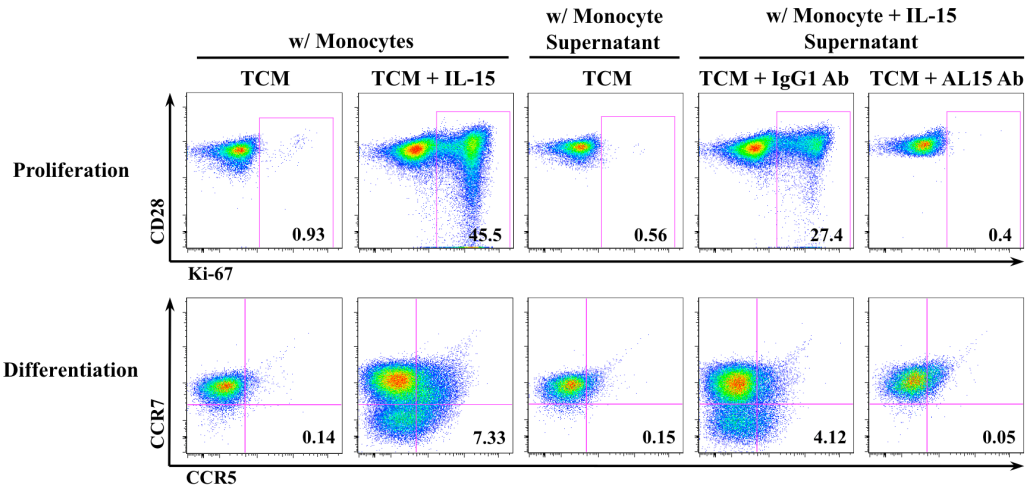

Figure 2-6 – The cell-free supernatant of monocytes cultured with IL-15 induces proliferation and differentiation of CD4 TCM to TEM – Sort-purified CD14+ monocytes were cultured in R10 with or without IL-15 for 2 days. The cell-free supernatant from these cultures was then incubated with sort-purified CD4 TCM either with anti-IL-15 Ab (ng/mL) or an IgG1 isotype control Ab (ng/mL). At day 7, cultures were stained for CD28, Ki-67, CCR7, and CCR5 expression and analyzed via flow cytometry. Shown are dot plots from a single RM, representative of six separate experiments.

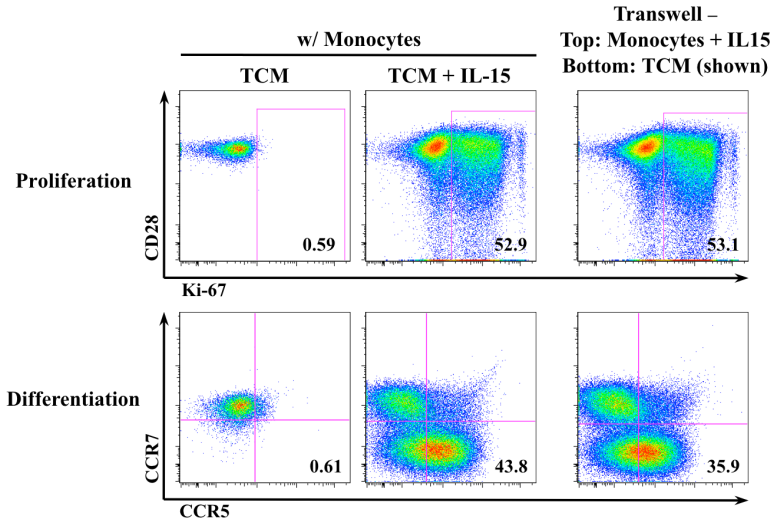

Figure 2-7 – Monocytes and IL-15 in the separate well of a transwell can induce CD4 TCM proliferation and differentiation to CD4 TEM – Sort purified CD4 TCM were cultured in bottom of transwell while CD14+ monocytes were placed with 50ng/mL rIL-15 in the top of transwell. At day 7, cultures were stained for CD28, Ki-67, CCR7, and CCR5 expression and analyzed via flow cytometry. Shown are dot plots from a single RM, representative of five separate experiments.

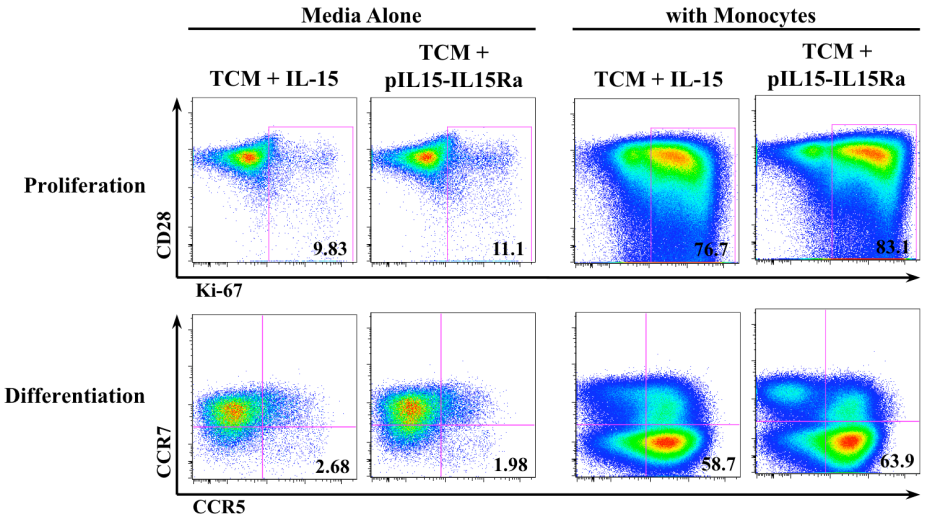

Figure 2-8 – Complexes of IL15-IL15Rα do not induce TCM proliferation and differentiation to TEM – Sort purified CD4 TCM were cultured *in vitro* with 50ng/mL rIL-15 or supernatant containing IL15-IL15Rα complexes for two weeks, with or without CD14+ monocytes. At day 7, cultures were stained for CD28, Ki-67, CCR7, and CCR5 and analyzed via flow cytometry. Shown are dot plots from a single RM, representative of three separate experiments.

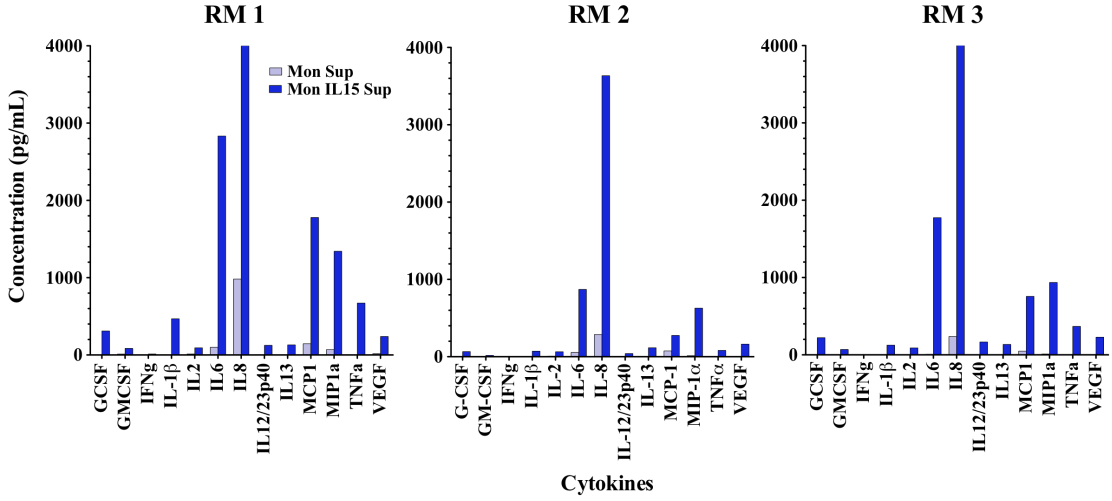

Figure 2-9 – Monocytes secrete IL-8 and IL-6 when cultured with IL-15 *in vitro* – Graphs show soluble cytokine concentrations (pg/mL) secreted by monocytes cultured in R10 alone (Mon Sup) or in R10 supplemented with IL-15 (Mon IL15 Sup) for each RM. Sort-purified CD14+ monocytes from 3 healthy RM were cultured *in vitro* with or without 50ng/mL IL-15 for 2 days. At day 2, supernatant was collected and analyzed for cytokines via luminex.

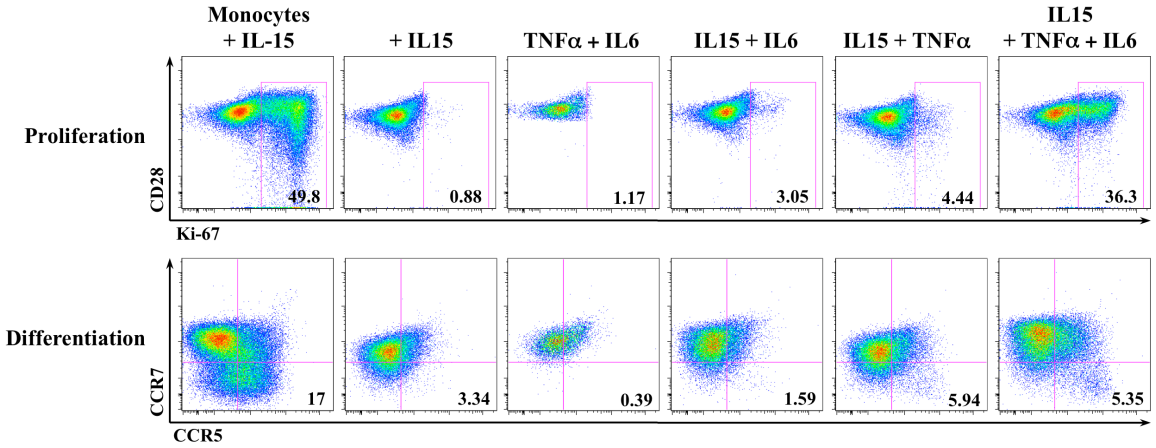

Figure 2-10 – CD4 TCM cultured with IL-15, TNFα, and IL-6 proliferate and show some differentiation to CD4 TEM – Sort-purified CD4 TCM were cultured *in vitro* with combinations of IL-15, IL-6, and TNFα, all at 50ng/mL. At day 7, cultures were stained for CD28, Ki-67, CCR7 and CCR5 and analyzed by flow cytometry. Shown are dot plots from one RM, representative of eight separate experiments.

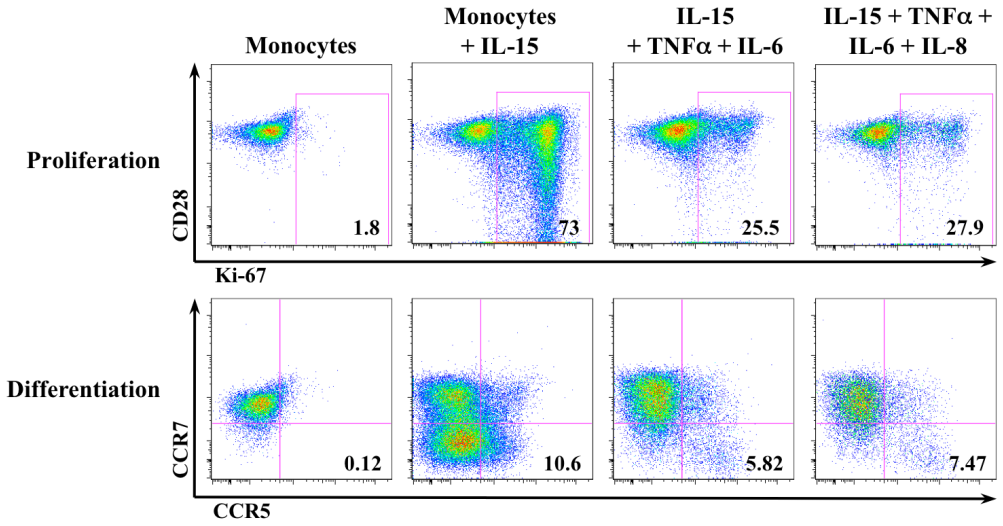

Figure 2-11 – IL-8 does not substantially increase proliferation and differentiation of CD4 TCM when cultured together with IL-15, TNFα, and IL-6 – Sort purified CD4 TCM were cultured with combinations of cytokines IL-15, TNFα, IL-6, and IL-8 at 50ng/mL. At day 7, cells were stained for CD28, Ki-67, CCR7 and CCR5 and analyzed by flow cytometry. Shown are dot plots from one RM, representative of five separate experiments.

Discussion

Because of the many complex and variable functions of IL-15 *in vivo*, we began our studies with *in vitro* experiments, first describing the cell signaling capabilities of the homeostatic cytokines IL-15 compared to IL-7. We observed that IL-15 and IL-7 have differing abilities to signal distinct RM lymphocyte populations via γc-mediated JAK3-STAT5 phosphorylation. Interestingly, whereas nearly all NK cells responded to exogenous doses of IL-15 by inducing STAT5 phosphorylation, most NK cell subsets did not induce STAT5 phosphorylation in response to doses of IL-7. Only the CD16- CD56+ NK cells were able to respond to high concentrations of IL-7 by phosphorylating STAT5. Our *in vitro* data, therefore, suggested that rhesus NK cells were also reliant on IL-15 mediated signaling *in vivo*, similar to mice. Indeed, our experiments administering anti-IL-15 Ab to RM (Chapter 3) resulted in nearly complete NK cell depletion as did a similar experiments in cynomolgous and rhesus macaques (130). These data suggest that RM NK cell reliance on IL-15 is a result of only being able to be signaled by IL-15 and not another homeostatic γc cytokine such as IL-7. Supporting this, we found that the CD16- CD56+ NK cell subset, which was the only subset responsive to IL-7, was the least depleted NK cell subset following antibody-mediated IL-15-signal blockade, suggesting that this population may receive homeostatic signals from IL-7 in the absence of IL-15.

We next focused on the ability of IL-15 and IL-7 to signal distinct T cell subsets. We observed that both IL-15 and IL-7 were able to signal all T cell subsets via STAT5 phosphorylation, though to varying degrees. Although there were slight differences in

the abilities of IL-15 and IL-7 to signal CD4 versus CD8 T cells, overall both CD4 and CD8 T cells exhibited similar patterns of STAT5 phosphorylation in response to doses of IL-15 and IL-7. The similar *in vitro* response of CD4 and CD8 T cells to IL-15 supports the accumulating data that IL-15 is imperative not only to CD8 T cell homeostasis, but also to CD4 T cell homeostasis as well (25, 32, 60, 110).

Regardless of CD4 or CD8 expression, IL-15 and IL-7 had differing abilities to induce phosphorylation of STAT5 in memory versus naïve T cells. Whereas effector memory phenotype subsets TEM and TTM were highly responsive to IL-15, TEM and TTM subsets were considerably less responsive to IL-7. This *in vitro* data potentially suggested that *in vivo* TEM and TTM populations were regulated primarily by IL-15 and to a lesser extent by IL-7. In contrast, TN and TCM subsets demonstrated a distinct phenotype, being highly responsive to IL-7 but only slightly responsive to IL-15. The result that TN and TCM cell subsets were more sensitive to IL-7 supports abundant data in the literature, which show that TN and TCM subsets' homeostatsis are primarily regulated by IL-7 *in vivo* (in addition to MHC interactions in the case of TN) (57-59, 157, 158). However, the observation that TN and TCM are able to induce STAT5 phosphorylation in response to IL-15, suggested that IL-15 was potentially involved in the regulation of these T cell subsets as well. Thus, overall our data predict that both IL-15 and IL-7 share regulation of TM homeostasis, though to varying degrees depending on the differentiation status of the TM subset.

To understand how IL-15- and IL-7-induced STAT5 phosphorylation affected downstream changes in different T cell subsets, we next cultured sort-purified T cell

populations *in vitro* with either IL-15 or IL-7. Notably, we observed that IL-15 induced the proliferation and differentiation of both TN and TCM to TEM *in vitro* when cultured with monocytes. In contrast, culture of either TN or TCM with IL-7 and monocytes led to only modest enhancement of T cell proliferation. Thus, IL-15 may regulate the homeostasis of TN and TCM populations by driving their differentiation to effector phenotype cells. Although not generally ascribed as a main function of IL-15, the ability of IL-15 to drive differentiation of effector memory T cells has been previously reported in the literature (25, 110).

Our *in vitro* data suggest that RM IL-15 is involved in the homeostasis of NK cells and both CD4 and CD8 T cells. Furthermore, our data predict that T cell dependence on IL-15 varies with the differentiation status of the T cell population. The phosphorylation and *in vitro* culture data indicate that IL-15 is a cytokine that primarily supports effector phenotype T cell populations' homeostasis and differentiation. To assess the extent to which TM subsets and NK cells are dependent on IL-15, in the next chapter we will explore the role of IL-15 *in vivo* by administering an anti-IL-15 antibody to maintain an IL-15-signal blockade.

Chapter 3 – Anti-IL-15 Ab administration to healthy RM

Contribution

Details and timing of antibody administration, tissue collection, necropsy and experiments of the primary groups of rhesus monkeys belonging to Picker cohorts 193 and 194 (N=15) were managed and planned by myself under guidance of Afam Okoye and Louis Picker. I performed and analyzed experiments described in Figures 3-1, 3-2, 3-3, 3-5, 3-6, 3-7, 3-9, 3-10, 3-11, and 3-17. During RM necropsy, Picker lab technicians assisted in tissue processing and cell isolation, to expedite time-sensitive experiments. Stan Shiigi often aided in cell sort-purification by operating the ARIA II. RM were cared for by Oregon National Primate Research Center (ONPRC) department of animal resources (DAR) technicians and staff. All surgical procedures including antibody dosing, necropsy, and harvesting of tissues were performed by veterinarians and/or veterinary assistants from Michael Axthelm's laboratory or ONPRC DAR. Additionally, three experimental procedures were performed by outside collaborators with tissues and cells collected from Picker cohorts 193 and 194. Immunostaining experiments were performed by Jake Estes with tissues fixed at necropsy (Figures 3-4, 3-8, 3-13, 3-14). Microarray analysis was performed by Rafick Sekaly with sort-purified PBMCs frozen in RLT buffer (Figure 3-15 and 3-16). Detection of CMV DNA was performed at VGTI virology core by Don Seiss with liver sections flash frozen at necropsy (Figure 3-18). A separate cohort of RM (Picker cohort 265, N=11) was administered anti-IL-15 Ab or IgG control Ab and then dosed with exogenous IL-7 (Figure 3-12). This study was managed by Afam Okoye, and all experiments were performed by his team in Louis Picker's lab.

Abstract

Preliminary *in vitro* studies indicated that the γc cytokine IL-15 supports the production, proliferation, and survival of effector-phenotype lymphocyte populations in RM; however, the non-redundant functions of IL-15 *in vivo* have not been fully characterized. To understand the role of IL-15 supporting lymphocyte homeostasis, we administered a rhesusized anti-IL-15 antibody (N=15) or an IgG1 control antibody (N=10) to healthy rhesus macaques biweekly, for a total of three doses given over six weeks. The anti-IL-15 Ab neutralized IL-15 mediated signaling via STAT5 phosphorylation, leading to near complete depletion of NK cells in the blood and tissues of RM compared to control treated animals. Additionally, anti-IL-15 Ab treatment led to an initial decline of CD4 and CD8 TEM absolute numbers, but this decline was countered by the onset of TEM homeostatic proliferation, potentially induced by an increased sensitivity to IL-7 in the absence of IL-15 mediated signaling. Although, the TEM homeostatic proliferative burst was associated with stabilization of absolute numbers in WB, TEM levels in the colon remained depleted and tissue expression of active caspase-3 was increased following anti-IL-15 Ab compared to IgG control Ab treatment. Moreover, microarray revealed that TEM expression profiles were dysregulated, with a signature indicating they were pre-apoptotic and turning over at an increased rate. Our studies thus reveal that IL-15 is necessary to maintain normal RM NK cell and effector memory T cell homeostasis *in vivo*.

Introduction

IL-15 is a γc cytokine that is involved in the homeostasis and activation of many cell types throughout the body, including memory T cells, NK cells, invariant NKT cells, intestinal intraepithelial lymphocytes (IELs), activated B cells, dendritic cells (DCs), macrophage, mast cells, and neutrophils (61-71). γc cytokines are a group of type I cytokines that share not only common structural features but also a common receptor, the γc (43-49). γc cytokine specificity and affinity is mediated by private receptors for each cytokine, designated their α-chains. To mediate signals, IL-15 binds to its heterotrimeric receptor composed of IL-15Rα, IL-2/15Rβ, and γc (65, 74-77). Binding the receptor initiates a signal cascade whereby JAK3 phosphorylation induces STAT5 phosphorylation, which causes STAT5 translocation to the nucleus and binding to specific DNA sequences (78). Via STAT5 activation, IL-15 favors pro-survival signals by up-regulating anti-apoptotic proteins such as Bcl-2 and downregulating pro-apoptotic proteins such as Bim in T cells and NK cells (53, 79-83). Because γc cytokines share common receptors, some of their biologic functions are overlapping and redundant, which has made it difficult to clarify the specific, non-redundant role of each γc cytokine *in vivo*.

A non-redundant role for IL-15 in lymphocyte homeostasis was demonstrated in IL-15/Rα-/- KO mice, which had reduced immune cell numbers and function. These mice had no NK cells and reduced numbers of CD8 T cells, activated CD8 memory T cells, NK T cells, γδ T cells, and IELs. Additionally, IL-15Rα-/- KO mice had smaller lymph nodes with less cells due to defective lymphocyte homing and reduced

proliferation (99). Likewise, IL-15-/- KO mice also had practically no NK cells and reduced numbers of NK T cells, CD8 T memory cells, and IELs (101). Both of these KO studies in mice demonstrated that without IL-15 mediated signals, NK cells were practically absent and no NK cell function could be observed, indicating that NK cells require IL-15 for development and function. The reduced number of memory CD8 T cells in the periphery but normal CD8 T cell numbers in the thymus of IL-15 pathway KO mice suggested that IL-15 controls proliferation and/or survival of these cells, but not their development (100, 101). Further studies indicated that during the contraction phase of a T cell response and the transition of effector to memory T cells, the absence of IL-15 signaling resulted in a much more drastic contraction phase and a much higher death rate of effector T cells (103, 104, 106, 107).

Later studies investigating the role of IL-15 by administering doses of exogenous IL-15 to RM *in vivo* indicated that the role of IL-15 regulating lymphocyte homeostasis is highly conserved throughout mammalian species. After IL-15 administration to RM, investigators observed a brief lymphopenia followed by lymphocytosis. IL-15 caused an increase in NK cell proliferation and absolute numbers over the course of treatment (114-116). T lymphocytes were also significantly affected by IL-15 administration, which caused an increase in CD4 and CD8 TM proliferation and absolute numbers. TEM populations demonstrated the highest increase in proliferation and absolute numbers, with TCM exhibiting lower increases in Ki-67 expression and absolute numbers. Additionally, CD8 T cells were more reactive to IL-15 than CD4 T cell counterparts (25, 114-116). IL-15 has been shown to induce cell migration causing a redistribution of

long-lived cells from circulation to tissues (25, 115). Alternatively, overstimulation with IL-15 and spikes of exogenous IL-15 were associated with increased cell death (114, 117). IL-15 treatment also increased the production of long-lived antigen specific CD4 and CD8 T cells (118, 119, 129). A more recent study found that anti-IL-15 Ab administration to cynomolgous macaques cause a depletion of NK cells and T cells, indicating RM lymphocyte regulation may be similar (130). Surprisingly, studies have shown that humans administered anti-IL-15 Ab had no NK cell depletion, but only T cell depletion (130, 131).

In our preliminary *in vitro* experiments described in Chapter 2, we observed that IL-15 is able to induce phosphorylation of STAT5 in NK cells and CD4 and CD8 T cell subsets. The majority of NK cells were only able to phosyphorylate STAT5 in response to IL-15 but not IL-7 *ex vivo*. In contrast, all T cells subsets could be signaled to induce phosphorylation of STAT5 by both IL-15 and IL-7, but responsiveness to IL-15 versus IL-7 varied with T cell differentiation status. Additionally, we observed that IL-15 could drive the *in vitro* proliferation of TEM and the differentiation of TCM to TEM. Our *in vitro* studies thus suggested that IL-15 supports effector cell populations through survival, proliferation, and differentiation. However, the complex mechanisms of IL-15 mediated homeostasis have not been fully elucidated. The goal of this chapter was to characterize the role of IL-15 regulating RM lymphocyte homeostasis *in vivo*. We developed and administered an anti-IL-15 Ab to mediate an IL-15 signaling blockade to healthy RM to assess how IL-15 controls NK cell and T cell homeostasis in the normal immune system.

Materials and Methods

Flow Cytometric Analysis

Polychromatic (8-12 parameter) flow cytometric analysis was performed on an LSR II instrument (BD) using Pacific Blue, AmCyan, FITC, PE, PE-Texas red, PE-Cy7, PerCP-Cy5.5, allophycocyanin (APC), APC-Cy7, and AlexaFlour 700 as the available fluorescent parameters. Instrument set up and data acquisition procedures were performed as previously described (155). List mode multiparameter data files were analyzed using FlowJo software. Criteria for delineating lymphocyte cell subsets: TN (live small lymphocytes, CD3+, CD28mid, CD95low, CCR7+, CCR5-); TCM (live small lymphocytes, CD3+, CD28high, CD95high, CCR7+, CCR5-); TTM (live small lymphocytes, CD3+ CD28high, CD95high, CCR7- and or CCR5+); TEM (live small lymphocytes, CD3+, CD28-, CD95high, CCR7-); Treg (CD3+, CD4+, CD25+, CD127mid); NK cells (live small lymphocytes, CD3-, CD20-, CD8bright, NKG2a+, CD14-), B cells (live small lymphocytes, CD3-, CD20+); monocytes (live large cells, CD14+, CD3-).

Antibodies

CD3 (SP34-2 BD Pharmingen), CD4 (L200 BD Pharmingen), CD8 (SKI BD Pharmingen, eBiosciences, BDIS), CD28 (CD28.2 Beckman Coulter, BD Pharmingen), CD95 (DX2 BD Pharmingen, eBiosciences), CCR5 (3A9 BD Pharmingen), CCR7 (15053 RandD Sysyems), Ki-67 (B56 BD Pharmingen), SA (BD Pharmingen), CD20 (L27 BDIS), CD27 (M-T271 BD Pharmingen), IgD (Southern Biotech),

Gd (5A6.E9 Invitrogen), PD1 (J105, eBisociences), B7 (FIB504, BD Pharmingen), CD56 (MEM-188 Invitrogen), CD16 (3G8 BD Pharmingen, Biolegend), NKG2A (Z199 Beckman Coulter), NKp46 (195314 RandD Systems), CD14 (M5E2 BD Pharmingen, RandD Systems), CD127 (hIL-7R-M21 BD Pharmingen), CD169 (7-239 Biolegend), HLA-DR (TU36 Invitrogen, Immu357 Beckman Coulter), CD23 (9P25 Beckman Coulter), CD25 (2A3 BD Pharmingen), CD69 (FN50 BD Pharmingen), STAT5 (47/Stat5(pY6) BD Pharmingen), BrdU (B44 BD Pharmingen).

Reagents

R10 media (RPMI (HyClone), 10% Fetal Bovine Serum (FBS), 100units/mL Penicillin, 10mg/mL Streptomycin (PenStrep) (Sigma), 200μM L-glutamine (Sigma))

R3 media (RPMI, 3% FBS, 100units/mL-10mg/mL PenStrep, 200μM L-glutamine)

IEL media (HBSS (Hyclone), 5% Bovine Growth Serum (BGS), 25mM HEPES buffer (Sigma), 100 IU/ml PenStrep, 2mM L-glutamine)

1X PAB (DPBS w 0.1% BSA and sodium azide)

Animals

Indian-origin RM (*Macaca mulatta*) were used in this study. Twenty-five healthy, adult (approximately ages 8-12) RM both male and female were used: 15 were administered anti-IL-15 Ab and 10 were administered IgG1 control Ab. Antibody doses were administered once every two weeks, 1X at 20mg/kg and 2X at 10mg/kg. BrdU doses were administered at 30mg/kg 3X within 24hrs at day 28-35 post antibody

administration. IL-7 doses were administered subcutaneously at 30μg/kg on days 35 and 42 post anti-IL-15 Ab or IgG1 control Ab dosing. All RM were housed at the Oregon National Primate Research Center according to standards of the Animal Care and Use Committee and the NIH Guide for the Care and Use of Laboratory Animals.

PBMC Isolation from whole blood

Whole blood was collected in ACD tubes. Whole blood was spun down for 15 minutes at 1800rpm to separate plasma. Plasma was collected and HBSS was added back to the blood to a total volume of no more than 30mL and mixed well. 14mL Ficoll was layered under the blood and tubes were spun at 3000rpm for 20 minutes. PBMCs were removed from the buffy coat with a transfer pipette and placed in a new 50mL conical (no more than 15mL). Cells were then washed with 35mL HBSS and spun for 15 minutes at 1800rpm. For cell sorting, cells were then re-suspended in 5mL 1X ACK Lysing Buffer (Biosource International) for less than 5 minutes, and 45mL HBSS was then added to stop lysis. Cells were spun for 8 minutes at 1800rpm. Cells were then washed 1X in R10 and re-suspended in fresh R10.

Lymphocyte isolation from bone marrow, tonsils, and lymph nodes

At necropsy, tissues were placed in a 50mL conical filled with approximately 25mL R10. For processing bone marrow, R10 and bone marrow material was simply resuspended using a 10mL pipette and filtered through a 70μm filter. Cells were washed with R10, spun and resuspended in R10 for counting.

Tonsils and lymph nodes were processed by placing each in a petri dish containing a metal screen and approximately 10mL R10. A glass pestule was then used to crush the tissue against the screen, releasing the lymphocytes into the media. Using a transfer pipette, the media containing the cells was then filtered through a 70μm filter into a 50mL conical. Collected cells were washed with R10, centrifuged 8 minutes at 1800rpm and the supernatant was aspirated. Cells were resuspended in fresh R10 for counting.

Lymphocyte isolation from spleen

Approximately a quarter-sized piece of spleen was placed in a petri dish on a metal screen in about 10mL of R10. Using forceps and a scalpel, the spleen was minced, and subsequently mashed on the screen using a glass pestule to release the lymphocytes into the media. Using a transfer pipette, the cells and R10 were then transferred from the petri dish and filtered with 70μm screen into a 50mL conical. The spleen and petri dish were washed with R10 additional times to maximize cell collection. Although multiple collection conicals were used, no more than 30mL of R10/cells was added to each 50mL conical. R10 was added to 30mL of any conical that had less than 30mL. 14mL Ficoll was then layered under the R10/cell mixture and tubes were spun at 3000rpm for 20 minutes. Lymphocytes were removed from the buffy coat with a transfer pipette and placed in a new 50mL conical (no more than 15mL). Cells were then washed with 35mL HBSS and spun for 15 minutes at 1800rpm. Cells were then washed 1X in R10 and re-suspended in fresh R10.

Lymphocyte isolation from gut, lung, and vaginal mucosa

At necropsy, small pieces of tissue were cleaned of debris and placed in a 50mL conical containing 30mL of IEL media. Once in IEL, tissue was cut into smaller pieces using scissors. The tissues were then agitated at 4˚C for 30 minutes on a shaker. After incubation, samples were spun at 1800rpm for 10min and supernatants were aspirated off. Tissue chunks were re-suspended in 45mL R10 and tubes were inverted to mix. Samples were again spun at 1800rpm for 10 minutes and the supernatant was aspirated off. Tissues pieces were washed once more with 45mL R10. After this second wash, tissue was placed into a 600mL container filled with 200mL R3 media containing DNAse and Collagenase. Samples were then incubated on a shaker for 45-60 minutes at RT. After incubation, R3 containing tissue was run through a 70µm filter into four 50mL conicals. R10 was added to conicals to 50mL and inverted to mix. Tubes were then centrifuged at 1800rpm for 15 minutes and the supernatant was aspirated off. Cell pellets were then washed with 45mL R10, centrifuged at 1800rpm for 10 minutes and the supernatant was again aspirated. Lymphocytes were finally resuspended in 10mL R10 for counting.

Lymphocyte isolation from liver and kidney –

At necropsy, approximately 80g of liver was collected, scored and placed in 200mL of R3 media containing DNAse and Collagenase. The container with liver was agitated at 37˚C for one hour. After incubation, the liver sections were filtered from the R3 medium using 70µm filters into four 50mL conical tubes. The conicals containing R3 and cells were centrifuged at 1800rpm for 15 minutes and the supernatant was aspirated off. The

cell pellets were resuspended in 20mL of R10 and 50uL DNAse was added to each tube and mixed by inversion. Subsequently, 12mL 35% Percol was underlaid, followed by 6mL of 60% Percol. Tubes were then centrifuged at 1000g for 20 minutes with low brake. After separation, the buffy coat and percol were removed with a transfer pipette and placed into a new 50mL conical. R10 was added to 50mL and tubes were centrifuged at 1800rpm for 20 minutes. The supernatant was then aspirated and cells were washed with 50mL R10. Samples were spun at 1800rpm for 8 minutes and the supernatant was aspirated. The cell pellets of each tube were then resuspended together in 10mL R10 media for counting.

Sort Purification of Cells

Whole blood was collected in ACD vacutainers and lymphocytes were isolated by density gradient separation as described above. Live lymphocytes were stained extracellularly in R10, on ice in the dark for 30 minutes. After incubation, cells were washed 1X with cold R10 and spun at 1500rpm for 10 minutes at 4˚C. Cells were then resuspended in cold R10 and kept on ice prior to sort and after sort purification. Cells were sorted using an ARIA II (BD).

Cellular Staining

Whole blood (150ul) was added to polystyrene flow tubes. For staining previously isolated tissue lymphocytes, $1x10^6$ cells were added to polystyrene flow tubes and washed 1X with IX PAB. Extracellular antibodies were added to appropriate tubes and

tubes were lightly vortexed and incubated in the dark for 30 minutes. In the case that biotin was used, the appropriate SA conjugated antibody was added and incubated for an additional 20 minutes. After incubation, 1mL lyse solution (BD) was added and tubes were vortexed and incubated at room temperature in the dark for 10 minutes. After 10 minutes, 3mL 1X PAB was added to each tube and tubes spun 5 minutes at1800rpm. Supernatant was decanted and 0.5mL 2X Perm buffer (BD) was added to each tube, vortexed and incubated 10 minutes at room temperature in the dark. Following incubation, cells were washed with 3mL 1X PAB, spun and the supernatant was decanted. Cells were permed one additional time then washed twice with 3mL 1X PAB. Extracellular antibodies were added and tubes were incubated at room temperature in the dark for 45 minutes. Cells were then washed with 3mL 1X PAB and were subsequently collected on an LSR II.

PhosFlow

Whole blood (100µL) was added to polystyrene flow tubes. Extracellular antibody stains were added and incubated in the dark at room temperature for 30 minutes. During last 15 minutes of surface stain, cytokine was spiked in (0-3.2ng diluted in 2µL 1X PBS) to blood. Samples were then incubated for 15 minutes at 37˚C. After 15 minutes, 2mL 1X BD PhosFlow Lyse/Fix diluted in water was added to blood. Samples were mixed well and incubated for 5 minutes at room temperature. After incubation, tubes were spun for 5 minutes at 1800rpm. The supernatant was then discarded and cells were washed 1X with 2mL 1X PBS. Samples were mixed well and spun for 5 minutes at 1800rpm. The

supernatant was then decanted. To samples, 1mL ice-cold 1X BD PhosFlow perm buffer IV diluted in 1X PBS was then added. Samples were mixed well and incubated for exactly 5 minutes at room temperature. After 5 minutes, 3mL 1X PAB was added to tubes and tubes were then spun 5 minutes at 1800rpm. The supernatant was decanted and samples were washed 1X with 1X PAB. Intracellular antibody was then added to samples and the samples were incubated 45 minutes at room temperature in the dark. Cells were washed 1X with 1X PAB. Samples were subsequently run on LSRII.

Intracellular Cytokine Staining (ICS) – PMBCs ($1X10^6$) were added to 5mL polypropylene flow tubes. Cells were washed 1X with RI0 and resuspended in 0.5mL R10. Peptides were added at desired concentrations along with costimulatory antibodies CD28pure and CD49dpure in 0.5mL R10. Samples were then incubated for 1 hour at 37˚C. After 1 hour, 1µL Brefeldin A (Biolegend) was added to each tube. Samples were then placed back at 37˚C for 8 hours. After 8 hours, samples were moved to 4˚C until staining. After incubation, ICS samples are stained normally as described above.

Cell Preparation for Microarray

Cell populations were sort purified based on phenotype and included CD8 TEM, CD4 TCM, and monoyctes. Sorted cells were collected in R10. Once purified, cells were spun down and supernatant was decanted. The cells were then resuspended in 1ml RLT buffer + 2BMe (Sigma) and placed immediately at -80˚C. Cells were then shipped to VGTI Florida for RNA isolation and microarray analysis.

CD4 TCM response to IL-7 during SIV infection – For cellular expression profiles, no less than 10,000 purified cells were resuspended in 1mL RLT buffer for RNA extraction and subsequent microarray analysis. Four cell types were purified by cell sorting: CD4 central memory T cells (CD4 TCM), CD8 TCM, CD4 T Naïve cells, and CD8 T effector memory cells (CD8 TEM). In 84 of the samples, CD4 TCM were incubated in R10 or R10 supplemented with 5ng or 50ng IL-7 for 0, 3, and 18 hours. In 77 of the samples, CD8 TCM were incubated in R10 or R10 supplemented with 5ng or 50ng IL-7 for 0, 3, and 18 hours. After the indicated time, the cells were washed with 1XPBS and resuspended in 350μL RLT buffer + 2BMe. The 46 additional samples are the single population purified cells resuspended in 1ml RLT buffer + 2BMe.

BrdU

Rhesus monkeys were administered BrdU 30mg/kg three times within 24 hours. Tissues were collected and processed for lymphocyte isolation. Cells were stained with extracellular antibodies and fixed and permeabilized as described above. Immediately after the final wash, Dnase was added to tubes. Following Dnase addition, intracellular antibodies including anti-BrdU were added and incubated as described above.

Microarray analysis

RNA was isolated using RNeasy Micro Kits (Qiagen), and the quantity and quality of the RNA was confirmed using a NanoDrop 2000c (Thermo Fisher Scientific) and an Experion Electrophoresis System. Samples (50 ng) were amplified using Illumina

TotalPrep RNA amplification kits (Ambion). The microarray analysis was conducted using 750 ng of biotinylated complementary RNA hybridized to HumanHT-12_V4 BeadChips (Illumina) at 58 °C for 20 h. The arrays were scanned using Illumina's iSCAN and quantified using Genome Studio (Illumina). The analysis of the GenomeStudio output data was conducted using the R and Bioconductor software packages. Quantile normalization was applied, followed by a $\log_2$ transformation. The LIMMA package was used to fit a linear model to each probe and perform (moderated) *t* tests or *F* tests on the groups being compared. To control the expected proportions of false positives, the FDR for each unadjusted *P* value was calculated using the Benjamini and Hochberg method implemented in LIMMA. Multidimensional scaling was used as a dimensionality reduction method in R to generate plots for the evaluation of similarities or dissimilarities between datasets. Ingenuity Pathway Analysis software (IPA, Ingenuity Systems) was used to annotate genes and rank canonical pathways. An immune response gene filter, constructed from innate and adaptive immune response gene queries of Gene Ontology (http://www.geneontology.org/), T cell activation and complement pathway genes from IPA and our own IFN- and inflammasome-response gene lists, was used where noted to reduce datasets for visualization before FDR estimation.

IL-7 ELISA

Plasma IL-7 was measured using the Quantikine HS Human IL-7 kit (RandD Systems) according to manufacturer's protocol. Briefly, previously collected plasma was thawed on ice. Once thawed, plasma was spun for 10 minutes at 10,000g at 4˚C. Plasma and

standards were incubated in the provided ELISA plate overnight at RT. After overnight incubation, wells were washed and IL-7 conjugate was added to each well. After incubation, wells were washed again and Substrate solution was added. Finally amplifier solution was added to each well followed by stop solution. Optical density was determined within 20 minutes using a microplate reader set to 490nm with wavelength correction set to 650nm.

Luminex

Plasma cytokine concentrations (excluding IL-7) were measured using the Cytokine Monkey Magnetic 29-Plex Panel Kit (Life Technologies) according to the manufacturer's instructions. This panel allowed for the quantitative determination of EGF, Eotaxin, FGF-basic, G-CSF, GM-CSF, HGF, IFN-γ, IL-1B, IL-1Ra, IL-2, IL-4, IL-6, IL-8, IL-10, IL-12, IL-15, IL-17, IP-10, I-TAC, MCP-1, MDC, MIF, MIG, MIP-1a, MIP-1b, RANTES, TNF-a, and VEGF. Briefly, previously collected plasma was thawed on ice. Once thawed, plasma was spun for 10 minutes at 10,000g at 4˚C. Sample plasma and standards were incubated with provided beads overnight at 4˚C. After incubation, detection antibody was added and incubated for 1 hour and the beads were subsequently washed. Streptavidin-RPE was added next and incubated for 30 minutes at room temperature. Finally, beads were washed and resuspended in wash buffer for acquisition using a Luminex 200 machine. Data was analyzed using MasterPlex QT and MasterPlex CT Software.

Immunohistochemistry and Quantitative Image Analysis

Immunohistochemistry was performed using a biotin-free polymer approach (Golden Bridge International, Inc.) on 5-µm tissue sections mounted on glass slides, which were dewaxed and rehydrated with double-distilled H2O. Heat induced epitope retrieval (HIER) was performed by heating sections in 0.01% citraconic anhydride containing 0.05% Tween-20 or 0.1M Tris-HCL pH 8.6 in a pressure cooker (Decloaking Chamber model DC2002; Biocare Medical) set at 122-125°C for 30 s. Slides were incubated with blocking buffer (TBS with 0.05% Tween-20 and 0.5% casein) for 10min. Slides were incubated with rabbit monoclonal anti-active caspase-3 (clone: 5A1E; Cell Signaling Technology), rabbit monoclonal anti-CD3 (clone: SP7; Thermo Scientific) or rabbit monoclonal anti-Phospho-Stat5 (Tyr694) (Clone: C11C5; Cell Signaling Technology) diluted in blocking buffer over night at 4oC. Slides were washed in 1X TBS with 0.05% Tween-20, endogenous peroxidases blocked using 1.5% (v/v) H2O2 in TBS (pH 7.4) for 10min, incubated with Rabbit Polink-2 HRP (Golden Bridge International, Inc.) according to manufacturer's recommendations and developed with Impact™ DAB (3,3′-diaminobenzidine; Vector Laboratories). Slides were washed in ddH2O, counterstained with hematoxylin, mounted in Permount (Fisher Scientific), and scanned at high magnification (x200) using the ScanScope CS System (Aperio Technologies) yielding high-resolution data from the entire tissue section. Representative regions of interest (ROIs; 500 um2) were identified and high-resolution images extracted from these whole-tissue scans. The percent area of the lymph nodes or lamina propria that stained for active

caspase-3, CD3+ T cells or Phospho-Stat5 were quantified using Photoshop CS5 and Fovea tools.

Results

Anti-IL15 specifically blocks IL-15 signaling via STAT5 phosphorylation

Our *in vitro* data suggested that IL-15 plays a considerable role in the homeostatic maintenance of NK cells and T cells in RM, but the exact function of IL-15 *in vivo* remains to be fully elucidated. Past studies in RM have used the addition of pharmacological levels of exogenous IL-15, which may or may not produce effects *in vivo* that reflect physiologic function. We therefore took an alternate approach and sought to knockdown IL-15 signaling in an effort to clarify the function of IL-15 *in vivo*. For that purpose, we developed an anti-IL-15 antibody for RM with the collaboration of Keith Reimann. The mouse, anti-human IL-15 clone, M111, which is cross reactive to rhesus IL-15, was "rhesusized" to make the antibody suitable for multiple administrations to RM. Similar to humanizing antibodies, rhesusizing the antibody entailed changing out mouse amino acid sequences for rhesus amino acid sequences in antibody constant regions and variable binding surfaces via cloning, without altering antibody affinity or specificity. We then administered three doses of either the anti-IL15 Ab or an IgG1 control antibody to healthy, adult rhesus macaques, once every two weeks (Figure 3-1).

We were unable to detect soluble IL-15 via luminex and ELISA in the plasma of most healthy rhesus macaques assayed, even prior to anti-IL-15 Ab administration because soluble IL-15 levels in plasma from these RM were very close to the limit of detection. Alternatively, to assess whether the anti-IL-15 antibody was blocking IL-15 mediated signals, phosflow analysis of STAT5 was used. At various timepoints after RM antibody dosing, we took blood samples and stimulated them *ex vivo* with increasing

concentrations of exogenous IL-15 and looked at changes in the induction of STAT5 phosphorylation in T cells. At baseline, there were no differences in the dose response curves of CD4 and CD8 TM to IL-15 between antibody treated groups. However, by day 1 post-treatment, CD4 TM and CD8 TM in WB from animals administered anti-IL15 Ab exhibited a decreased ability to induce STAT5 phosphorylation in response to exogenous IL-15 compared to control animals (Figure 3-2A). This block of CD4 and CD8 TM IL-15-mediated STAT5 phosphorylation persisted through day 14 after a single dose of anti-IL-15 Ab. Administering subsequent doses of anti-IL-15 Ab every two weeks maintained an IL-15 signal blockade throughout antibody treatment (Figure 3-2A). We estimated the half maximal effective concentration (EC50) from the IL-15 dose response curves of CD4 TM and CD8 TM for each rhesus at a given time point after anti-IL-15 dosing. Animals treated with anti-IL-15 Ab showed a statistically significant increase in CD4 and CD8 TM EC50 to IL-15 compared to IgG1 Ab treated RM.

To examine changes in the ability of specific T cell populations to respond to IL-15 and IL-7 over the course of antibody treatment, we graphed the change in the ability of a particular T cell population to respond to a single dose of cytokine, the minimal dose that elicited a maximal response in our dose response curves *in vitro*. Indeed, the response of all T cell populations to 8ng IL-15 was significantly diminished after anti-IL-15 Ab treatment compared to controls (Figure 3-2B). Interestingly, the percent of CD4 and CD8 TEM able to respond to 4ng IL-7, which is the minimal dose for a maximal response in the IL-7 dose response curves, was overall significantly increased in anti-IL-15 treated animals compared to controls (Figure 3-3). The percent of CD4 and CD8 TN,

TCM and TTM able to respond to 4ng IL-7 over the course of anti-IL15 treatment remained unchanged compared to control treated subjects. This data indicates that as anti-IL-15 Ab treatment inhibits the responsiveness of T cells to IL-15, the percent of TEM that are able to respond to IL-7 increases.

To further confirm a specific IL-15-signal blockade and determine the extent to which tissues were affected as well, we collaborated with Jake Estes to evaluate the tissues of anti-IL-15 Ab versus IgG1 control Ab treated RM via phospho-STAT5 immunostaining. It was observed that overall phospho-STAT5 staining was significantly reduced in lymph nodes (LN) from anti-IL-15 Ab treated RM compared to controls (Figure 3-4). The reduction of phospho-STAT5 in tissues after anti-IL-15 Ab treatment suggests that the antibody is effectively working to inhibit IL-15 mediated signals *in vivo*. A complete inhibition of STAT5 phosphorylation in tissues was not expected as other factors including IL-7 and IL-2, which are not blocked by the anti-IL-15 Ab, also signal via STAT5. These results combined with the phosflow data together suggest that anti-IL-15 administration was able to block IL-15-mediated signals in the peripheral blood and this effect extended into the tissues as well.

Anti-IL-15 administration results in near complete NK cell depletion

Once we confirmed that the anti-IL-15 Ab was effectively blocking IL-15-mediated signaling *in vivo*, we next sought to analyze the effect this had on lymphocyte populations throughout the body. Strikingly, NK cells were almost completely depleted after anti-IL15 Ab treatment *in vivo*. NK cell depletion was not observed at day 1 post-

treatment, but by day 7 total NK cell numbers dropped to approximately 10% of baseline levels, and were maximally depleted by two to three weeks after initiation of treatment (Figure 3-5). Although all NK cell subsets showed significant levels of depletion, NK cell populations depleted to different extents. The most abundant population of NK cells in the peripheral blood is the CD16+ CD56- cytotoxic effector NK cell population and it was depleted to the greatest extent, being over 95% depleted. The CD16- CD56- NK cells were depleted to about 25% of baseline levels, and the CD16- CD56+ NK cell populations were reduced to around 40% of baseline levels. This data supports previous data in mice that show NK cells are reliant on IL-15 *in vivo* for maintenance and function. Reliance on IL-15 does, however, vary among NK cell populations.

We observed significant depletion of NK cells in the peripheral blood over the course of anti-IL-15 Ab treatment, but we wanted to find the extent to which the antibody was penetrating tissues and depleting NK cells throughout the body. To answer this question, lymphocytes were isolated from the tissues of anti-IL-15 Ab and IgG1 control Ab treated RM at necropsy and stained to determine NK cellularity throughout the tissue. It was found that the percentage of NK cells of tissue lymphocytes was significantly reduced in all tissues examined from anti-IL-15 Ab treated RM (Fig 3-6A, B). This data along with the WB data shows that the anti-IL-15 antibody regimen was sufficient to significantly deplete NK cells throughout the entire body.

T Cell Dynamics

We next looked at the effects of anti-IL15 Ab on T cell homeostasis when administered to healthy rhesus monkeys. In response to anti-IL15 Ab treatment, CD4 and CD8 TEM populations in the peripheral blood were initially depleted to approximately 30-40% of baseline levels at day 14 compared to control treated animals (Figure 3-7). However, beginning around day 21, CD4 and CD8 TEM in the WB exhibited a significant increase in Ki-67 expression. TEM induction of Ki-67 after anti-IL-15 Ab treatment was highly unexpected because TEM induce Ki-67 expression in response to IL-15 administration. Notably, this proliferative burst of CD4 TEM and CD8 TEM was associated with a stabilization of absolute cell numbers with slow recovery towards pre-treatment levels by day 35 (Figure 3-7). TEM proliferation was also observed in BAL, with CD4 and CD8 populations significantly increasing their Ki-67 levels after anti-IL-15 Ab treatment compared to controls (Figure 3-8). Although no depletion of absolute numbers was observed for transitional phenotype cells, both CD4 and CD8 TTM populations demonstrated a significant increase in Ki-67 expression that was only slightly attenuated compared to the proliferative burst of TEM populations (Figure 3-7). TEM were also depleted in tissues of RM following anti-IL-15 Ab compared to IgG Ab treatment as shown by a significant reduction of CD3+ T cells in the colon lamina propria in RM via immunostaining (Figure 3-9). This indicates that although the homeostatic response normalized TEM blood counts, it did not completely replenish the tissue TEM compartment. There were no observed changes to either the

absolute numbers or Ki-67 expression of CD4 and CD8 TN and TCM populations after anti-IL-15 Ab treatment.

To understand where in the body TEM were proliferating in response to anti-IL-15 treatment, at the approximate peak of TEM proliferation (days 28-35) rhesus monkeys were dosed three times with BrdU within 24 hours prior to being necropsied. Tissues were harvested and lymphocytes were isolated and analyzed for BrdU incorporation. As BrdU is incorporated into actively proliferating cells, our technique of dosing with BrdU followed by immediate necropsy allowed us to detect cells that proliferated within the previous 24hrs. This offered a more accurate indication of the location of TEM proliferation than Ki-67 expression, which can be maintained for several days following cell proliferation during which time cell migration may occur (24). We observed a significant increase in BrdU incorporation of TEM most notably in the liver, lungs, and kidneys of anti-IL-15 Ab treated rhesus monkeys compared to controls (Figure 3-10). Although there are extremely limited numbers of TEM phenotype cells in lymph nodes, the few TEM that were observed displayed significantly increased BrdU incorporation in anti-IL-15 Ab treated RM compared to control treated animals. We did not observe increased TEM BrdU incorporation in mucosal tissues such as the BAL, colon, ileum, jejunum or vaginal mucosa after anti-IL-15 Ab dosing compared to controls. Taken all together, it seems that TEM proliferation is widespread, excluding mucosal tissues.

TEM proliferation is not driven FC receptor binding

We considered the possibility that TEM proliferation was indirectly being driven by anti-IL-15-immune complexes binding Fc receptors and represented an artifact of antibody dosing. To test this possibility, two animals were dosed with anti-IL-15 LALA antibody, which is the same rhesusized clone M111 that bears a two amino acid mutation at the Fc receptor-binding site rendering the site inactive. Animals dosed with the Fc-receptor binding site mutated antibody displayed similar phenotypes to anti-IL15 Ab treated animals compared to controls for all parameters assayed including IL-15 signal blockade, NK cell depletion and T cell dynamics. The anti-IL15 LALA Ab dosed animals were therefore grouped as anti-IL15 Ab treated monkeys for all analysis.

Tissues have higher caspase3 staining after anti-IL-15 antibody

We analyzed the tissues of anti-IL-15 Ab versus IgG1 control Ab treated RM to determine if there were any global changes to tissues after anti-IL-15 Ab dosing *in vivo*. The most striking change to tissues in response to anti-IL-15 Ab treatment was a significant increase active caspase-3 in multiple tissues. In both the colon and LN, the percent of active caspase-3 in the tissues increased from approximately 1% to 4% after anti-IL-15 Ab compared to IgG Ab dosing of RM (Figure 3-11, 3-12). Moreover, the increased active caspase-3 in tissues after anti-IL-15 Ab treatment was observed in areas where T cells are known to reside; in the colon, increased active caspase-3 was observed in the lamina propria, and in LN increased active caspase-3 was observed in the T cell zones. An increase in markers of cell death and pre-apoptotic cells in tissues populated

with TEM, combined with our data showing increased Ki-67 expression in TEM, together suggest that TEM are proliferating and turning over at an increased rate. Additionally supporting increased TEM turnover, TEM cell numbers in WB leveled off at approximately baseline levels, despite continued TEM proliferation, but tissues remained TEM depleted.

Microarray reveals that TEM are turning over at an increased rate

We observed that after anti-IL-15 Ab administration *in vivo*, TEM cells were induced to proliferate, but analysis of tissues showed significantly increased active caspase-3, indicating increased cellular apoptosis. To understand the overall effect of anti-IL-15 Ab treatment on CD8 TEM expression profiles, we sorted CD8 TEM from anti-IL-15 Ab and IgG control Ab treated RM before treatment and at the approximate peak of TEM proliferation, day 28. In collaboration with Rafick Sekaly, we analyzed the gene expression profiles of the CD8 TEM by microarray according to the described bioinformatic analysis (Figure 3-13). It was observed that, after anti-IL-15 Ab treatment, more CD8 TEM showed entry into cell cycle as indicated by induction of GADD45A, COX5a, and decreased expression of NFATC1 (Figure 3-14), matching our observations of increased Ki-67 staining by flow cytometry. CD8 TEM also demonstrated an increased activation status following anti-IL-15 Ab administration *in vivo*, as demonstrated by the induced T cell activation genes LAT, ITK, FYN, FKBP1A, HLA-DR, and VAV. Notably, CD8 TEM showed decreased expression of death receptor signaling genes TNFRSF1A, BIRC3, TNFRSF10A, and BCL2 and an increase in genes

NDUFA3, CYC1, NDUFV2, and PRDX5, which are associated with mitochondrial dysfunction, indicating that these proliferating TEM are dysregulated and potentially pre-apoptotic (Figure 3-14). Again, TEM demonstrated an increase in proliferation associated with an increase in markers of cell death, indicating that following anti-IL-15 Ab treatment, TEM homeostasis is dysregulated and TEM are turning over at an increased rate.

TEM become more responsive to IL-7 after IL-15 blockade

Because TEM proliferation was induced only after substantial depletion of the population, we considered that the proliferative burst of TEM was an IL-15 independent homeostatic response to keep TEM levels relatively stable in the body in the absence of IL-15 mediated signals. As there are several cytokines associated with T cell homeostasis, we thought it maybe possible that another cytokine level was changing in the absence of IL-15 that was taking over for IL-15 maintenance of T cells as a homeostatic backup and inducing TEM proliferation. To test this hypothesis we measured cytokine levels in the plasma of anti-IL-15 Ab treated RM compared to IgG Ab treated control monkeys throughout the course of treatment by luminex analysis. We found no changes in the concentrations of plasma IL-7, IL-1β, IL-2, IL-12, or TNFα after anti-IL-15 Ab administration (Figure 3-15). It should be noted that we were only able to test plasma for a panel of known cytokines that have defined reagents. Our data does not exclude the possibility that other cytokines we did not measure were changing in response to anti-IL-15 Ab administration.

Although changes in IL-7 levels were not observed in anti-IL-15 Ab treated animals, our data suggests that IL-7 still could be a factor involved in the TEM proliferative burst because an increased percentage of TEM become responsive to IL-7 after anti-IL-15 Ab dosing (Figure 3-3). To test the relevance of this observation *in vivo*, RM were administered anti-IL-15 Ab or an IgG control Ab every two weeks for 8 weeks for a total of five doses. On days 35 and 42 post antibody treatment, all RM were administered doses of IL-7. Intriguingly, after anti-IL-15 Ab dosing, CD4 and CD8 TEM showed a significant increase in absolute numbers in response to IL-7 compared to IgG control Ab treated RM (Figure 3-16). Whereas CD8 TEM absolute numbers modestly increased about two fold, CD4 TEM absolute numbers were increased 100 fold after anti-IL-15 Ab compared to IgG Ab dosing. This data confirms that both CD4 and CD8 TEM responsiveness to IL-7 changes following an *in vivo* IL-15 signaling blockade.

Other lymphocyte populations

As IL-15 depletion has not been fully described in RM previously, we examined several populations of immune cells to understand the entire effect of anti-IL-15 Ab administration *in vivo*. Absolute numbers of B cells and total B cell proliferation did not change over the course of antibody dosing (Fig 3-17). Also, T regulatory cell numbers remained constant, as did proliferation. Overall, as documented previously, these cell populations are not reliant on IL-15 mediated signals *in vivo*.

rhCMV is not reactivated after anti-IL-15 Ab treatment

TEM proliferation was prominent in the livers of anti-IL-15 Ab treated rhesus monkeys. It is known that rhCMV-specific TEM responses are high in livers as this a location of virus reactivation. We considered that in response to NK cell and TEM depletion, rhCMV may be reactivating in the livers of anti-IL-15 Ab treated RM and be driving a TEM proliferative burst. To assay for virus reactivation we measured viral load in the livers of anti-IL-15 Ab and IgG control Ab treated animals by real time PCR. However, no viral DNA could be detected in any of the livers assayed from either group of RM (Figure 3-18).

Results – Chapter 3 Figures – Anti-IL-15 Ab administration to healthy RM

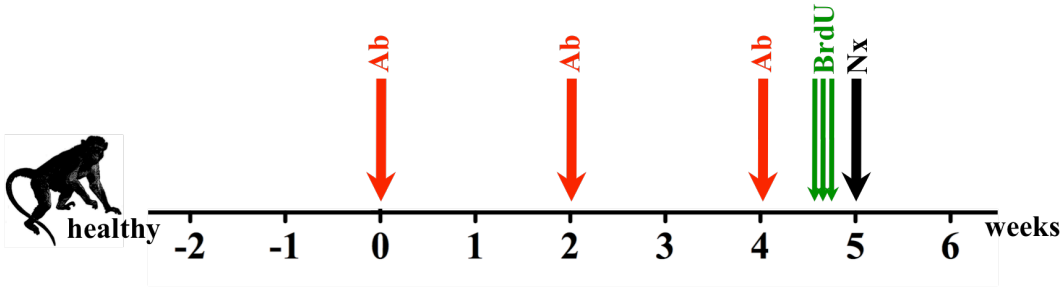

Figure 3-1 – Schematic of anti-IL-15 Ab administration to healthy RM – Healthy rhesus monkeys were administered 3 doses of anti-IL15 Ab or IgG1 control Ab biweekly. Animals were dosed one time with antibody at 20mg/kg followed by subsequent doses at 10mg/kg. RM were administered 3 doses of BrdU at 30mg/kg prior to necropsy.

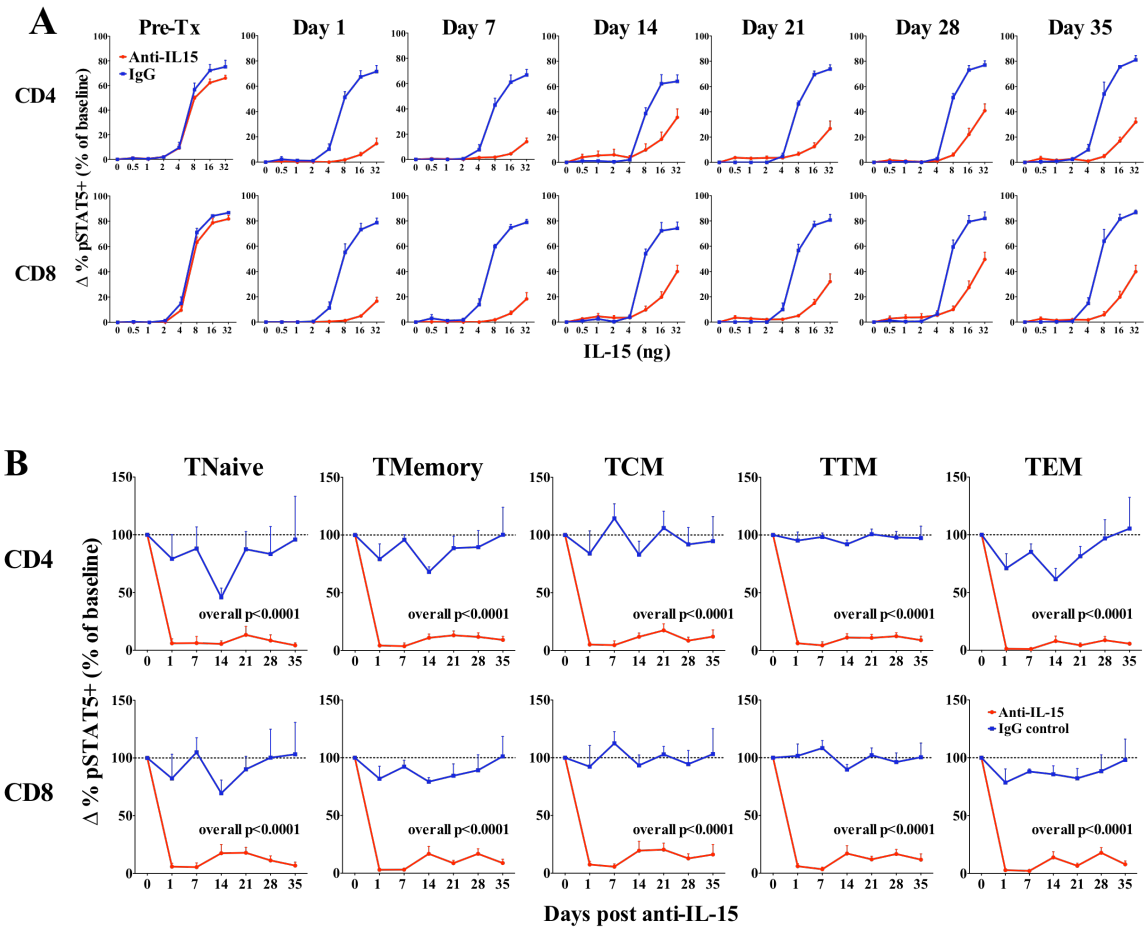

Fig 3-2 – Anti-IL-15 Ab specifically blocks IL-15 signaling via STAT5 phosphorylation - At various time points during antibody treatment, whole blood samples were stimulated *ex vivo* with cytokines, and cells were then stained and analyzed via flow-cytometry for T cell phenotype and induction of STAT5 phosphorylation. (A) Graphs show % of CD4 TM and CD8 TM that induce STAT5 phosphorylation in response to increasing concentrations (0, 0.5, 1, 2, 4, 8, 16, and 32ng) of IL-15; Anti-IL-15, N=9 (red); IgG control, N=5 (blue). (B) Shows T cell populations' change in %STAT5 phosphorylation in response to 8ng IL-15 over time. Statistical analysis evaluated using repeated measures analysis of variance (rANOVA) with Tukey-Kramer adjustment to control for multiple comparisons.

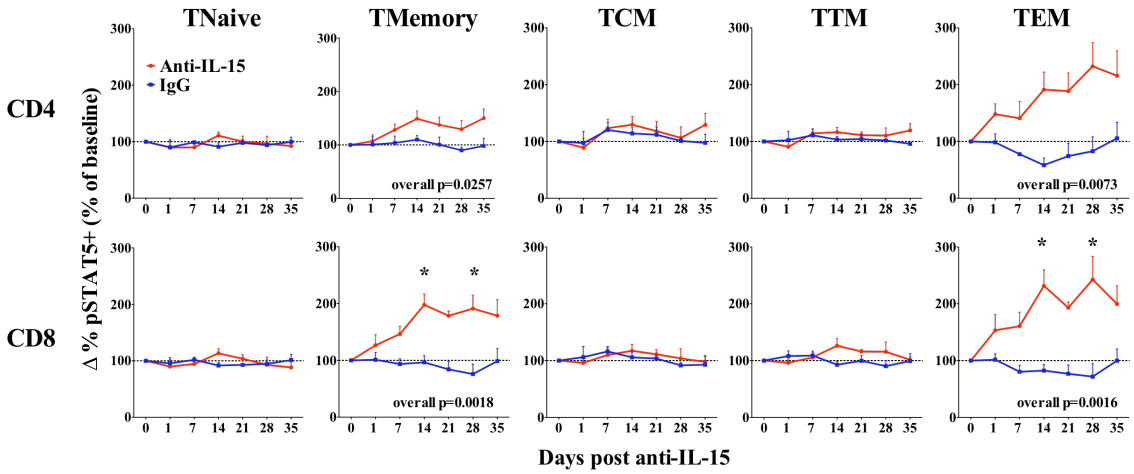

Figure 3-3 – An increased percentage of CD4 and CD8 TEM become responsive to IL-7 after anti-IL-15 Ab treatment – Post-antibody treatment, whole blood samples were taken and stimulated ex vivo with 4ng IL-7. Cells were then stained for T cell phenotypic markers and phospho-STAT5. Graphs show T cell populations' % of baseline STAT5 phosphorylation in response to 4ng IL-7 over time. Anti-IL-15 Ab (red, N=9), IgG control Ab (blue, N=7), * $p<0.05$. Statistical analysis evaluated using rANOVA with Tukey-Kramer adjustment.

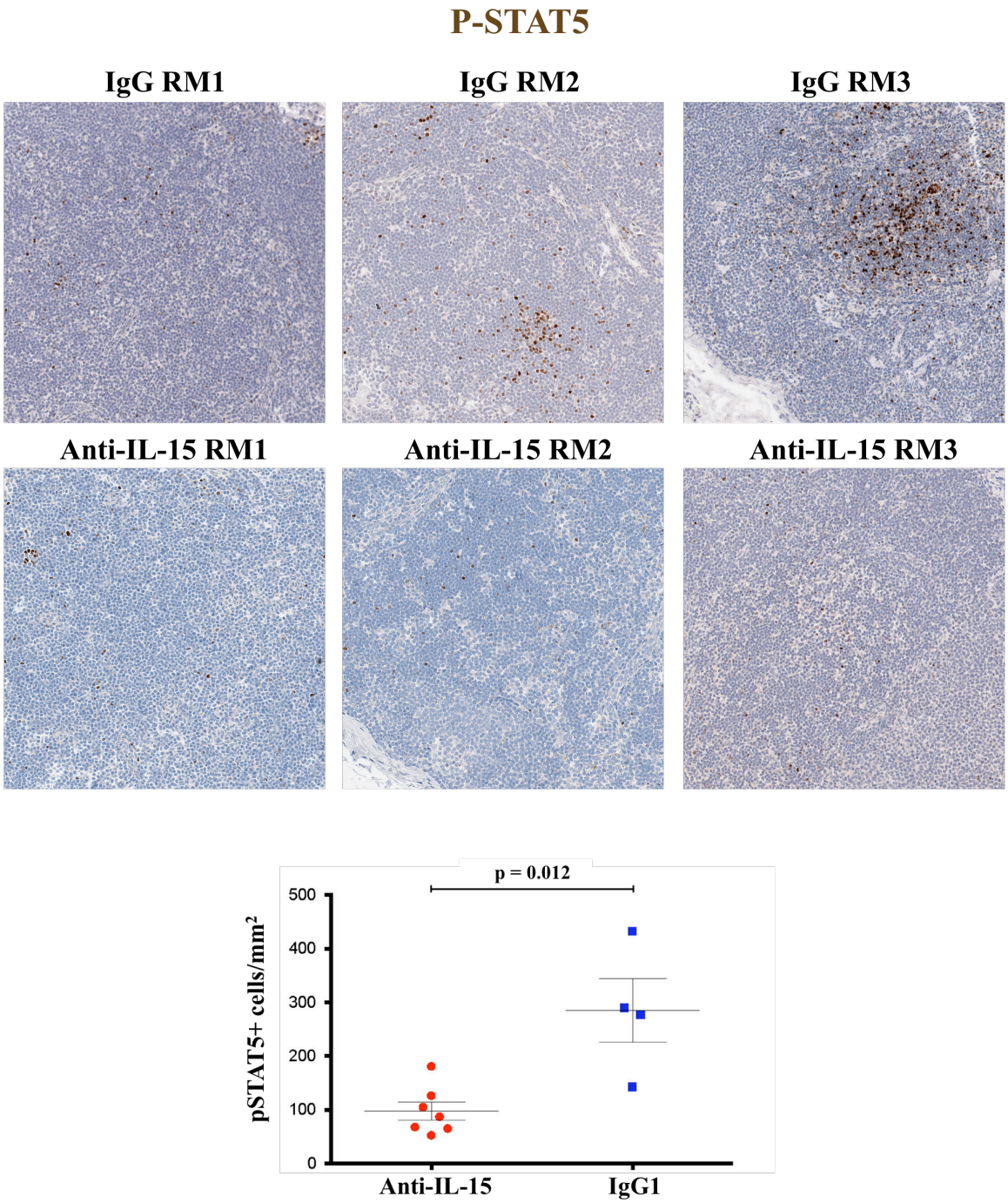

Figure 3-4 – Phospho-STAT5 is reduced in tissues after anti-IL-15 Ab treatment – Images at top show phospho-STAT5 (brown) immunostaining of axillary LN following anti-IL-15 Ab (bottom images) or IgG control Ab (top images) treatment. Graph shows quantification of the number of phospho-STAT5+ cells/mm^2 following anti-IL-15 Ab (red, N=7) or IgG1 control Ab (blue, N=4) treatment. p values based on Mann-Whitney test.

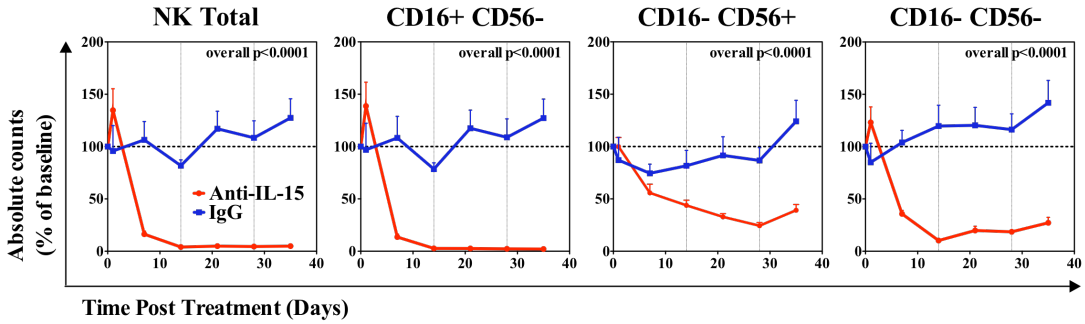

Figure 3-5 – NK cell populations are depleted in WB after anti-IL-15 Ab treatment *in vivo* – Shown are indicated NK cell populations absolute counts in WB graphed as percent of baseline. WB was stained for NKG2α, CD16, and CD56 and analyzed by flow cytometry over the course of anti-IL-15 Ab (red, N=9) or IgG1 control Ab (blue, N=5) treatment. Gray, vertical lines indicate day antibody was administered to RM. Statistical analysis evaluated using rANOVA with Tukey-Kramer adjustment to control for multiple comparisons.

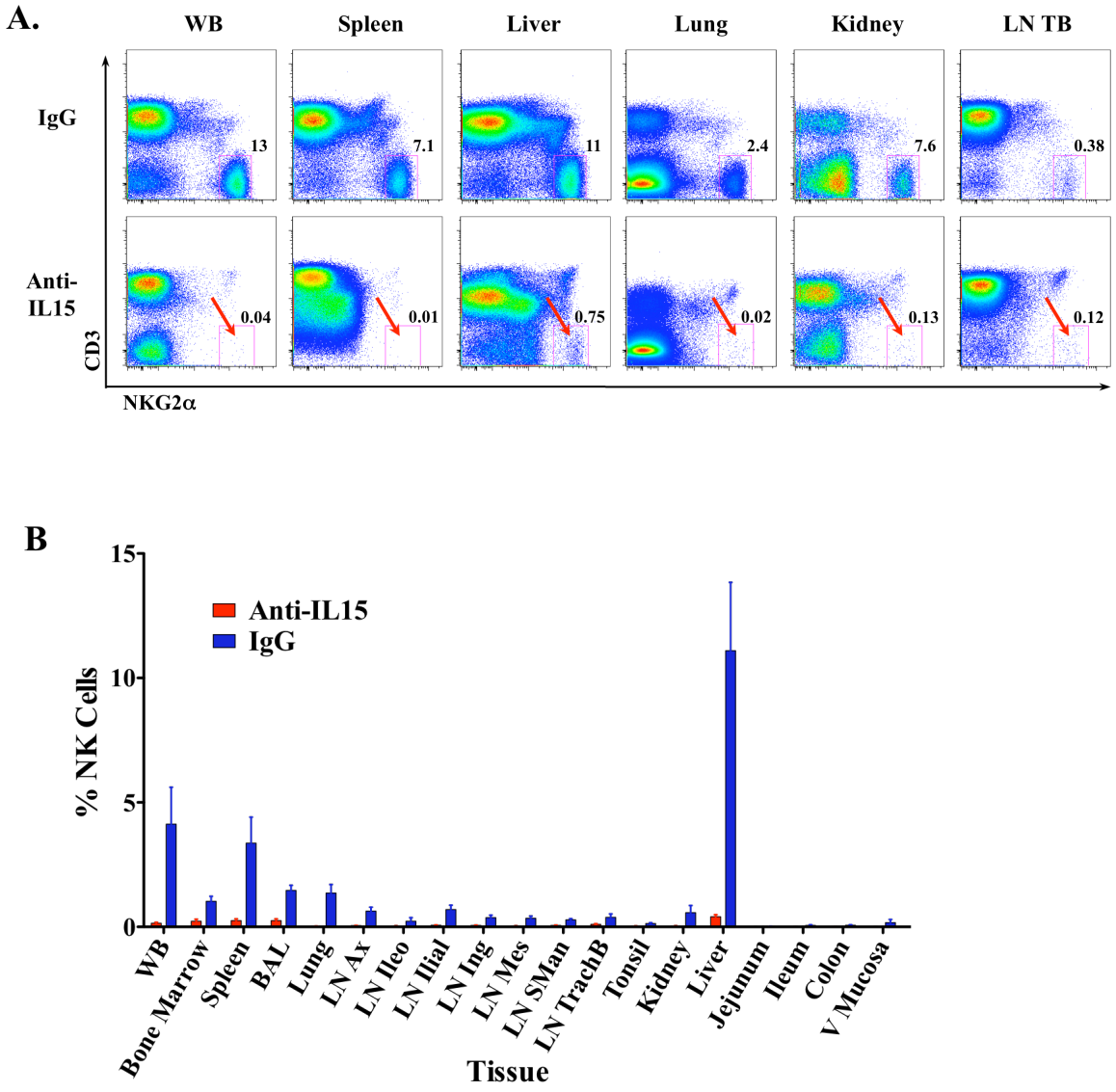

Figure 3-6 – NK cells are depleted in tissues after anti-IL-15 Ab treatment – At days 28-35 post anti-IL-15 Ab or IgG1 control Ab dosing, RM were necropsied and tissues lymphocytes were isolated. Collected cells were stained with NK cell phenotypic markers and analyzed by flow. Shown in (A) are representative animals' dot plots of NK cells in tissues and (B) are the means of NK cell percentages of total lymphocytes for each tissue from both anti-IL-15 Ab (red, N=9) and IgG control Ab (blue, N=5) treated groups.

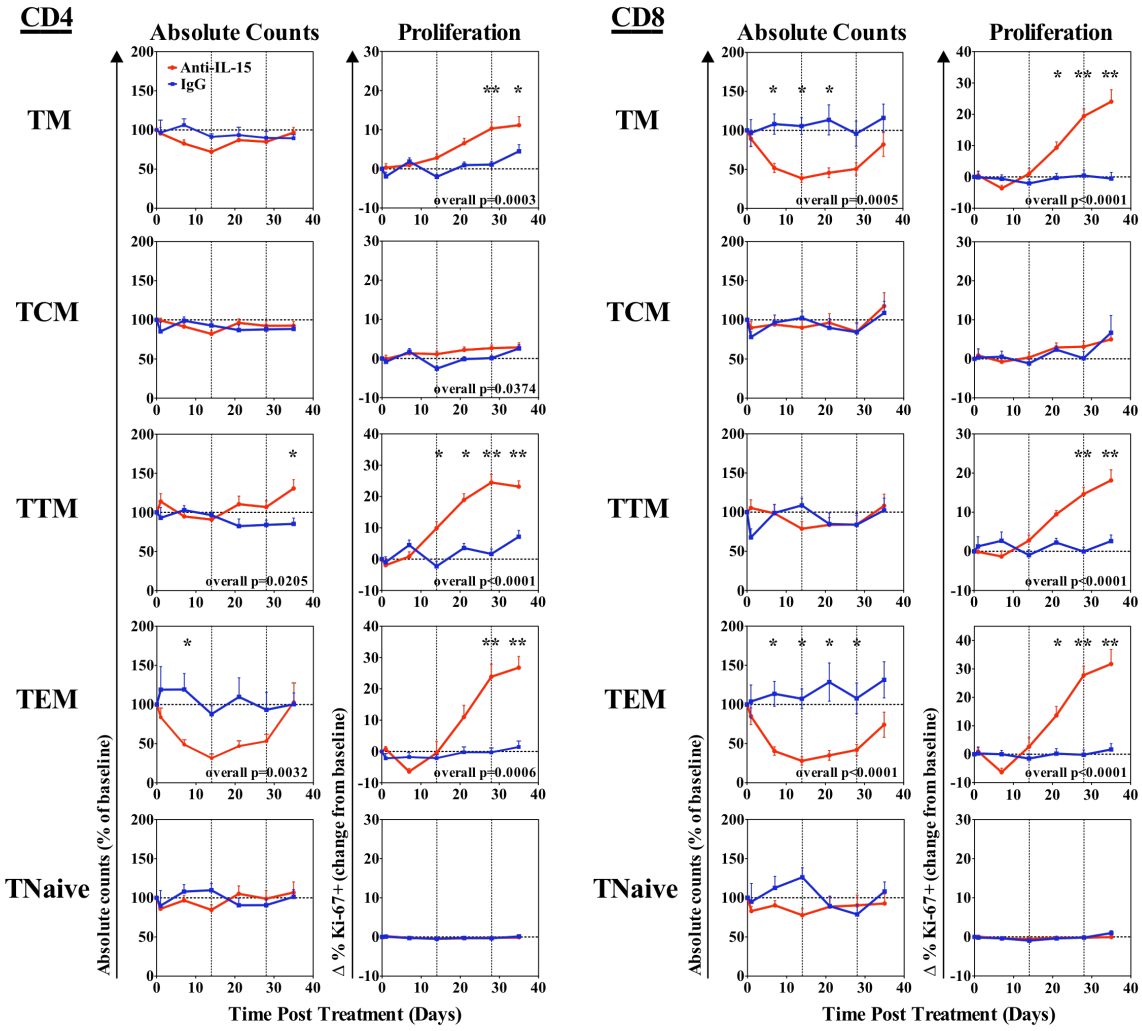

Figure 3-7 – T cell dynamics during anti-IL-15 Ab treatment in healthy RM – Shown are CD4 and CD8 T cell populations absolute counts and proliferation in WB. WB was stained for T cell markers and Ki-67 at time points post anti-IL-15 Ab (red, N=9) or IgG1 control Ab (blue, N=5) administration. Gray, vertical lines indicate the days antibody was administered to RM. * $p<0.05$, **$p<0.0001$. Statistical analysis evaluated using rANOVA with Tukey-Kramer adjustment to control for multiple comparisons.

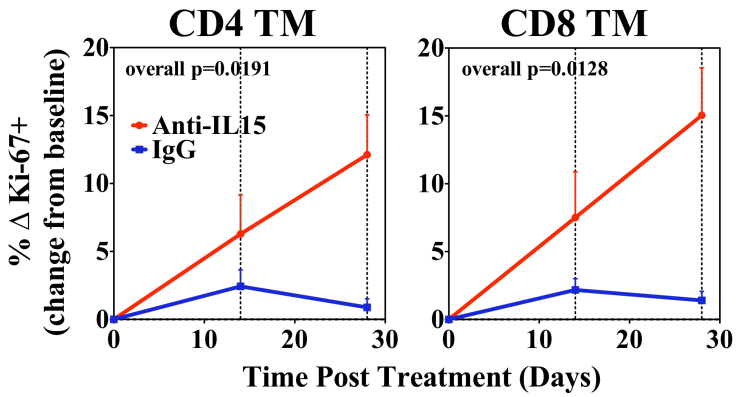

Figure 3-8 – TEM in BAL are induced to proliferate after anti-IL-15 Ab treatment – BAL was collected at indicated time points post anti-IL-15 Ab (red, N=9) or IgG1 control Ab (blue, N=5) administration and stained for T cell markers and Ki-67. Graphs show percent change in TEM Ki-67+ cells. Gray, vertical lines indicate days antibody was administered to RM. Statistical analysis evaluated using rANOVA with Tukey-Kramer adjustment to control for multiple comparisons.

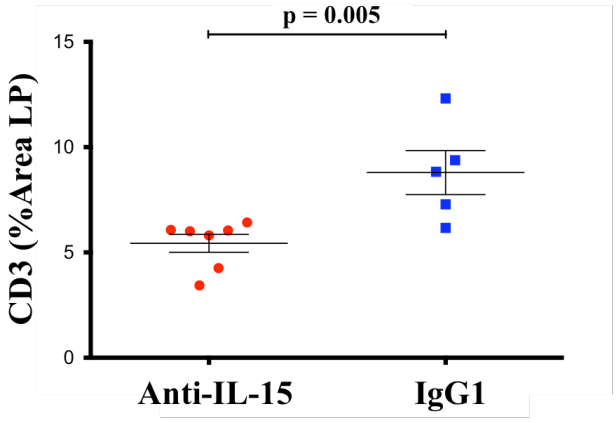

Figure 3-9 – CD3+ T cells are reduced in the colon lamina propria of anti-IL-15 Ab treated RM – Quantification of the percent area of the colon lamina propria that is CD3+ via immunostaining following anti-IL-15 Ab (red, N=7) or IgG control Ab (blue, N=5) treatment of RM. p value based on the Mann-Whitney test.

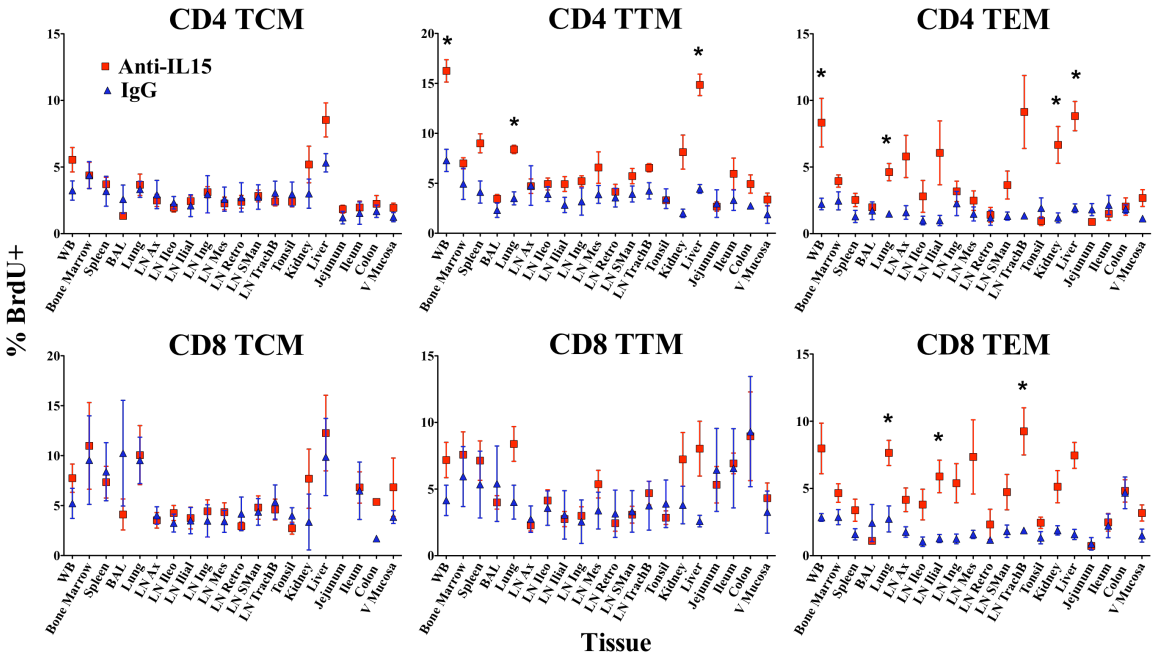

Figure 3-10 – TEM proliferation induced in response to anti-IL-15 Ab treatment is widespread, but most notable in the liver, lung, and kidney – At days 28-35 anti-IL-15 Ab (red, N=7) or IgG1 control Ab (blue, N=5) treated RM were dosed with BrdU prior to necropsy. Tissue lymphocytes were isolated and stained for T cell markers and BrdU. Graphs show T cell populations' percent BrdU+ cells. * $p<0.05$, Wilcoxon rank sum test.

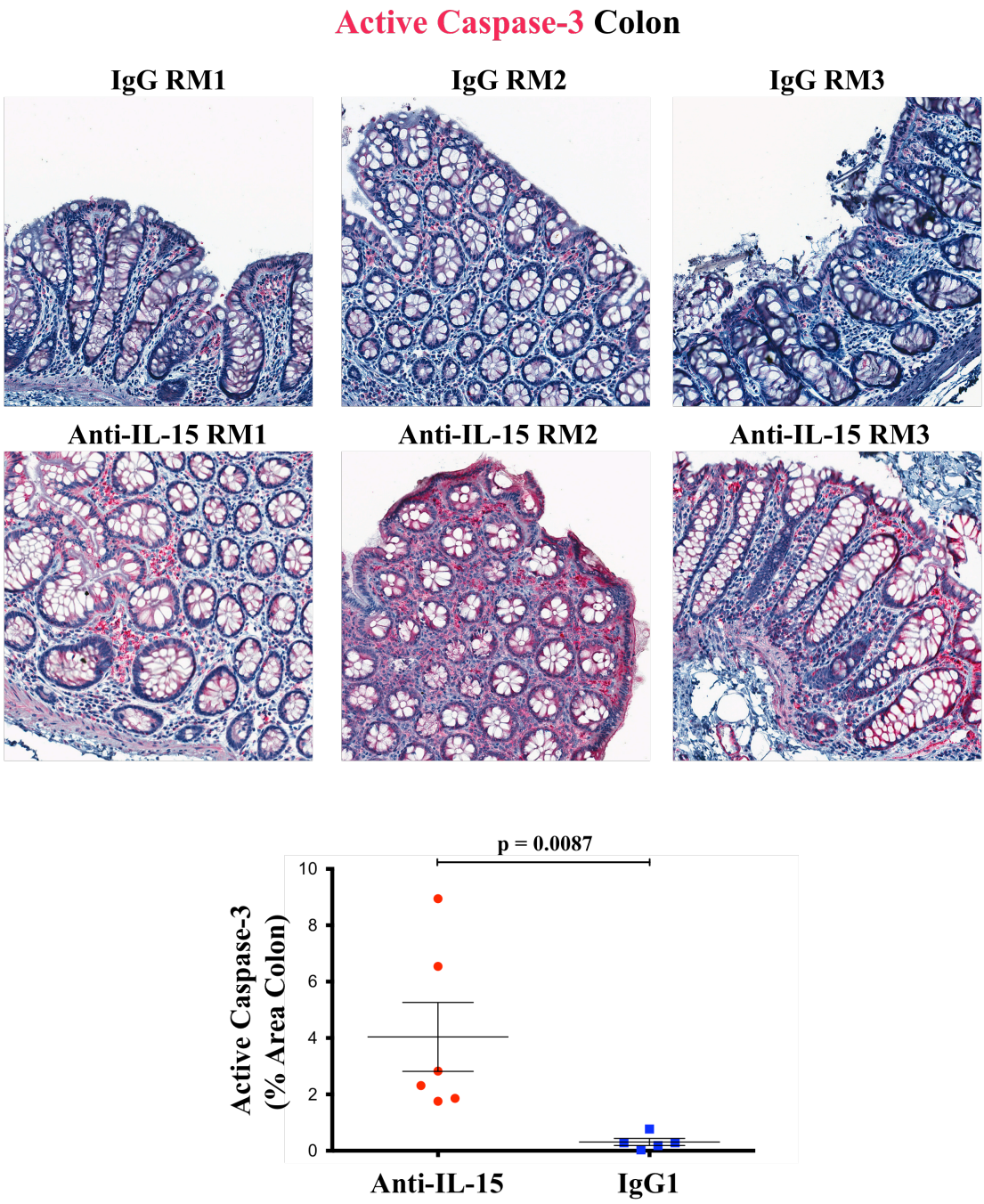

Figure 3-11 – Active caspase-3 is increased in the colon of RM treated with anti-IL-15 Ab – Images show active-caspase-3 (red) immunostaining of colon following anti-IL-15 Ab (bottom images) or IgG control Ab (top images) treatment. Graph shows quantification of the percent area of the colon that is active caspase-3 positive in anti-IL-15 Ab (red, N=6) or IgG1 control Ab (blue, N=5) treated RM. p values based on Mann-Whitney test.

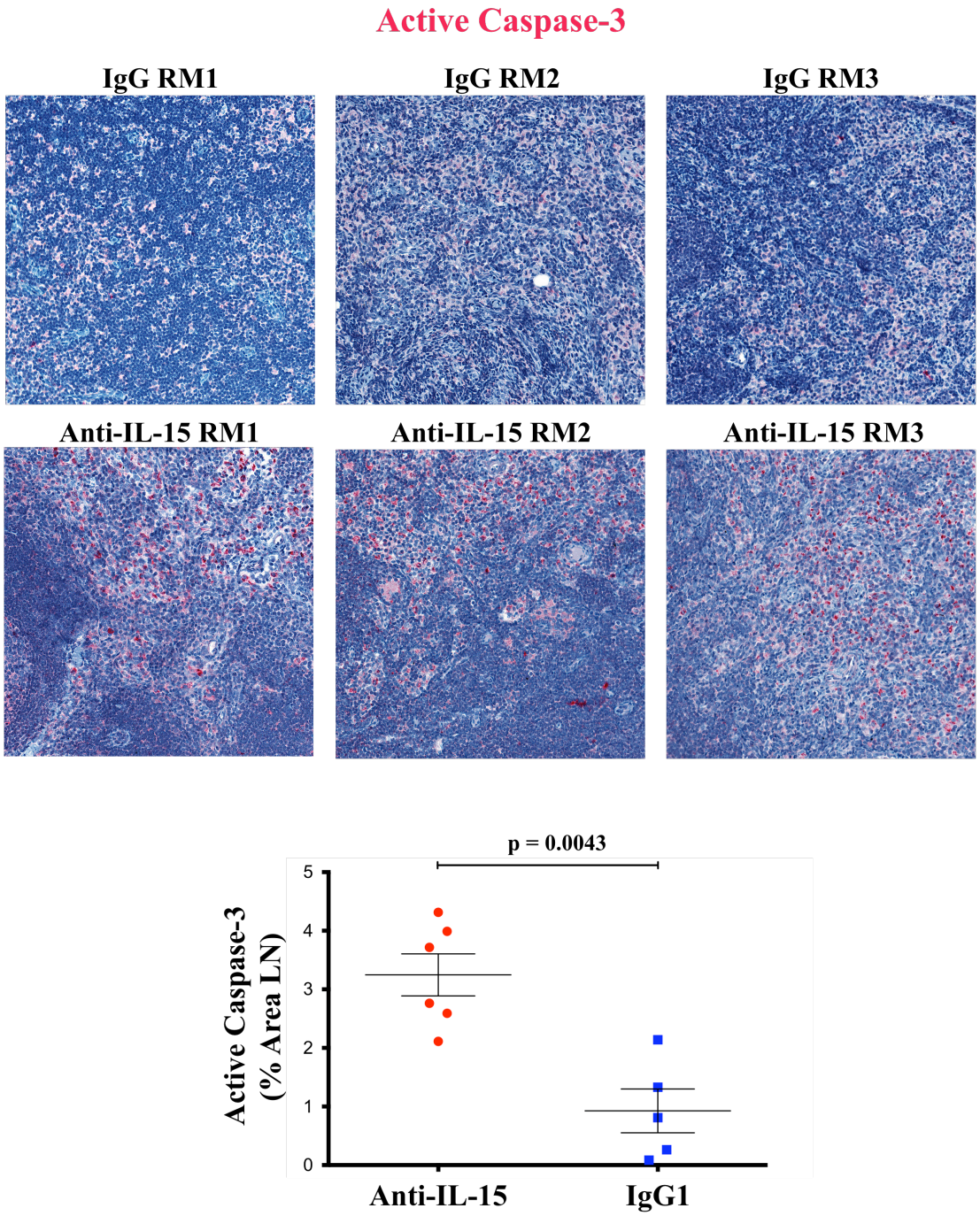

Figure 3-12 – Active caspase-3 is increased in the LN of RM treated with anti-IL-15 Ab – Images show active-caspase-3 (red) immunostaining of LN following anti-IL-15 Ab (bottom images) or IgG control Ab (top images) treatment. Graph shows quantification of the percent area of the LN that is active caspase-3 positive in anti-IL-15 Ab (red, N=6) or IgG1 control Ab (blue, N=5) treated RM. p values based on Mann-Whitney test.

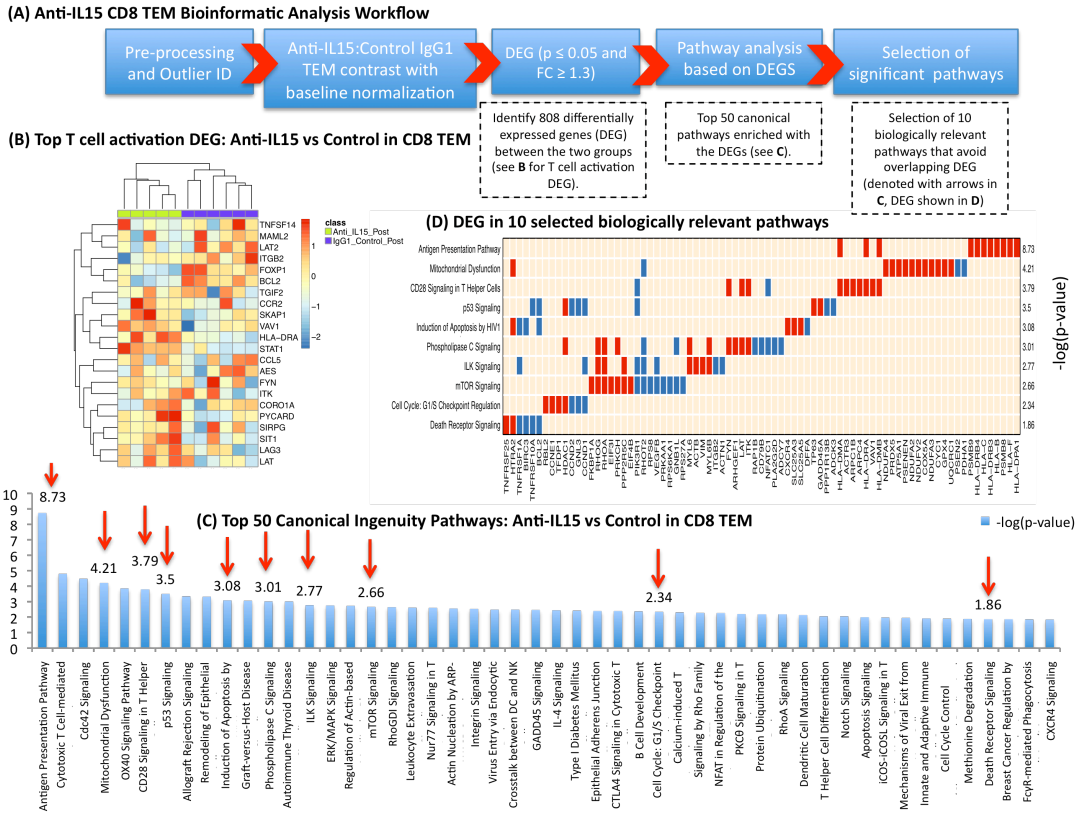

Figure 3-13 – Bioinformatic Analysis Workflow – Analysis of the genome array output data was conducted using the R statistical language (URL http://www.R-project.org/) and Bioconductor, an open source project for the analysis and comprehension of high-throughput genomic data (Bioconductor: Open software development for computational biology and bioinformatics R. Gentleman, V. J. Carey, D. M. Bates, B.Bolstad, M. Dettling, S. Dudoit, B. Ellis, L. Gautier, Y. Ge, and others 2004, Genome Biology, Vol. 5, R80). (A) Flow chart for bioinformatic selection of significantly differential genes (DEG), top pathways and selected pathways. Arrays displaying unusually low median intensity, low variability, or low correlation relative to the bulk of the arrays were discarded from the rest of the analysis. Quantile normalization was then applied to the remaining arrays, followed by a log2 transformation. For each cell type, normalized gene expression from anti-IL15 Ab treated samples (with their pre-treatment baseline expression subtracted) was contrasted with IgG1 control Ab treated control samples (with their respective pre-treatment expression removed). Only the genes that had a nominal p-value of 0.05 (by a Student's t-test) and an absolute fold change of (+/-) 1.3 were deemed as differentially expressed between the two groups (808 genes). (B) Selected T cell activation DEGs from the 808 (filter developed from Fukazawa et al., 2012) are shown in a heat map with gene expression shown as a gene-wise standardized expression (*z* score). (C) Canonical pathway analysis was performed with the IPA package from Ingenuity Systems. Only the pathways with a p-value of 0.05, as determined by Fischer exact test, were considered significant. The top 50 pathways are shown with red arrows and the –log(p-values) denoting the 10 pathways selected that are relevant to the biology in this experiment and avoid overlapping DEGs between pathways. (D) Lastly, the DEG membership of the 10 selected canonical pathways from IPA are shown (red = 2-fold or higher up-regulated, blue = 2-fold or higher down-regulated).

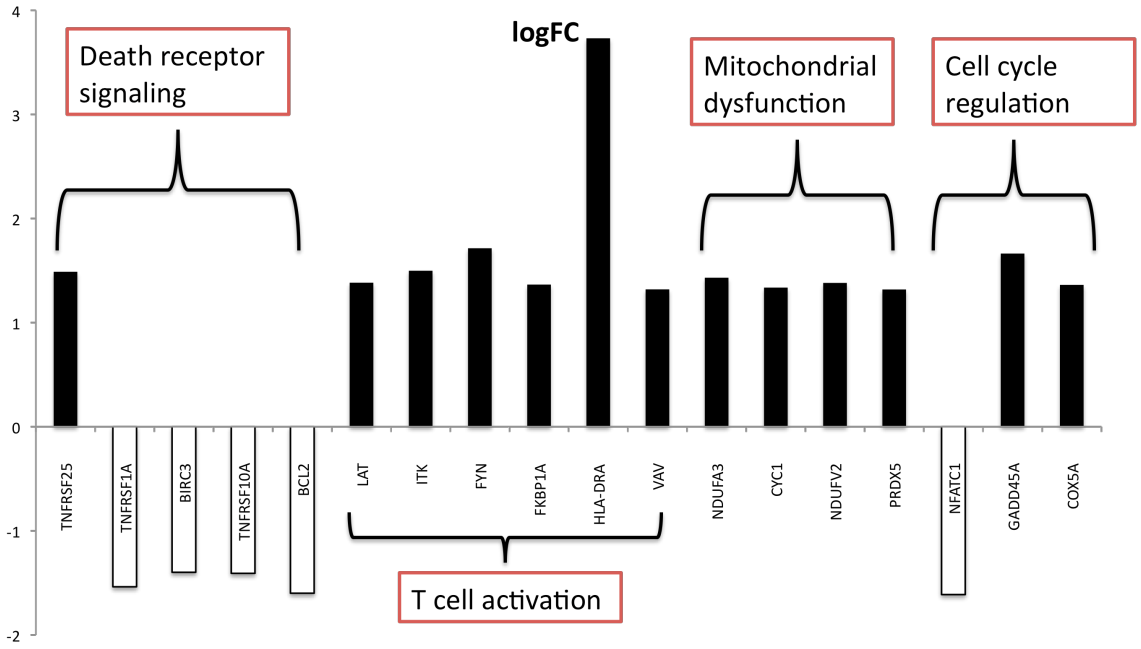

Figure 3-14 – Transcriptomic profiling after anti-IL-15 Ab treatment reveals that CD8 TEM are dysregulated and becoming apoptotic – Transcriptomic profiling performed on sort-purified CD8 TEM obtained from anti-IL-15 Ab (N=6) or IgG control Ab (N=6) treated healthy RM. Graph shows fold changes of gene expression in CD8 TEM from anti-IL-15 Ab as compared to CD8 TEM from IgG control Ab treated RM.

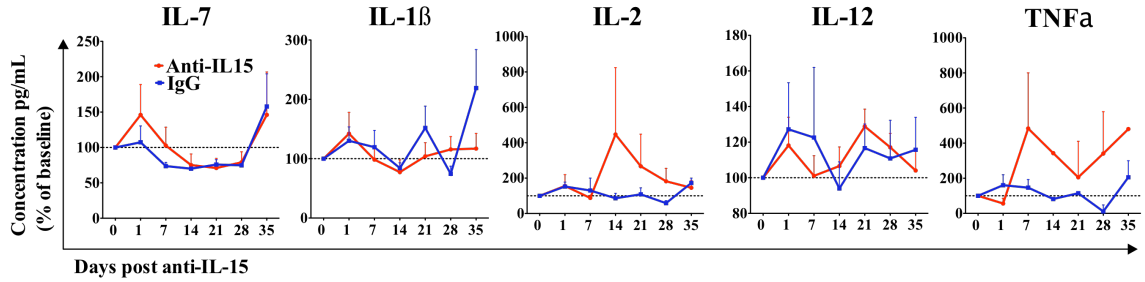

Figure 3-15 – Plasma IL-7 concentrations do not change in response to anti-IL-15 Ab treatment – Plasma collected at indicated time points post anti-IL-15 Ab (red, N=5) or IgG1 control Ab (blue, N=5) treatment was analyzed via ELISPOT for IL-7 and via luminex for IL-1B, IL2, IL-12, and TNFα. Graphs show percent of baseline concentration for each cytokine.

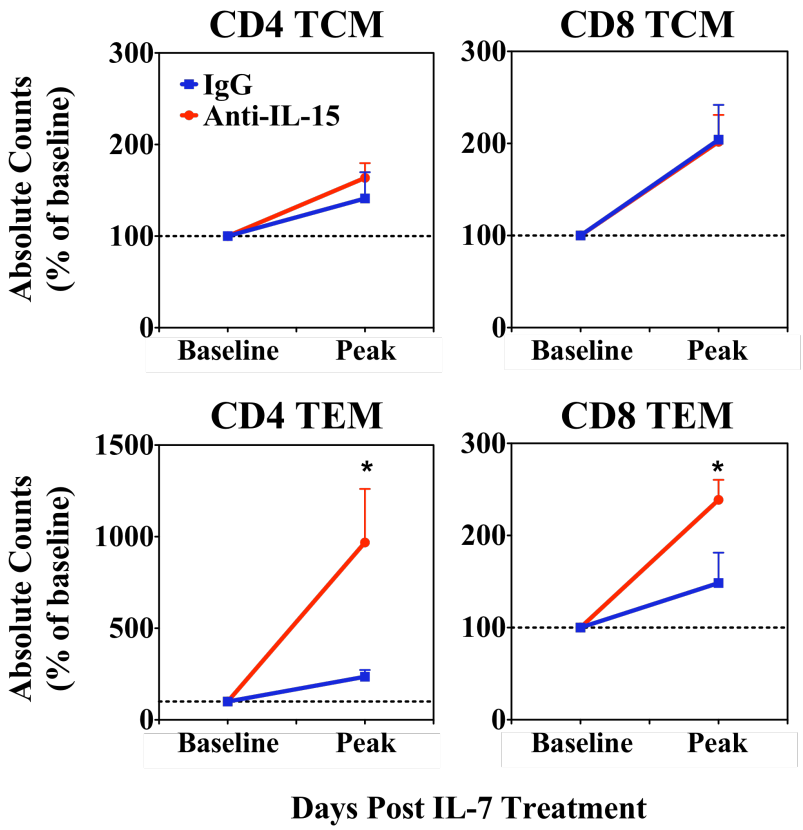

Figure 3-16 – IL-7 dosing increases the absolute numbers of CD4 and CD8 TEM in anti-IL-15 Ab treated RM – Graphs show peak change (day 14 post IL-7 dosing) in absolute counts of TCM (top) and TEM (bottom) in response to IL-7 dosing. RMs were administered anti-IL-15 Ab (red, N=6) or IgG1 control Ab (blue, N=5) biweekly for 8 weeks for a total of 5 doses. On day 35 and day 42 post anti-IL-15 Ab treatment, both groups of RM were administered doses of IL-7 subcutaneously. WB was analyzed for T cell markers over the course of treatment. * $p<0.05$, Wilcoxon rank sum test.

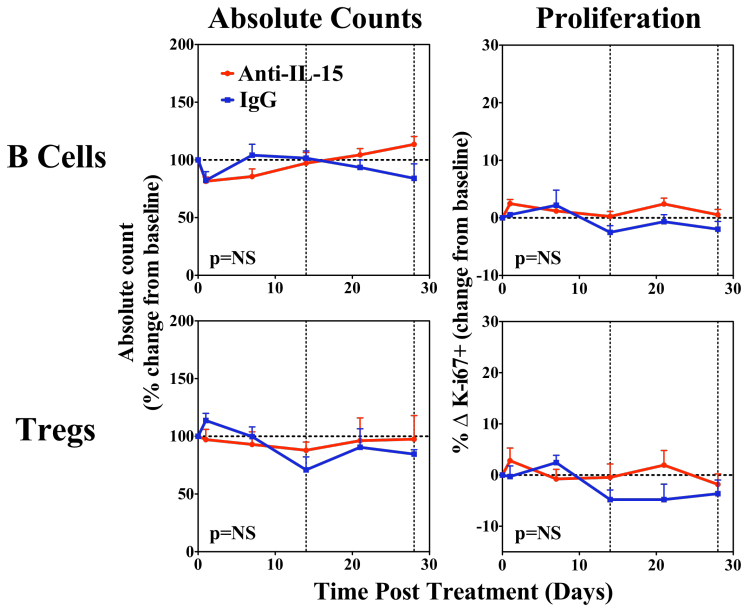

Figure 3-17 – B cell and Treg populations are not changed after anti-IL-15 Ab administration – Graphs show B Cell and Treg absolute counts and proliferation in WB following anti-IL-15 Ab (red, N=7); IgG1 control Ab (blue, N=4). treatment. WB was stained for CD20 (B Cells), CD127 and CD25 (Tregs) and analyzed via flow cytometry. Gray vertical lines indicate days antibody was administered to RM. P=NS (Not Significant) - Statistical analysis evaluated using rANOVA with Tukey-Kramer adjustment to control for multiple comparisons.

Treatment	Animal	Viral Load - Copies per µg DNA
Anti-IL15	Rh20235	< 30 copies/µg DNA
Anti-IL15	Rh23045	< 30 copies/µg DNA
Anti-IL15	Rh22196	< 30 copies/µg DNA
IgG Control	Rh22179	< 30 copies/µg DNA
IgG Control	Rh24271	< 30 copies/µg DNA
IgG Control	Rh19913	< 30 copies/µg DNA

Figure 3-18 – rhCMV DNA was not detected in the livers of anti-IL-15 Ab treated RM - RNA isolated from the livers of anti-IL-15 Ab or IgG1 control Ab was analyzed via real-time qPCR for rhCMV viral DNA.

Discussion

To characterize the role of IL-15 *in vivo,* we used the approach of administering a rhesusized anti-IL-15 Ab to healthy RM to understand how an IL-15 signal blockade would affect lymphocyte homeostasis in a healthy immune system. Similar to previous studies in humans and rhesus macaques, anti-IL-15 antibody treatment was well tolerated by all RM, with no adverse side effects observed after multiple dosing (130, 131). Moreover, *in vivo* anti-IL-15 Ab administration to RM effectively neutralized IL-15 signaling, causing a significant decrease in STAT5 phosphorylation in tissues as was verified by phosflow and immunostaining assays. Thus, our studies support the use of anti-IL-15 Ab *in vivo* in RM, where it may have parallels to dosing in humans.

Anti-IL-15 Ab administration to healthy RM caused a significant depletion of NK cells in the WB and tissues of RM, which persisted over the course of antibody treatment. Our data confirms in rhesus macaques what previous studies have shown in other species; IL-15 mediated signaling is mandatory for NK cell generation and maintenance *in vivo* (99, 101, 122, 123, 130). Although all RM NK cell subsets were dependent on IL-15, the CD16+ CD56- NK cell population was most reliant on IL-15 mediated signaling, an observation made in a previous macaque study (114). Notably, we found that the CD16- CD56+ NK cell subset, which was the only subset responsive to IL-7, was the least depleted NK cell subset, suggesting that this population may receive homeostatic signals from IL-7 in the absence of IL-15. The ability of anti-IL15 Ab to practically eliminate NK cells throughout the peripheral blood and tissues of RM make it a valuable tool to test the various roles of NK cell function in health and disease.

Anti-IL-15 Ab treatment of healthy rhesus macaques revealed several aspects of TM homeostasis. Our *in vitro* data showed that IL-15 can drive the proliferation and differentiation of TN and TCM to TEM, an observation which has been reported in the literature (25, 110). Thus, in the absence of IL-15 mediated signaling, we may have expected an increase in TN or TCM absolute numbers as fewer of these cells were induced to differentiate to TEM. However, our data administering anti-IL-15 Ab to RM showed no change to TN or TCM absolute numbers or Ki-67 expression in WB over the course of treatment. Thus, TN and TCM differentiation to TEM may be an *in vitro* artifact caused by physiologically irrelevant high doses of cytokine. We did observe an initial decline in TEM absolute numbers following anti-IL-15 Ab treatment, which may in part be due to decreased production of TEM from recently differentiated TN and TCM. It is therefore possible that IL-15 is inducing some TEM differentiation from TN and TCM *in vivo*. It is more likely, however, the decline in TEM absolute numbers is caused by decreased viability of TEM.

Interestingly, anti-IL-15 Ab treatment of healthy rhesus macaques revealed a unique facet of TEM homeostasis. In the absence of IL-15 signaling, TEM numbers initially declined to approximately 30-40% of baseline levels. Strikingly, after two weeks of anti-IL-15 Ab dosing, TEM exhibited a burst of proliferation that corresponded with an increase in cell absolute numbers back to pre-treatment levels in WB. Our data suggest that TEM proliferation represents a homeostatic response to declining absolute numbers rather than the anti-IL-15 Ab exhibiting an activating role *in vivo*. Previous studies have reported that although some antibodies against γc cytokines displayed

blocking effects *in vitro*, the same antibodies became activating *in vivo* and amplified cytokine mediated signaling (159-164). Notably, in cases where an antibody against a γc cytokine demonstrated *in vivo* cytokine signal amplification, all observed *in vivo* effects were activating with no blocking effects. Our anti-IL-15 Ab, in contrast, showed blocking effects *in vivo,* such as decreased phospho-STAT5 levels, NK cell depletion, and T cell depletion, thus confirming our anti-IL-15 Ab caused an IL-15 signal blockade *in vivo*. We also considered that T cells maybe indirectly induced to proliferate in response to anti-IL-15 Ab forming immune complexes that stimulate Fc receptors. To test this possibility we administered the same anti-IL-15 Ab with a mutated Fc receptor-binding site and observed this had no effect on antibody mediated IL-15 signal blockade, T cell or NK cell dynamics. We thus concluded that the TEM proliferation observed two weeks following anti-IL-15 Ab treatment was not an artifact of the antibody dosing itself, but rather indicated a separate homeostatic event.

We considered that, during anti-IL-15 Ab administration, a homeostatic factor other than IL-15 maybe inducing TEM proliferation as a backup system to maintain population numbers *in vivo* in the absence of IL-15 signaling. Measurements of plasma cytokine levels revealed no changes in other known immune-modulating cytokines including IL-7, TNFα, and IL-12. Interestingly, despite the fact that IL-7 levels were not changed in the plasma of anti-IL-15 Ab compared to IgG control Ab treated RM, our data suggest that IL-7 could be involved in the observed homeostatic TEM proliferation. Our phosflow data revealed that a significantly increased percent of both CD4 and CD8 TEM were able to induce STAT5 phosphorylation in response to IL-7 *ex vivo* after anti-IL-15

Ab treatment compared to control Ab treatment. Confirming this observation *in vivo*, when anti-IL-15 Ab treated RM were dosed with IL-7, CD4 and CD8 TEM absolute numbers significantly increased compared to IgG control Ab treated RM dosed with IL-7. Interestingly, a previous study in RM showed that *in vivo* JAK3 inhibition caused CD8 and CD4 T cell depletion, but T cell numbers only rebounded after cessation of inhibitor dosing (129). This study suggests that a separate JAK3 mediated signaling event, potentially IL-7 signaling, may be involved in the proliferation and accumulation of CD4 and CD8 TEM cells after IL-15 signal blockade in our system. Taken together and in line with our *in vitro* signaling data, it is likely that TEM are able to receive homeostatic signals from both IL-15 and IL-7 *in vivo* that help maintain TEM numbers despite immune system perturbations.

We further characterized the anti-IL-15 Ab induced TEM proliferation by identifying where in the RM TEM were proliferating. To that end, we dosed RM with BrdU at the peak of anti-IL-15 Ab induced TEM proliferation and immediatedly harvested tissues to monitor BrdU incorporation, and thus proliferation of TEM throughout the body. We observed significantly increased proliferation of TEM in WB, LN, kidney, lung, and liver, but we did not observe increased TEM BrdU incorporation in mucosal sites such as the BAL, colon, jejunum, ileum, or vaginal mucosa. This restriction of the homeostatic TEM proliferation to select tissues and organs further implicates that IL-7 is involved in the TEM homeostatic proliferative response. Although stromal fibroblastic reticular cells in lymphoid organs have been observed as primary producers of IL-7 (165, 166), IL-7 expression has also been detected in liver and kidney

tissue as well (167). Thus, TEM proliferation was observed primarily in sites known to produce IL-7.

Because TEM proliferation was widespread in the body, we used immunostaining to visualize multiple tissues throughout the body to help identify any systemic phenotypic effects that were associated anti-IL-15 Ab compared to IgG1 control Ab treatment in RM. Interestingly, after anti-IL-15 Ab administration, we observed a significant increase of active caspase-3 staining in tissues of RM compared to IgG control Ab dosing. Active caspase-3 has been shown to be a cellular mediator of apoptosis, likely indicating that cell death is increased in multiple RM tissues after IL-15 signal blockade (168).

An increase in active caspase-3 expression, indicating widespread cellular apoptosis was initially surprising because we observed the induction of TEM proliferation and rebound of absolute numbers in WB suggesting that the TEM population was receiving homeostatic signals that were supporting their renewal after depletion following IL-15 signal blockade. However, despite accumulation of TEM absolute numbers to baseline levels in WB, TEM continued to proliferate throughout anti-IL-15 Ab administration potentially suggesting the population numbers were unstable. Furthermore, TEM remained relatively depleted in some tissues such as the colon following anti-IL-15 Ab treatment and TEM homeostatic proliferation. In an effort to understand these observations, we used microarray to analyze TEM expression profiles at the peak of their proliferative response to anti-IL-15 Ab compared to IgG control Ab administration. We observed an upregulation of activation and cell cycling genes indicating the cells had been induced to proliferate. Interestingly, there was also an

increase in mitochondrial dysfunction genes associated with a deficit in cell energy. Our data thus suggests that TEM are becoming activated and entering into cell cycle, but once into cell cycle the TEM do not have adequate energy to complete replication and become pre-apoptotic; taken together, this data indicate that TEM are turning over at an increased rate.

From our experiments administering anti-IL-15 Ab to RM, we observed that *in vivo*, IL-15 primarily functions to maintain effector lymphocyte homeostasis. IL-15 supports NK cell generation and survival in RM and IL-15 supports normal TEM homeostasis *in vivo*. In the absence of IL-15 mediated signaling, TEM numbers are maintained, but TEM exhibit a high-turnover homeostasis.

Chapter 4 – Anti-IL-15 Ab administration to SIV-infected RM

Contribution

I managed tissue processing of RM belonging to Picker cohort 167, which administered anti-IL-15 Ab to chronically SIV-infected RM. Additionally, I performed experiments and analyzed data included in figures 4-1, 4-2, 4-3, 4-4, 4-5, 4-6, 4-7, and 4-9. Afam Okoye managed both Picker cohorts 167 and 183 under the guidance of Louis Picker. Experiments of Picker cohort 183, which administered anti-IL-15 Ab to acutely SIV-infected RM, were performed by Afam Okoye's team in Louis Picker's lab. Picker cohort 183 experiments are shown in figures 4-10, 4-11, 4-12, 4-13, 4-14, 4-15, 4-16, 4-17, 4-19, and 4-20. Stained cells from both picker cohorts 167 and 183 were collected on an LSR II by the LSR team in Louis Picker's lab. RM were cared for by ONPRC DAR technicians and staff. All surgical procedures including antibody dosing, necropsy, and harvesting of tissues, was performed by veterinarians and/or veterinary assistants from Michael Axthelm's laboratory or from ONPRC DAR. Additionally, RM SIV plasma viral loads were measured by outside collaborators Mike Piatak and Jeff Lifson (Figures 4-8 and 4-18).

Abstract

Increased IL-15 levels have been observed following pathogenic HIV/SIV-infection, and IL-15 has been implicated in the pathogenic hyperimmune activation that characterizes HIV/SIV infection. IL-15 activity might provide benefit to an HIV/SIV infected host by support of anti-viral T and NK cell effectors, and/or contribute to HIV/SIV pathogenesis by support of hyperimmune activation. To better understand the role of IL-15 in pathogenic SIV-infection, we first treated 18 chronically SIVmac239-infected RM with 6 doses of the rhesusized anti-IL15 antibody, M111, (N=9) or IgG isotype control antibody (N=9) biweekly, over a 10-week period. We next investigated the effect of anti-IL-15 Ab dosing on acute SIV infection by administering 23 RM anti-IL-15 M111 (N=15) or IgG isotype control (N=8) antibody before and up to 8 weeks post SIVmac239-infection. In both cohorts, anti-IL15 Ab was highly efficient at neutralizing IL-15 signaling *in vivo* and caused a near complete depletion of NK cells in the blood and tissues. Throughout anti-IL-15 Ab dosing, CD4 and CD8 TEM exhibited a high-turnover homeostasis, but long-term CD4 TEM absolute counts in blood and tissues remained unchanged compared to IgG control Ab treatment during both chronic and acute SIV-infection. Despite these notable changes to immune cell populations, viral replication rates and disease progression during chronic and acute SIV infection were comparable to those of control animals. These studies suggest that increased IL-15 levels during SIV infection do not play a central role in driving disease progression and that NK cells do not play a significant role in either controlling SIV replication or promoting SIV pathogenesis.

Introduction

Studies have implicated that CD4 T cell depletion during HIV/SIV pathogenesis is caused not only by direct virus induced cell death, but also by a homeostatic dysregulation of the CD4 T cell population over time. The common γc cytokine IL-15 is known to regulate memory T cell homeostasis and has been implicated in the pathogenic hyperimmune activation that characterizes HIV/SIV-infection. It has been observed that during acute HIV and SIV infection, IL-15 levels are significantly increased (111, 135, 139). It is unclear, however, whether increased IL-15 levels play a role in exacerbating HIV/SIV disease or promoting immunity.

Several lines of evidence support a role for IL-15 in promoting immunity during HIV/SIV infection. First, IL-15 stimulates the expansion of virus-specific T cell responses (25, 111, 112, 118, 119, 141). Many recent studies administering IL-15 as an adjuvant during HIV/SIV vaccination protocols have demonstrated that IL-15 increased viral-specific T cell responses during T cell priming (142-152). Additionally, the ability of IL-15 to differentiate, expand and maintain the viability of CD4 TEM may help preserve this population after viral depletion. Further suggesting that increased IL-15 does not worsen SIV pathogenesis, it was shown that short term IL-15 treatment did not change the SIV plasma viral load of either ART treated or untreated SIV-infected RM (25). Administration of IL-15 to chronically SIV-infected macaques did not result in changes to viral loads either (141, 153). Similarly, a JAK/STAT inhibitor administered to chronically SIV-infected RM induced modest, transient increase to viral load (128). It therefore remains uncertain whether increased IL-15 levels protect against HIV/SIV

disease progression through support of anti-viral effectors such as CD8 T cells and NK cells and through support of CD4 TEM populations numbers by inducing CD4 T cell differentiation.

Alternatively, IL-15 may play a role driving HIV/SIV pathogenesis. By differentiating and expanding CD4 TM populations and, in particular, up-regulating the SIV/HIV co-receptor CCR5, IL-15 may simply produce more targets for SIV/HIV and contribute to the depletion of central memory T cell populations. In this regard, administration of IL-15 to chronically SIV-infected rhesus monkeys on ART delayed viral suppression and did not reconstitute CD4 T cells at mucosal sights (153). Moreover, administration of IL-15 to rhesus macaques during acute SIV infection increased viral set point and accelerated disease progression despite higher SIV-specific CD8 T cell responses (112). Increased IL-15 cytokine concentrations have been correlated to increased viral loads (111, 135, 139). One study measured significantly higher plasma IL-15 levels during acute SIV infection, which correlated with increased immune activation and increased susceptibility of CD4 TM to SIV infection (111). Indeed, incubation of CD4 T cells with IL-15 increased the infection rate of CD4 T cells by SIV *in vitro* (111). It should be noted that despite the observed correlation between IL-15 and disease outcome, Okoye et al. documented that CD8 depletion of SIV infected RM resulted in a spike of IL-15 that caused dramatic CD4 TEM expansion. While the CD8 depleted monkeys succumbed to rapid disease progression, blockade of IL-15 inhibited the CD4 TEM proliferation, but did not prevent rapid disease progression (154).

Our *in vitro* data described in Chapter 2 suggested that RM IL-15 is involved in the homeostasis of NK cells and both CD4 and CD8 TM cells. Additionally, our data predicted that T cell dependence on IL-15 varies with the differentiation status of the T cell population, and that IL-15 is a cytokine that primarily supports effector phenotype T cell populations' homeostasis and differentiation. In our experiments administering anti-IL-15 Ab to RM described in Chapter 3, we confirmed that *in vivo* IL-15 supports NK cell generation and survival in RM, and IL-15 supports normal TEM homeostasis. In the absence of IL-15 mediated signaling, TEM numbers were initially depleted, but TEM exhibited a high-turnover homeostasis that was associated with normalized TEM absolute numbers. Our data supports that *in vivo* IL-15 primarily functions to maintain effector lymphocyte homeostasis. Because IL-15 is a crucial regulator of CD4 and CD8 TEM and NK cell homeostasis, we wanted to understand how increased IL-15 levels during pathogenic SIV-infection of RM were affecting CD4 TM homeostasis and SIV pathogenesis. In this chapter we investigated the role of IL-15 in pathogenic SIV-infection by treating both chronically and acutely SIV-infected RM with anti-IL-15 Ab or an IgG control Ab.

Materials and Methods

Animals

A total of 45 male and female adult Indian-origin RMs (*Macaca mulatta*) were used in this study. For chronic SIV-infection studies, 22 male and female adult, chronically SIVmac239-infected RM were used. RM were infected with SIVmac239 for 200-600 days prior to use in this study. Animals were inoculated with SIVmac239 via various routes and doses. SIV-dose administration ranged from 50 TCID50 – 3000 TCID50 and included rectal, vaginal and intravenous inoculations. For acute-phase studies, twenty-three healthy, adult RMs were used. Seven RM were administered three doses of anti-IL-15 Ab prior to SIV-infection, eight RM were administered 8 doses of anti-IL-15 Ab prior to and during acute SIV-infection, and eight RM were administered 8 doses of IgG control Ab prior to and during acute SIV-infection. Antibody was administered once every two weeks, first at 20mg/kg and subsequent doses were administered at 10mg/kg. At day 42 post-antibody administration, all 23 RM were inoculated intra-rectally with a high titer dose of SIVmac239 at 3000 TCID50. All RM were housed at the Oregon National Primate Research Center according to standards of the Animal Care and Use Committee and the NIH Guide for the Care and Use of Laboratory Animals.

Flow Cytometric Analysis

Polychromatic (8-12 parameter) flow cytometric analysis was performed on an LSR II instrument (BD) using Pacific Blue, AmCyan, FITC, PE, PE-Texas red, PE-Cy7, PerCP-Cy5.5, allophycocyanin (APC), APC-Cy7, and AlexaFlour 700 as the available

fluorescent parameters. Instrument set up and data acquisition procedures were performed as previously described (155). List mode multi-parameter data files were analyzed using FlowJo software. Criteria for delineating lymphocyte cell subsets: TN (live small lymphocytes, CD3+, CD28mid, CD95low, CCR7+, CCR5-); TCM (live small lymphocytes, CD3+, CD28high, CD95high, CCR7+, CCR5-); TTM (live small lymphocytes, CD3+ CD28high, CD95high, CCR7- and or CCR5+); TEM (live small lymphocytes, CD3+, CD28-, CD95high, CCR7-); Treg (CD3+, CD4+, CD25+, CD127mid); NK cells (live small lymphocytes, CD3-, CD20-, CD8bright, NKG2a+, CD14-), B cells (live small lymphocytes, CD3-, CD20+); monocytes (live large cells, CD14+, CD3-).

Antibodies

CD3 (SP34-2 BD Pharmingen), CD4 (L200 BD Pharmingen), CD8 (SKI BD Pharmingen, eBiosciences, BDIS), CD28 (CD28.2 Beckman Coulter, BD Pharmingen), CD95 (DX2 BD Pharmingen, eBiosciences), CCR5 (3A9 BD Pharmingen), CCR7 (15053 RandD Sysyems), Ki-67 (B56 BD Pharmingen), SA (BD Pharmingen), CD20 (L27 BDIS), CD27 (M-T271 BD Pharmingen), IgD (Southern Biotech), Gd (5A6.E9 Invitrogen), PD1 (J105, eBisociences), B7 (FIB504, BD Pharmingen), CD56 (MEM-188 Invitrogen), CD16 (3G8 BD Pharmingen, Biolegend), NKG2A (Z199 Beckman Coulter), NKp46 (195314 RandD Systems), CD14 (M5E2 BD Pharmingen, RandD Systems), CD127 (hIL-7R-M21 BD Pharmingen), CD169 (7-239 Biolegend),

HLA-DR (TU36 Invitrogen, Immu357 Beckman Coulter), CD23 (9P25 Beckman Coulter), CD25 (2A3 BD Pharmingen), CD69 (FN50 BD Pharmingen), STAT5 (47/Stat5(pY6) BD Pharmingen), BrdU (B44 BD Pharmingen).

Reagents

R10 media (RPMI (HyClone), 10% Fetal Bovine Serum (FBS), 100units/mL Penicillin, 10mg/mL Streptomycin (PenStrep) (Sigma), 200μM L-glutamine (Sigma))

R3 media (RPMI, 3% FBS, 100units/mL-10mg/mL PenStrep, 200μM L-glutamine)

IEL media (HBSS (Hyclone), 5% Bovine Growth Serum (BGS), 25mM HEPES buffer (Sigma), 100 IU/ml PenStrep, 2mM L-glutamine)

1X PAB (DPBS w 0.1% BSA and sodium azide)

PBMC Isolation from whole blood

Whole blood was collected in ACD tubes. Whole blood was spun down for 15 minutes at 1800rpm to separate plasma. Plasma was collected and HBSS was added back to the blood to a total volume of no more than 30mL and mixed well. 14mL Ficoll was layered under the blood and tubes were spun at 3000rpm for 20 minutes. PBMCs were removed from the buffy coat with a transfer pipette and placed in a new 50mL conical (no more than 15mL). Cells were then washed with 35mL HBSS and spun for 15 minutes at 1800rpm. For cell sorting, cells were then re-suspended in 5mL 1X ACK Lysing Buffer (Biosource International) for less than 5 minutes, and 45mL HBSS was then added to

stop lysis. Cells were spun for 8 minutes at 1800rpm. Cells were then washed 1X in R10 and re-suspended in fresh R10.

Lymphocyte isolation from lymph nodes

At necropsy, tissues were placed in a 50mL conical filled with approximately 25mL R10. Lymph nodes were processed by placing each one in a petri dish containing a metal screen and approximately 10mL R10. A glass pestule was then used to crush the tissue against the screen, releasing the lymphocytes into the media. Using a transfer pipette, the media containing the cells was then filtered through a 70µm filter into a 50mL conical. Collected cells were washed with R10, centrifuged 8 minutes at 1800rpm and the supernatant was aspirated. Cells were resuspended in fresh R10 for counting.

Sort Purification of Cells

Whole blood was collected in ACD vacutainers and lymphocytes were isolated by density gradient separation as described above. Live lymphocytes were stained extracellularly in R10, on ice in the dark for 30 minutes. After incubation, cells were washed 1X with cold R10 and spun at 1500rpm for 10 minutes at 4˚C. Cells were then resuspended in cold R10 and kept on ice prior to sort and after sort purification. Cells were sorted using an ARIA II (BD).

Proliferation and Differentiation Cultures

PBMCs from whole blood were sort purified based on phenotype. Purified cells were plated in a 48-well plate in 1mL R10 at a cell density of 150,000 to 300,000 cells per mL. Cytokine and antibodies were spiked into the culture at the concentration described, and cultures were gently mixed. Cells were then placed in culture at 37˚C for two weeks. At day 7, the culture was resuspended and half the culture (0.5mL) was removed for phenotype analysis by flow cytometry. An equal amount of fresh R10 was added back to the remaining culture, which was placed back at 37˚C for the remaining 7 days. At day 14, the entire culture was resuspended and taken for phenotype analysis.

Cellular Staining

Whole blood (150ul) was added to polystyrene flow tubes. For staining previously isolated tissue lymphocytes, $1x10^6$ cells were added to polystyrene flow tubes and washed 1X with IX PAB. Extracellular antibodies were added to appropriate tubes and tubes were lightly vortexed and incubated in the dark for 30 minutes. In the case that biotin was used, the appropriate SA conjugated antibody was added and incubated for an additional 20 minutes. After incubation, 1mL lyse solution (BD) was added and tubes were vortexed and incubated at room temperature in the dark for 10 minutes. After 10 minutes, 3mL 1X PAB was added to each tube and tubes spun 5 minutes at1800rpm. Supernatant was decanted and 0.5mL 2X Perm buffer (BD) was added to each tube, vortexed and incubated 10 minutes at room temperature in the dark. Following incubation, cells were washed with 3mL 1X PAB, spun and the supernatant was decanted. Cells were permed one additional time then washed twice with 3mL 1X PAB.

Extracellular antibodies were added and tubes were incubated at room temperature in the dark for 45 minutes. Cells were then washed with 3mL 1X PAB and were subsequently collected on an LSR II.

PhosFlow

Whole blood (100µL) was added to polystyrene flow tubes. Extracellular antibody stains were added and incubated in the dark at room temperature for 30 minutes. During last 15 minutes of surface stain, cytokine was spiked in (0-3.2ng diluted in 2µL 1X PBS) to blood. Samples were then incubated for 15 minutes at 37˚C. After 15 minutes, 2mL 1X BD PhosFlow Lyse/Fix diluted in water was added to blood. Samples were mixed well and incubated for 5 minutes at room temperature. After incubation, tubes were spun for 5 minutes at 1800rpm. The supernatant was then discarded and cells were washed 1X with 2mL 1X PBS. Samples were mixed well and spun for 5 minutes at 1800rpm. The supernatant was then decanted. To samples, 1mL ice-cold 1X BD PhosFlow perm buffer IV diluted in 1X PBS was then added. Samples were mixed well and incubated for exactly 5 minutes at room temperature. After 5 minutes, 3mL 1X PAB was added to tubes and tubes were then spun 5 minutes at 1800rpm. The supernatant was decanted and samples were washed 1X with 1X PAB. Intracellular antibody was then added to samples and the samples were incubated 45 minutes at room temperature in the dark. Cells were washed 1X with 1X PAB. Samples were subsequently run on LSRII.

Intracellular Cytokine Staining (ICS) – PMBCs ($1X10^6$) were added to 5mL polypropylene flow tubes. Cells were washed 1X with RI0 and resuspended in 0.5mL R10. Peptides were added at desired concentrations along with costimulatory antibodies CD28pure and CD49dpure in 0.5mL R10. Samples were then incubated for 1 hour at 37˚C. After 1 hour, 1µL Brefeldin A (Biolegend) was added to each tube. Samples were then placed back at 37˚C for 8 hours. After 8 hours, samples were moved to 4˚C until staining. After incubation, ICS samples are stained normally as described above.

BrdU

Rhesus monkeys were administered BrdU 30mg/kg three times within 24 hours. Tissues were collected and processed for lymphocyte isolation. Cells were stained with extracellular antibodies and lysed and permeabilized as described above. Immediately after the final wash, Dnase was added to tubes. Following Dnase addition, intracellular antibodies including anti-BrdU were added, incubated, and washed normally.

Luminex

Plasma cytokine concentrations (excluding IL-7) were measured using the Cytokine Monkey Magnetic 29-Plex Panel Kit (Life Technologies) according to the manufacturer's instructions. This panel allowed for the quantitative determination of EGF, Eotaxin, FGF-basic, G-CSF, GM-CSF, HGF, IFN-γ, IL-1B, IL-1Ra, IL-2, IL-4, IL-6, IL-8, IL-10, IL-12, IL-15, IL-17, IP-10, I-TAC, MCP-1, MDC, MIF, MIG, MIP-1a, MIP-1b, RANTES, TNF-a, and VEGF. Briefly, previously collected plasma was thawed on ice.

Once thawed, plasma was spun for 10 minutes at 10,000g at 4˚C. Sample plasma and standards were incubated with provided beads overnight at 4˚C. After incubation, detection antibody was added and incubated for 1 hour and the beads were then subsequently washed. Streptavidin-RPE was added next and incubated for 30 minutes at room temperature. Finally, beads were washed and resuspended in wash buffer for acquisition using a Luminex 200 machine. Data was analyzed using MasterPlex QT and MasterPlex CT Software.

Virus Quantification

Plasma SIV RNA was assessed using a real-time RT-PCR assay with a threshold sensitivity of 30 SIV gag RNA copy equivalents per milliliter of plasma as described previously (169). Amplification primers included forward primer (SGAG21), 5'-GTCTGCGTCATPTGGTGCATTC-3'; reverse primer (SGAG22), 5'-CACTAGKTGTCTCTGCACTATPTGTTTTG-3', and probe (pSGAG23), 5'-(FAM) CTTCPTCAGTKTGTTTCACTTTCTCTTCTGCG-(BHQTM1)-3'.

Results

CD4 TEM are the most efficiently targeted cells by most SIV/HIV because they constitutively express CCR5, the SIV/HIV co-recteptor. Pathogenic CCR5-tropic SIV-infection of RM results in the rapid depletion of most CCR5+ CD4 TEM in effector sites such as the lung and gut lamina propria within days of initial infection (31). Antigen-stimulated systemic immune activation causes TCM proliferation and differentiation to TEM in order to supply the peripheral effector sites with adequate TEM to fight local infection. It was shown that SIV infection initiates a persistent hyper-proliferative state among CD4 (and CD8) memory T cells (32). During pathogenic HIV/SIV-infection and chronic immune activation, studies have reported abnormal homeostatic cytokine levels, including increased IL-15 plasma concentrations (111). Indeed, we have observed that IL-15 levels are generally increased in the plasma and tissues of SIV-infected RM (Figure 4-1). We additionally observed that sort-purified CD4 T cells from chronically SIV-infected RM were unable to respond normally to homeostatic cytokines, having a delayed proliferation response to both IL-15 and IL-7 *in vitro* (Figure 4-2).

To better understand the role of IL-15 in pathogenic SIV-infection, eighteen chronically SIVmac239-infected RM were administered six doses of the rhesusized anti-IL-15 Ab, M111, (N=9) or an IgG1 isotype control Ab (N=9) once every two weeks for ten weeks (Figure 4-3). Animals were defined as chronically infected if they were infected with SIV for at least 100 days, had plateau-phase viral loads and had less than two percent CD4 T cells in BAL. Over the course of antibody treatment, the WB from the chronically SIV-infected RM was monitored via phosflow, and we observed anti-IL-

15 Ab treatment blocked IL-15 mediated STAT5 phosphorylation *ex vivo* compared to IgG control Ab treatment (data not shown).

Similar to our observations in healthy RM described in Chapter 3, anti-IL15 Ab was highly efficient at depleting NK cells in chronically SIV-infected RM (Figure 4-4). NK cells showed differential reliance on IL-15, with CD16+ CD56- NK cells being depleted to the highest extent and showing over 95% depletion compared to baseline levels. CD16- CD56- NK cells were also significantly depleted, being reduced by 90%, and CD16- CD56+ NK cells were the least depleted NK cell population, only being reduced to about 50% of baseline levels compared to control antibody treated monkeys. These data further support that NK cells are reliant on IL-15 signals *in vivo,* and that NK cell reliance on IL-15 does not change during chronic SIV-infection.

We next examined T cell population dynamics in the chronically SIV-infected monkeys during anti-IL-15 Ab administration. Consistent with our observations in healthy, SIV-negative RM described in Chapter 3, absolute numbers of CD8 T cells decreased after anti-IL-15 Ab dosing compared to IgG control Ab dosed animals (Fig 4-6). The reduction in total CD8 T cell absolute numbers was due primarily to reductions of the CD8 TEM population numbers, whereas CD8 TCM and CD8 TTM absolute numbers remained unchanged over the course of Ab treatment. Beginning at day 14, both CD8 TEM and to a lesser extent CD8 TTM populations showed a significant increase in Ki-67 expression. Increased CD8 T cell proliferation was associated with CD8 T cell numbers rising back to baseline levels after approximately three doses of anti-IL-15 Ab, despite continued anti-IL-15 Ab administration. Although CD8 T cell

numbers were able to rebound after depletion and proliferation, CD8 T cells continued to proliferate after baseline numbers in WB were re-achieved, throughout the course of antibody treatment. In chronically SIV-infected RM, CD4 TEM numbers initially declined slightly, but after several doses of anti-IL15 Ab, CD4 TEM numbers were not significantly reduced compared to control treated monkeys (Figure 4-5). Additionally, only CD4 TEM and not CD4 TTM populations showed an increase in proliferation following anti-IL15 Ab administration, a finding that differed from our studies in healthy RM. Analysis of lymphocytes in the BAL demonstrated that resident CD8 TEM and the few remaining CD4 TEM had increased levels of Ki-67 following anti-IL-15 Ab administration compared to IgG Ab control (Fig 4-7).

Our *in vivo* IL-15 signal blockade caused significant changes to both NK cell and T cell population dynamics during SIV-infection, and we wanted to establish how these changes affected SIV disease progression. In collaboration with Mike Piatak, we measured SIV plasma viral loads and found they remained stable and unchanged between IgG control and anti-IL-15 Ab treated groups (Figure 4-8). Also, there were no differences in CD4 T cell depletion of BAL or WB following treatment with anti-IL-15 Ab compared to IgG Ab during the course of chronic SIV-infection (Figure 4-9, 4-6). We observed that following anti-IL-15 Ab administration, there were no significant clinical changes to SIV-infected RM compared to control IgG Ab administration. Moreover, anti-IL-15 Ab treatment did not accelerate the time to end stage disease in RM compared to IgG control Ab treatment (data not shown). Taken together, anti-IL-15 Ab administration did not significantly alter the rate of SIV replication or SIV pathogenesis.

Anti-IL-15 Ab on acute-phase SIV pathogenesis

Although an *in vivo* blockade of IL-15 signaling did not change the progression of SIV pathogenesis when administered during chronic phase SIV-infection, it may be that IL-15 plays a role driving disease progression early on, causing permanent damage to the immune system during acute-phase infection. Indeed, it was observed that IL-15 administration had more profound effects on T cell dynamics and viral load when administered during acute phase of viral infection as opposed to during chronic infection (112, 141). We therefore next tested the effect of anti-IL-15 Ab treatment before and during acute-phase SIV-infection. Antibodies were dosed to RM once every two weeks. Seven RM were given three doses of anti-IL-15 Ab prior to SIV infection, eight RM were given eight doses of anti-IL-15 Ab prior to and during acute SIV infection; and eight RM were given eight doses of IgG1 control Ab both prior to and throughout acute phase SIV-infection. At week six after initiation of antibody treatment, all animals were inoculated intra-rectally with a high-titer dose (3000 TCID50) of SIVmac239, which was sufficient to infect all animals (Fig 4-10).

Consistent with previous cohorts, the anti-IL-15 Ab significantly depleted NK cells from the peripheral blood of RM compared to IgG control Ab (Figure 4-11). CD16+ CD56- NK cell populations were almost completely depleted after two doses of anti-IL-15 Ab and remained depleted throughout acute SIV-infection until approximately ten weeks after the cessation of antibody therapy in both anti-IL-15 Ab treated groups. The CD16- CD56+ and CD16- CD56- NK cell populations also depleted significantly after anti-IL-15 Ab treatment, but proceeded to decline more slowly and only fully

depleted after the fourth dose of antibody. Due to the long-term nature of this study, we were able to follow NK cell population rebound after cessation of antibody treatment. Total NK cell numbers did not begin to increase until close to ten weeks after stopping anti-IL-15 Ab dosing, as was observed after treatment with either three or eight doses of anti-IL-15 Ab. The fact that NK cells did not replenish in RM for nearly ten weeks supports that IL-15 is necessary not only for NK cell survival, but also for early NK cell generation and development.

We next evaluated T cell dynamics following anti-IL-15 Ab administration during acute SIV-infection. After anti-IL-15 Ab treatment but prior to SIV-infection, RM showed a depletion of CD8 TEM absolute numbers (Figure 4-13), consistent with our previously treated cohorts. After two weeks, CD8 TEM, and to a lesser extent CD8 TTM, exhibited a significant increase in Ki-67 expression that remained raised over the course of anti-IL15 Ab dosing. At day 42 post anti-IL-15 Ab or IgG control Ab treatment, RM were infected intra-rectally with SIV. Following SIV-infection, CD8 TEM and CD8 TTM from anti-IL-15 Ab treated RM did not show any further increases in proliferation. In contrast, during IgG control Ab treatment, CD8 TEM and CD8 TTM exhibited a large burst of proliferation that lasted only a few weeks after SIV-infection. Whereas the RM from the IgG control Ab group quickly resolved the induction of CD8 TEM and TTM proliferation post SIV-infection, CD8 TEM and TTM proliferation remained high throughout acute SIV-infection during the course of anti-IL15 Ab treatment. We observed no differences in CD8 TCM proliferation or absolute numbers following anti-IL-15 Ab compared to IgG control Ab administration during acute SIV-

infection. Although there were no changes to CD8 TN proliferation, anti-IL-15 Ab treatment unexpectedly led to long-term depletion of CD8 TN absolute numbers in WB.

Following anti-IL-15 Ab administration, CD4 TEM absolute numbers were initially depleted compared to IgG control Ab dosing, similar to CD8 TEM and our observations in previous RM cohorts (Figure 4-12). After several weeks post anti-IL-15 Ab dosing, CD4 TEM and more moderately, CD4 TTM, exhibited a burst in proliferation compared to IgG Ab treated RM. Of note, after acute SIV-infection post-antibody dosing, CD4 TEM depleted more rapidly in anti-IL-15 Ab treated RM compared to IgG control Ab. By day 42 post SIV-infection, however, there was no difference in CD4 TEM absolute numbers among anti-IL-15 Ab and IgG control Ab treated groups. Following SIV-infection of IgG control Ab treated RM, CD4 TTM and CD4 TEM were induced to proliferate. Whereas CD4 TTM proliferation remained increased throughout SIV infection, CD4 TEM proliferation was quickly resolved in the IgG control treated RM. SIV infection following anti-IL-15 Ab treatment, in contrast, led to an initial decrease in CD4 TEM proliferation that then increased at 2 weeks post-infection and remained high over Ab treatment. We observed no differences in CD4 TCM and CD4 TN proliferation between anti-IL-15 antibody and IgG control Ab dosed groups during acute SIV-infection. In all antibody treated groups, CD4 TCM showed an initial decrease in proliferation after SIV-infection, followed by a rebound to levels higher than baseline that remained increase throughout observation. Similar to CD8 TN, CD4 TN exhibited long-term depletion of absolute numbers following anti-IL-15 Ab administration compared to IgG control Ab.

In the BAL, CD4 and CD8 TEM showed increased Ki-67 expression after anti-IL-15 Ab compared to IgG control Ab treatment (Figure 4-14). Although TEM from BAL sustained high levels of proliferation over the course of anti-IL-15 Ab treatment, CD4 TEM from anti-IL-15 Ab treated RM showed only slightly increased proliferation, and CD8 TEM exhibited no increased proliferation following SIV infection. In contrast, TEM from IgG control Ab treated RM were induced to proliferate following SIV infection, but proliferation was quickly resolved.

Following SIV-infection, TEM from anti-IL-15 Ab treated RM showed sustained, high levels of proliferation throughout antibody treatment and acute SIV-infection, rather than the quick burst and resolution of TEM proliferation seen in IgG control Ab treated RM. In healthy RM (Chapter 3) we observed that sustained, increased proliferation of TEM during anti-IL-15 Ab dosing was associated with a high turnover of TEM. To determine if anti-IL-15 Ab increased TEM turnover during SIV-infection, anti-IL-15 Ab or IgG control Ab treated SIV-infected RM were given three doses of BrdU within 24 hours. BrdU appearance and loss was then monitored in the BAL and WB of treated RM. Analysis of the BAL showed that an increased percent of TEM incorporated BrdU from anti-IL-15 Ab treated RM than IgG control Ab treated RM (Figure 4-15). Thirty to thirty-five percent of CD4 TEM showed BrdU incorporation after anti-IL-15 Ab treatment as compared to 20% of CD4 TEM that incorporated BrdU following IgG control Ab dosing. Fifteen to twenty percent of CD8 TEM showed BrdU incorporation after anti-IL-15 Ab treatment as compared to less than ten percent of CD8 TEM that showed BrdU incorporation following IgG control Ab administration. Peak TEM BrdU

incorporation was reached on the same day in all antibody treated groups. After peak BrdU incorporation, however, the percent of BrdU-positive TEM from both anti-IL-15 Ab and IgG control Ab treated groups rapidly declined to similar levels over the same time period. By day 14, the same percent of CD4 TEM and CD8 TEM from both anti-IL-15 Ab and IgG control Ab treated groups showed BrdU incorporation that disappeared slowly over a similar time course (Figure 4-15). Analysis of the WB revealed that TCM and TTM cell populations showed no differences in the appearance and loss of BrdU (Figure 4-16). For both CD4 and CD8 populations, after the peak of BrdU incorporation, TCM and TTM cell subsets from both anti-IL-15 Ab and IgG control Ab treated RM showed loss of BrdU-positive cells at the same rate; BrdU-positive cells quickly declined to around 20% of peak levels by day 10, then depletion leveled off and only declined to approximately 5-10% by day 60. Of note, we observed that CD4 and CD8 TEM from anti-IL-15 Ab treated RM demonstrated significantly increased appearance and loss of BrdU in the WB compared to IgG control Ab treatment. In anti-IL-15 Ab treated RM, the percent of BrdU-positive CD4 TEM declined rapidly to approximately 50% of peak incorporation within 10 days before leveling off and only depleting to 20-30% of peak by day 60. In contrast, in IgG control Ab treated RM, the percent of BrdU-positive CD4 TEM depleted only to 80% of peak incorporation by day 10 before leveling off and declining to 50% of peak BrdU incorporation by day 60. The percent of BrdU-positive CD8 TEM in anti-IL-15 Ab treated animals exhibited fast decline to 20% of peak levels by day 7, followed by slow decline to 5-10% by day 60. Following IgG control Ab treatment, the percent of BrdU-positive CD8 TEM decreased to only 40% by day 10,

before leveling off and further declining to 20% by day 60. Taken together, CD4 and CD8 TEM appear to be turning over at higher rates in WB and BAL following anti-IL-15 Ab compared to IgG control Ab treatment.

Anti-IL-15 Ab administration had potent effects decreasing TEM absolute numbers, which was followed by increased TEM proliferation, suggesting that IL-15 does play a major role supporting TEM population homeostasis *in vivo*. TEM function has also been shown to be dependant on IL-15 signals and SIV-specific TEM responses have been shown to be augmented by IL-15 both *in vivo* and *in vitro* (119). To determine the role that IL-15 signaling plays in the development and function of T cell responses during acute SIV-infection, we monitored SIV-specific CD4 and CD8 T cell responses following anti-IL-15 Ab or IgG control Ab administration via intracellular cytokine staining (ICS). Indeed, we observed decreases to total SIV-specific responses in WB after treatment with anti-IL-15 Ab during acute-SIV infection as compared to IgG control Ab treatment. Additionally, we observed more profound decreases to CD4 and CD8 total SIV-specific responses in the BAL (Figure 4-17). Taken together, this data shows that IL-15 not only plays a role in T cell homeostasis but also that IL-15 plays role in the maintenance or generation of antigen specific T cells during SIV-infection.

We observed profound alterations to lymphocyte populations during anti-IL-15 Ab treatment of RM during acute SIV infection. Notably, NK cell populations were almost completely depleted and TEM populations were initially depleted, but TEM were subsequently characterized by increased proliferation, activation, and turnover. During the course of anti-IL-15 Ab administration, once NK cells depleted and TEM were

maximally proliferating, RM were inoculated with a high-titer dose of SIV. We monitored plasma viral loads to evaluate how the IL-15 signaling blockade and the resultant change to lymphocyte populations during acute SIV-infection affected viral replication. Surprisingly, despite the drastic alterations to NK cell and T cell populations caused by either regimen of anti-IL-15 Ab dosing, there were no changes to either peak or plateau-phase SIV viral loads compared to IgG control Ab treated RM (Figure 4-18). Consistent with no differences in viral replication, the rate of CD4 T cell depletion in the BAL and WB was equivalent in anti-IL-15 Ab and IgG control Ab treated RM (Figure 4-19). Long-term survival of these RM was monitored for 400 days and while the anti-IL-15 Ab treated groups showed slight indications of early AIDS progression, the survival rates were not statistically different of RM treated with anti-IL-15 Ab versus IgG conrol Ab (Figure 4-20).

Results – Chapter 4 Figures – Anti-IL-15 Ab administration to SIV-infected RM

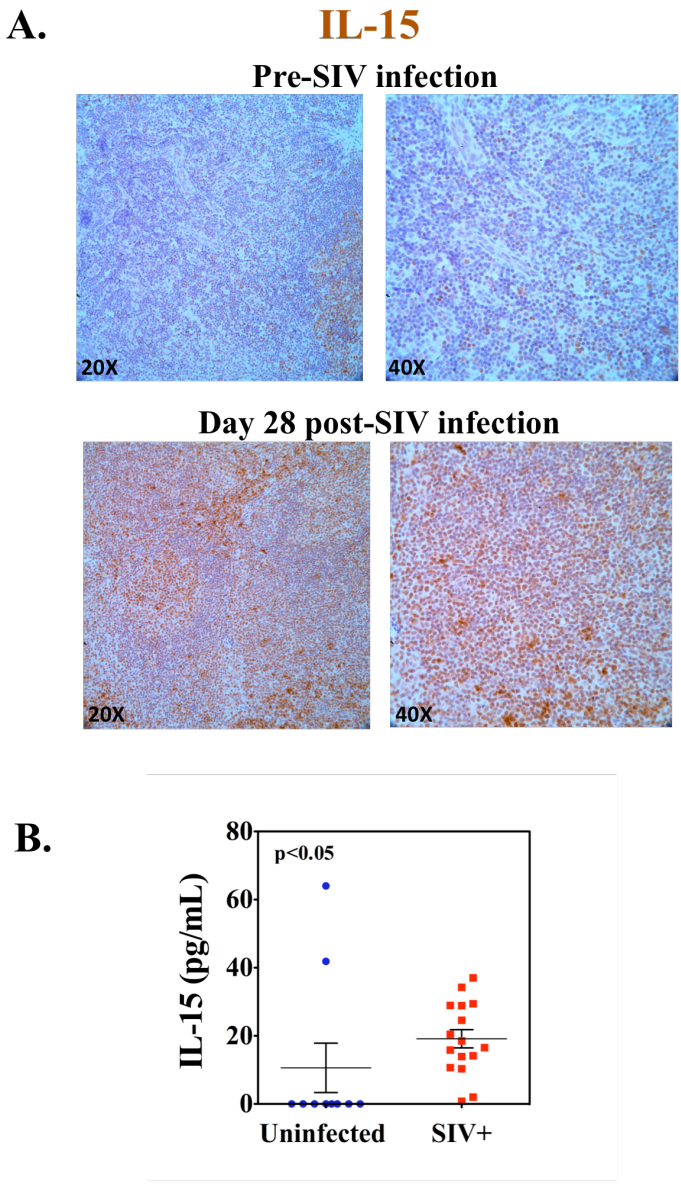

Figure 4-1 – Plasma and tissue IL-15 levels are increased during SIV-infection - (A) IL-15 immunostaining (brown) of LN from a representative RM before (top) and at day 28 post SIV-infection (bottom). B. Plasma IL-15 concentrations (pg/mL) of uninfected RM (N=10, blue) and SIVmac239 infected RM (N=16, red). p value measured by Mann-Whitney test.

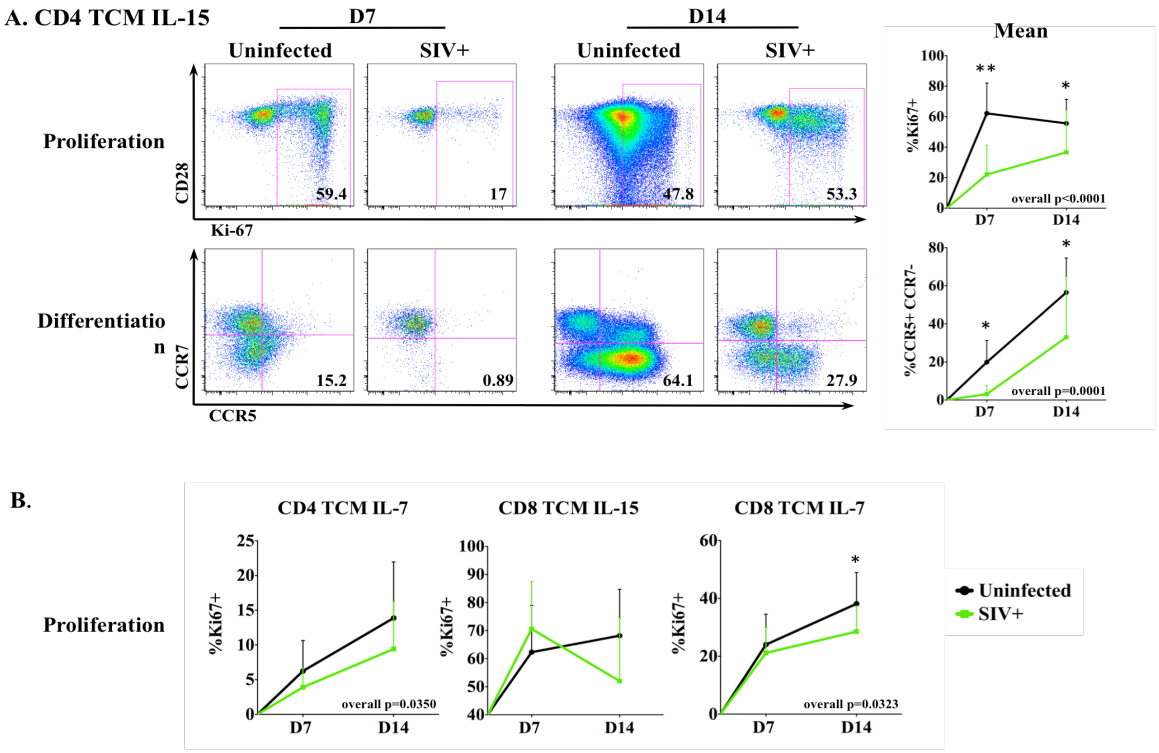

Figure 4-2 – CD4 TCM from SIV-infected RM have a delayed proliferation and differentiation response to IL-15 – Sort-purified CD4 TCM and CD8 TCM from healthy, uninfected RM (black) or SIV-infected RM (green) were cultured *in vitro* for 14 days with 20µM PMPA and 50ng/mL rIL-15 or 50ng/mL rIL-7. At day 7 and day 14 cultures were stained for CD28, Ki-67, CCR7 and CCR5. (A) Left panels show representative RM dot plots of CD4 TCM proliferation (top) and differentiation (bottom) response to IL-15. Panels on right show mean proliferation (top) and differentation (bottom) of uninfected RM (N=19); and SIV-infected (N=21). Panels in (B) show mean responses of CD4 TCM to IL-7 of healthy RM (N=19) and SIV+ RM (N=23); CD8 TCM to IL-15 of healthy RM (N=11) and SIV+ RM (N=11); CD8 TCM to IL-7 of healthy RM (N=14) and SIV+ RM (N=20). * $p<0.05$, ** $p<0.0001$. Statistical analysis evaluated using repeated measures ANOVA with Tukey-Kramer adjustment to control for multiple comparisons.

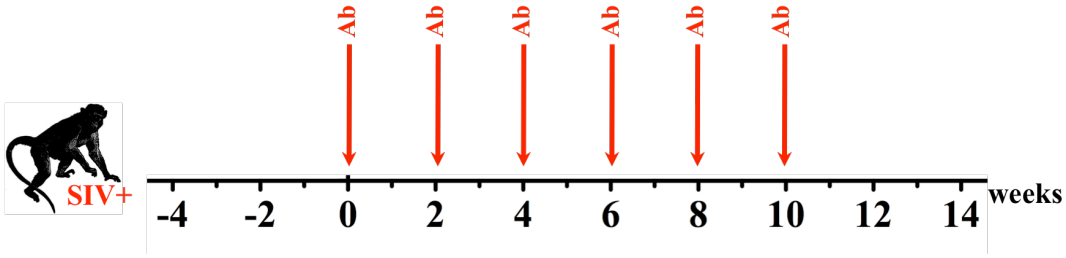

Figure 4-3 – Schematic of anti-IL-15 Ab administration to chronically SIV-infected RM – Chronically SIV-infected rhesus monkeys were administered 6 doses of anti-IL-15 Ab or IgG1 control antibody biweekly. Animals were dosed with antibody once at 20mg/kg followed by 5 doses at 10mg/kg.

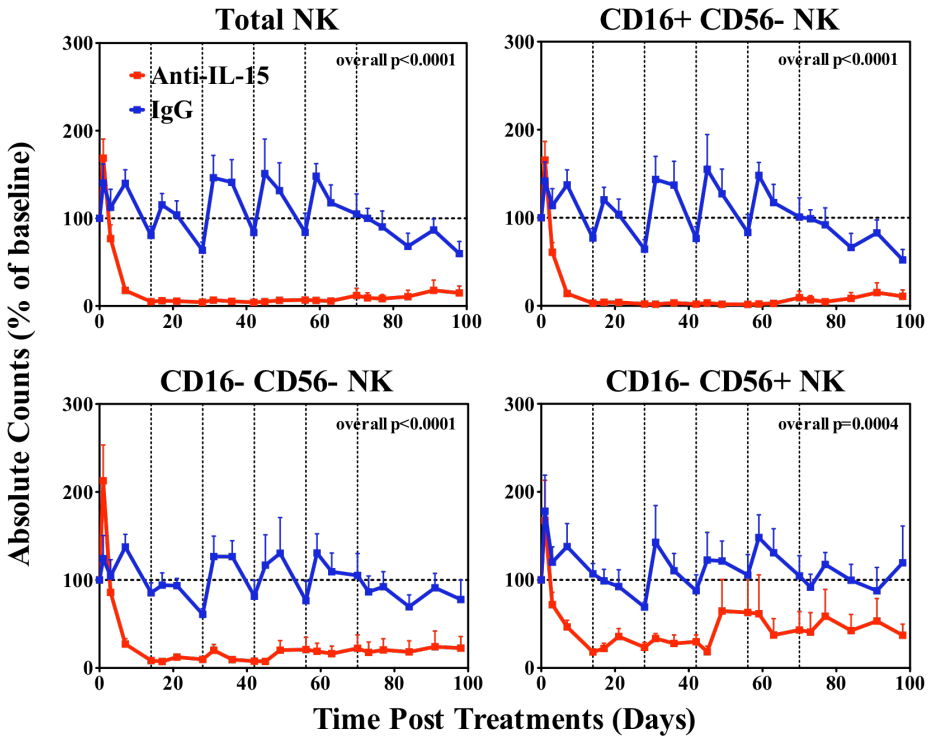

Figure 4-4 – NK cells are depleted in WB after anti-IL-15 Ab treatment to chronically SIV-infected RM – Shown are indicated NK cell populations absolute counts in WB graphed as percent of baseline, following anti-IL-15 Ab (red, N=9) or IgG1 control Ab (blue, N=9) treatment. WB from chronically SIV-infected RM was stained for NKG2a, CD16, and CD56 and analyzed by flow cytometry. Gray vertical lines indicate days antibody was administered to RM. Statistical analysis was evaluated using repeated measures ANOVA with Tukey-Kramer adjustment to control for multiple comparisons.

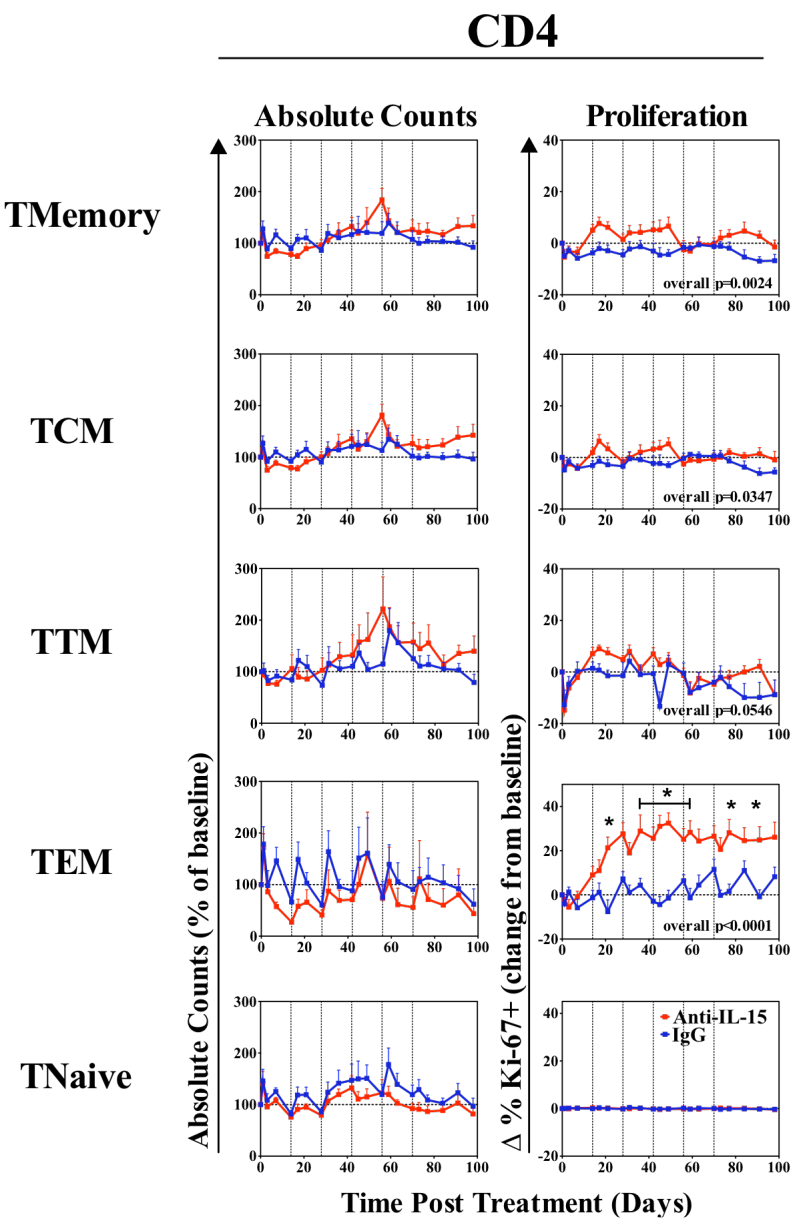

Figure 4-5 - CD4 T cell dynamics during anti-IL-15 Ab administration to chronically SIV-infected RM– Shown are CD4 T cell populations' absolute counts and proliferation in WB graphed as percent of baseline following anti-IL-15 Ab (red, N=9) or IgG1 control Ab (blue, N=9) administration. WB was stained for T cell markers and Ki-67 and analyzed via flow cytometry. Gray, vertical lines indicate days antibody was administered to RM. * $p<0.05$, Statistical analysis was evaluated using repeated measures ANOVA with Tukey-Kramer adjustment to control for multiple comparisons.

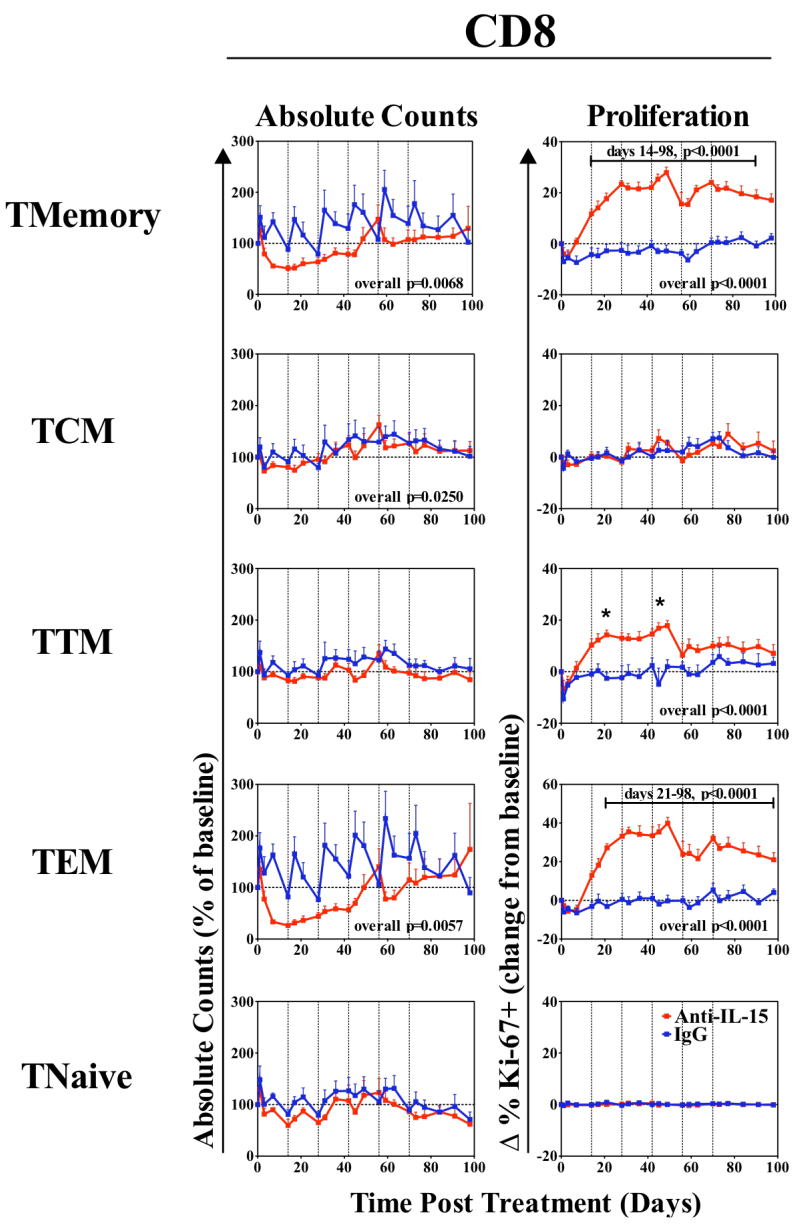

Figure 4-6 - CD8 T cell dynamics during anti-IL-15 Ab administration to chronically SIV-infected RM– Shown are CD8 T cell populations' absolute counts and proliferation in WB graphed as percent of baseline following anti-IL-15 Ab (red, N=9) or IgG1 control Ab (blue, N=9) administration. WB was stained for T cell markers and Ki-67 and analyzed via flow cytometry. Gray, vertical lines indicate days antibody was administered to RM. * $p<0.05$, Statistical analysis was evaluated using repeated measures ANOVA with Tukey-Kramer adjustment to control for multiple comparisons.

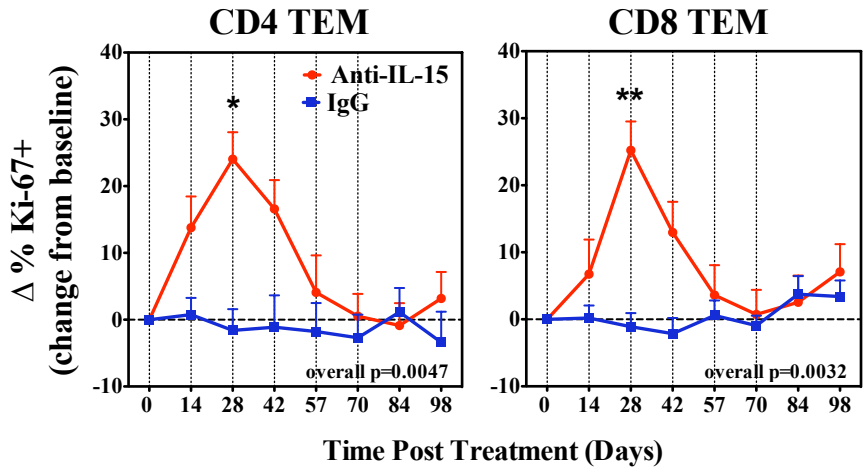

Figure 4-7 - CD4 and CD8 TEM in BAL of chronically SIV-infected RM are induced to proliferate after anti-IL-15 Ab treatment – BAL was collected at indicated time points post anti-IL-15 Ab (red, N=9) or IgG1 control Ab (blue, N=5) administration and stained for T cell markers and Ki-67. Graphs show percent change in TEM Ki-67+ cells. Gray vertical lines indicate days antibody was administered to RM. * $p<0.05$, **$p<0.0001$. Statistical analysis evaluated using repeated measures ANOVA with Tukey-Kramer adjustment to control for multiple comparisons.

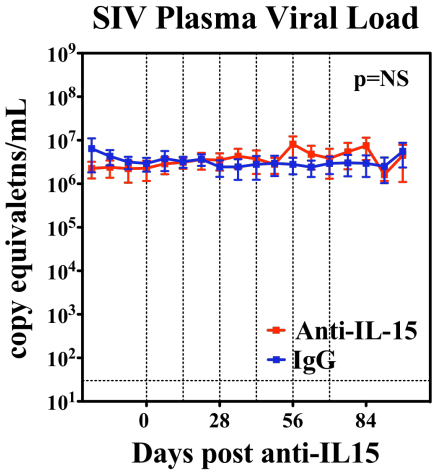

Figure 4-8 – Chronic-phase SIV viral loads are not changed in RM after anti-IL-15 Ab treatment - Plasma viral loads of chronically infected RM following anti-IL-15 Ab (red, N=9) or IgG1 control Ab (blue, N=9) administration. Gray vertical lines indicate days antibody was administered to RM. p=Not significant (NS) - Statistical analysis was evaluated using repeated measures ANOVA with Tukey-Kramer adjustment to control for multiple comparisons.

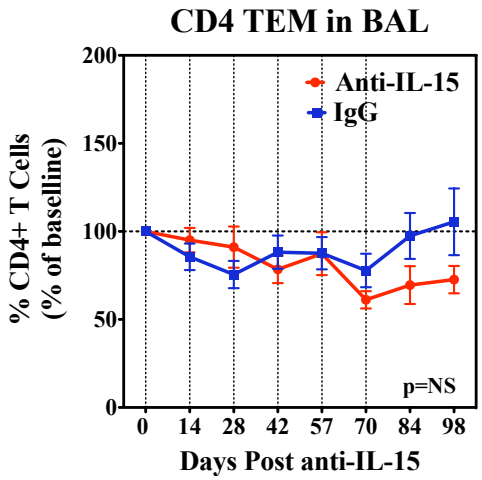

Figure 4-9 – Anti-IL-15 Ab treatment does not change CD4 T cell depletion in the BAL during chronic SIV-infection – Graph shows the percentage of CD4+ T cells in BAL graphed as percent of baseline. Anti-IL-15 Ab (red, N=9) or IgG1 control Ab (blue, N=9). Gray vertical lines indicate days antibody was administered to RM. p=Not significant (NS) - Statistical analysis was evaluated using repeated measures ANOVA with Tukey-Kramer adjustment to control for multiple comparisons.

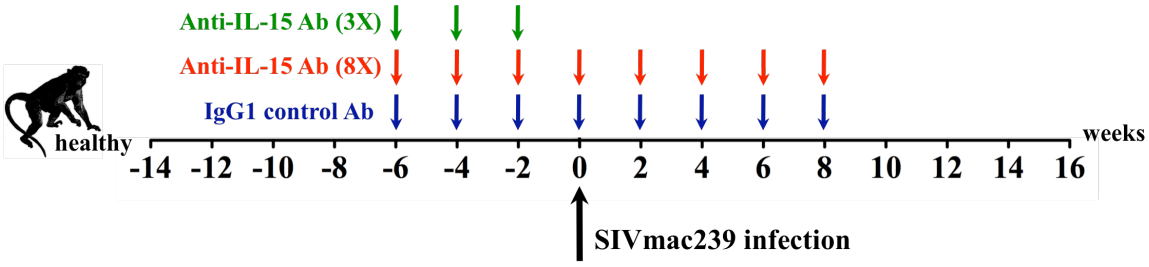

Figure 4-10 – Schematic of anti-IL-15 Ab administration to RM during acute SIV-infection – Healthy RM were treated with: 3 doses of anti-IL-15 Ab prior to SIV infection (N=7, green); 8 doses of anti-IL-15 Ab prior to and during SIV infection (N=8, red); or 8 doses of IgG1 control Ab prior to and during acute phase SIV-infection (N=8, blue). Doses of antibody were administered every two weeks, the first dose administered at 20mg/kg and all subsequent doses administered at 10mg/kg. At week six after initiation of antibody treatment, all animals were inoculated intra-rectally with a high-titer dose of SIVmac239.

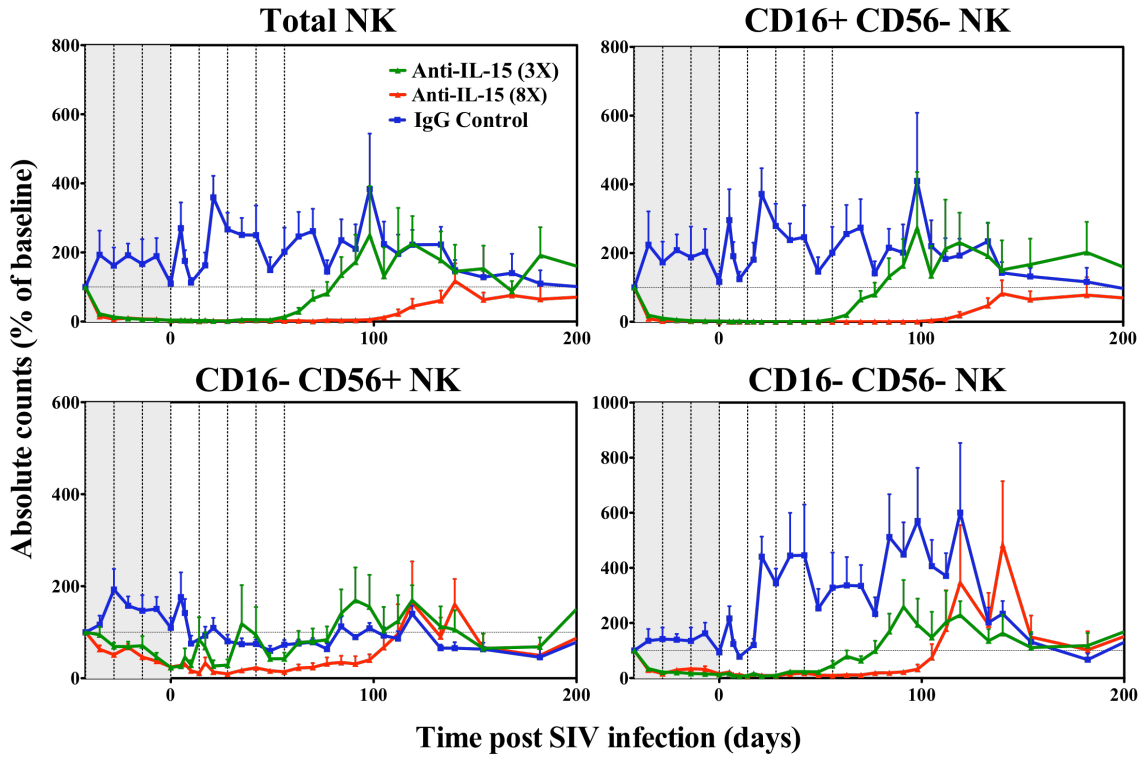

Figure 4-11 - NK cells were depleted in WB after anti-IL-15 Ab administration to RM before and during acute SIV-infection – WB from acutely SIV-infected RM was stained for NKG2α, CD16, and CD56 and analyzed by flow cytometry over the course of anti-IL-15 Ab 3X (green, N=7), anti-IL-15 Ab 8X (red, N=8), or IgG1 control Ab (blue, N=8) treatment. Shown are indicated NK cell populations absolute counts graphed as percent of baseline. Gray vertical lines indicate days antibody was administered to RM.

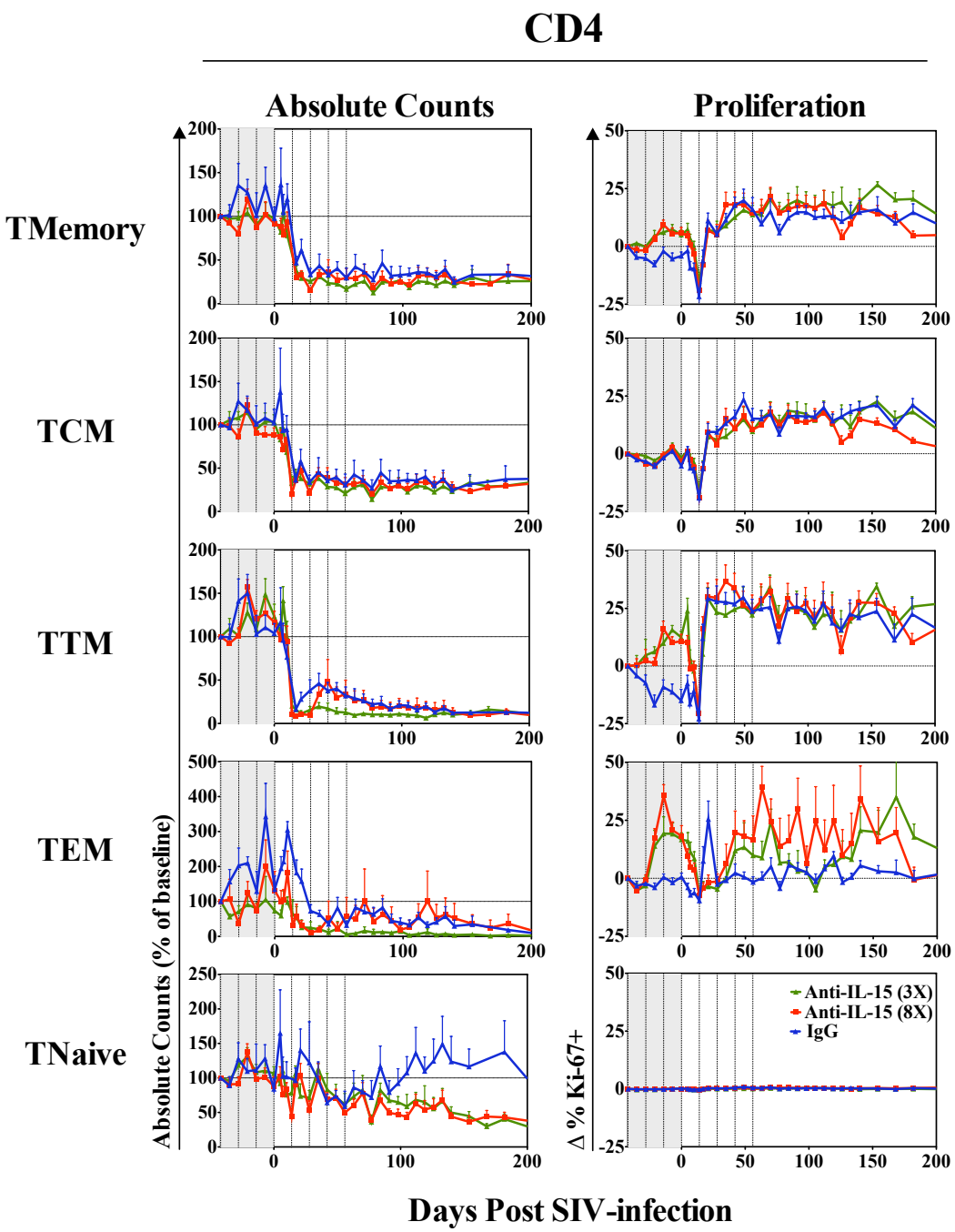

Figure 4-12 – Acute SIV-infection CD4 T cell dynamics during anti-IL-15 Ab treatment – Shown are CD4 T cell population absolute counts and proliferation in WB graphed as percent of baseline following anti-IL-15 Ab 3X (green, N=7), anti-IL-15 Ab 8X (red, N=8), or IgG1 control Ab (blue, N=8) treatment. WB from acutely SIV-infected RM was stained for T cell markers and Ki-67 and analyzed via flow cytometry. Gray vertical lines indicate days antibody was administered to RM.

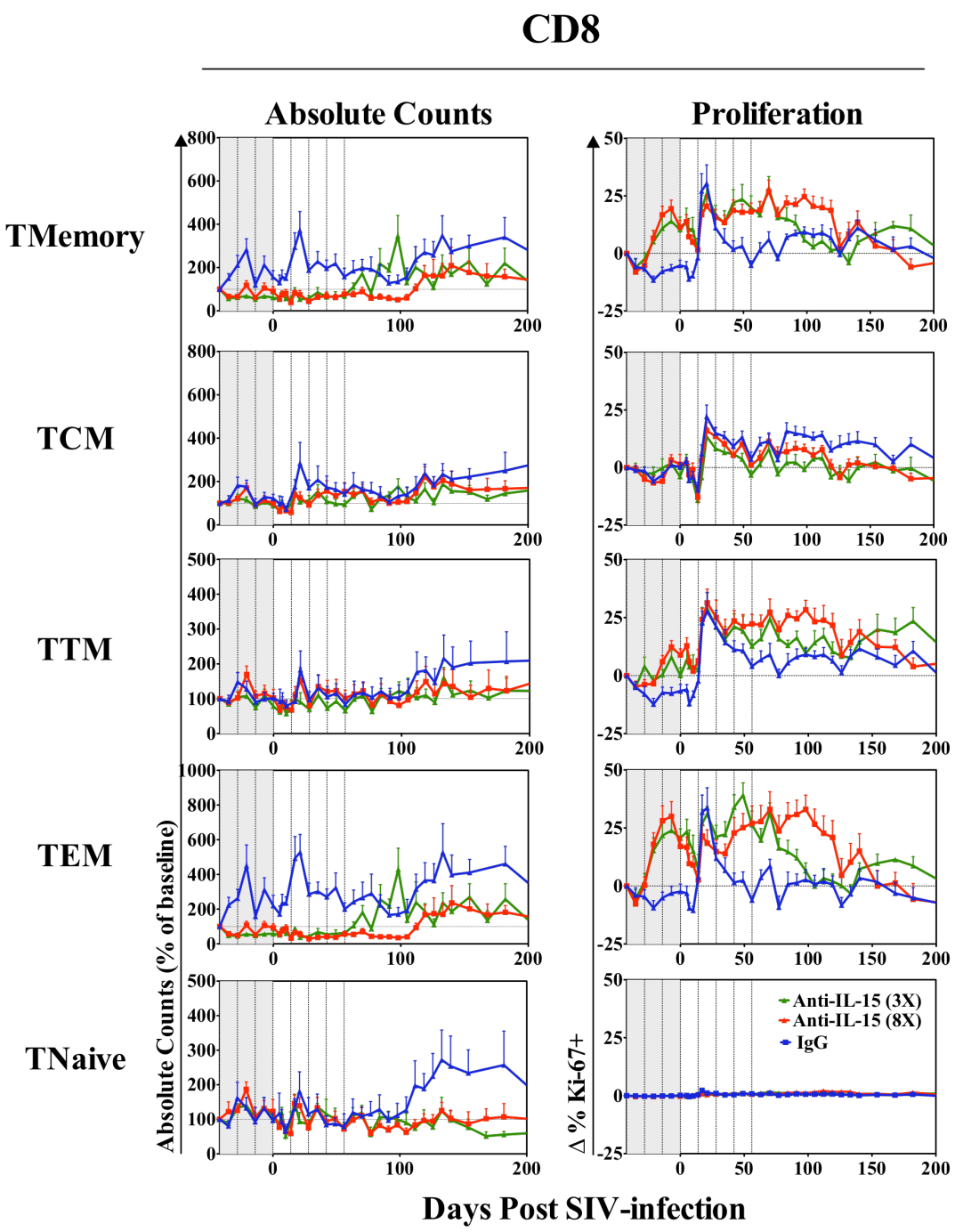

Figure 4-13 - Acute SIV-infection CD8 T cell dynamics during anti-IL-15 Ab treatment – WB from acutely SIV-infected RM was stained for T cell markers and Ki-67 at time points post anti-IL-15 Ab 3X (green, N=7), anti-IL-15 Ab 8X (red, N=8), or IgG1 control Ab (blue, N=8) treatment. Shown are CD4 T cell population absolute counts and proliferation graphed as percent of baseline. Gray vertical lines indicate days antibody was administered to RM.

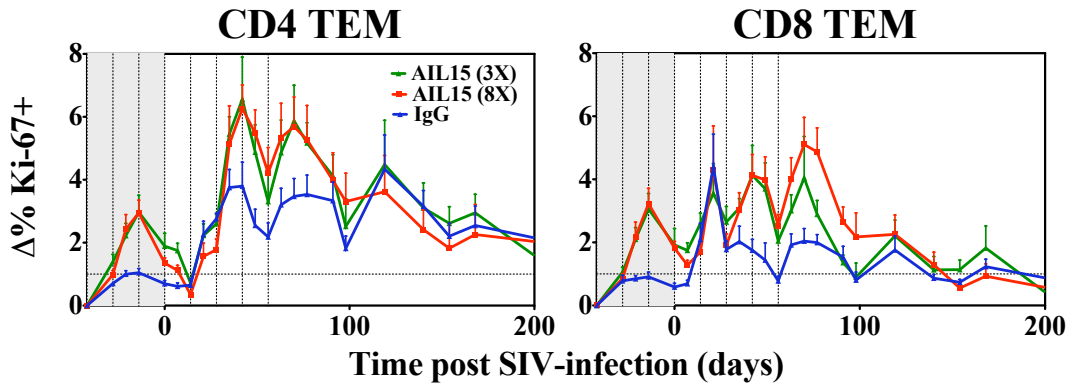

Figure 4-14 - TEM in BAL from acutely SIV-infected RM are induced to proliferate after anti-IL-15 Ab treatment – BAL was collected at indicated time points post anti-IL-15 Ab 3X (green, N=7), anti-IL-15 Ab 8X (red, N=8), or IgG1 control Ab (blue, N=8) administration and stained for T cell markers and Ki-67. Graphs show percent change in TEM Ki-67+ cells. Gray vertical lines indicate days antibody was administered to RM.

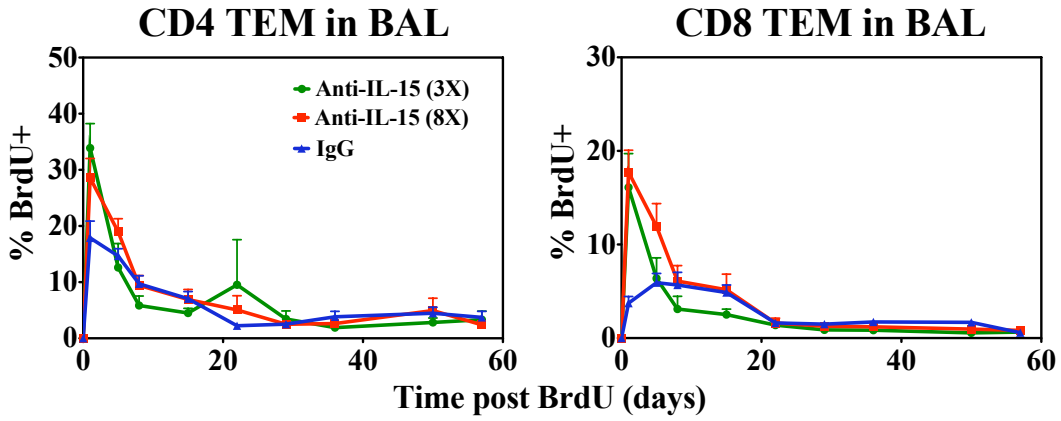

Figure 4-15 – Anti-IL15 Ab increases TEM turnover in the BAL during acute SIV infection – At day 40 post SIV infection, RM were administered BrdU 3X within 24hrs. BAL was collected at indicated time points and stained for T cell markers and BrdU. Graphs show percent change in CD4 and CD8 TEM BrdU+ cells from baseline. Anti-IL-15 Ab 3X (green, N=7), anti-IL-15 Ab 8X (red, N=8), or IgG1 control Ab (blue, N=8).

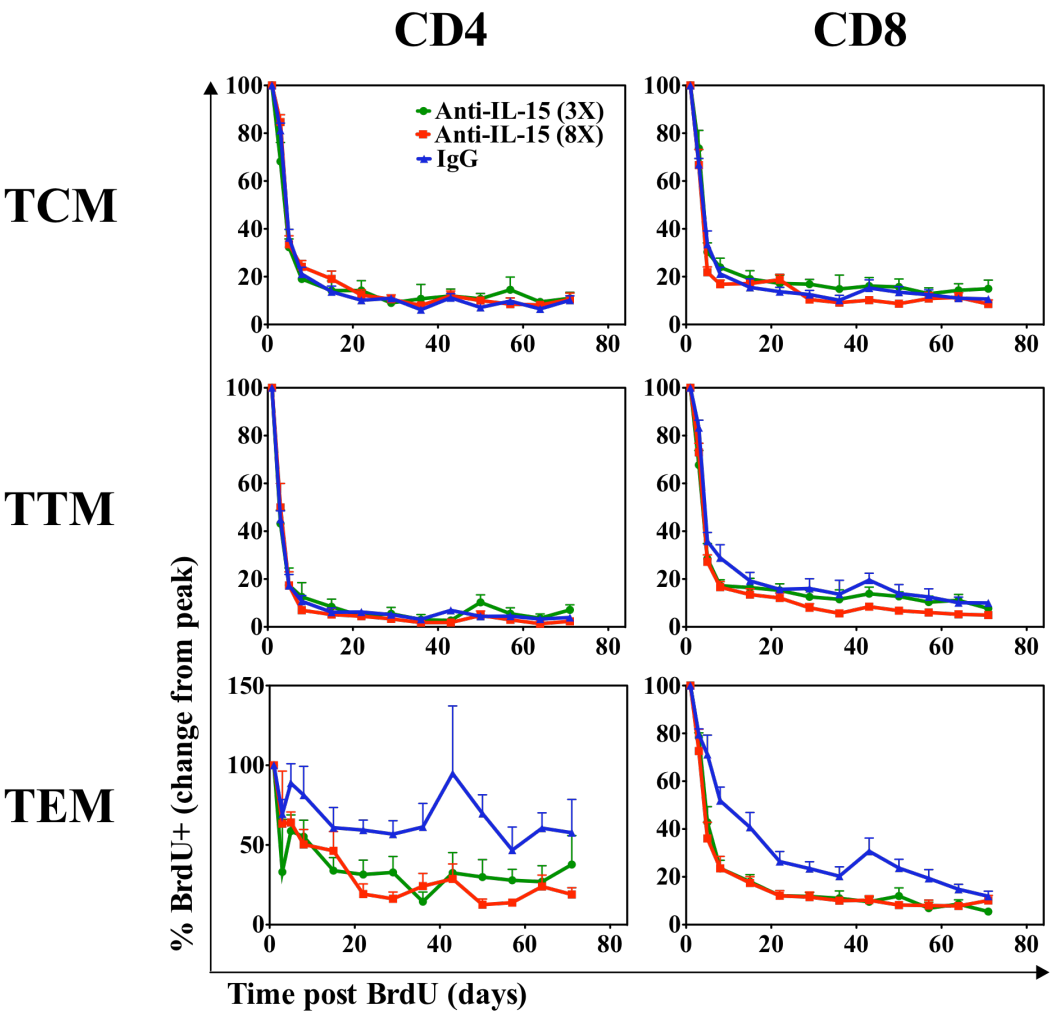

Figure 4-16 – Anti-IL15 Ab increases TEM turnover in WB during acute SIV infection – At day post SIV infection, RM were administered 30mg/kg BrdU 3X within 24hrs. WB was collected at indicated time points and stained for T cell markers and BrdU. Graphs show percent change in CD4 and CD8 T cell subsets BrdU+ cells from peak BrdU incorporation. Anti-IL-15 Ab 3X (green, N=7), anti-IL-15 Ab 8X (red, N=8), or IgG1 control Ab (blue, N=8).

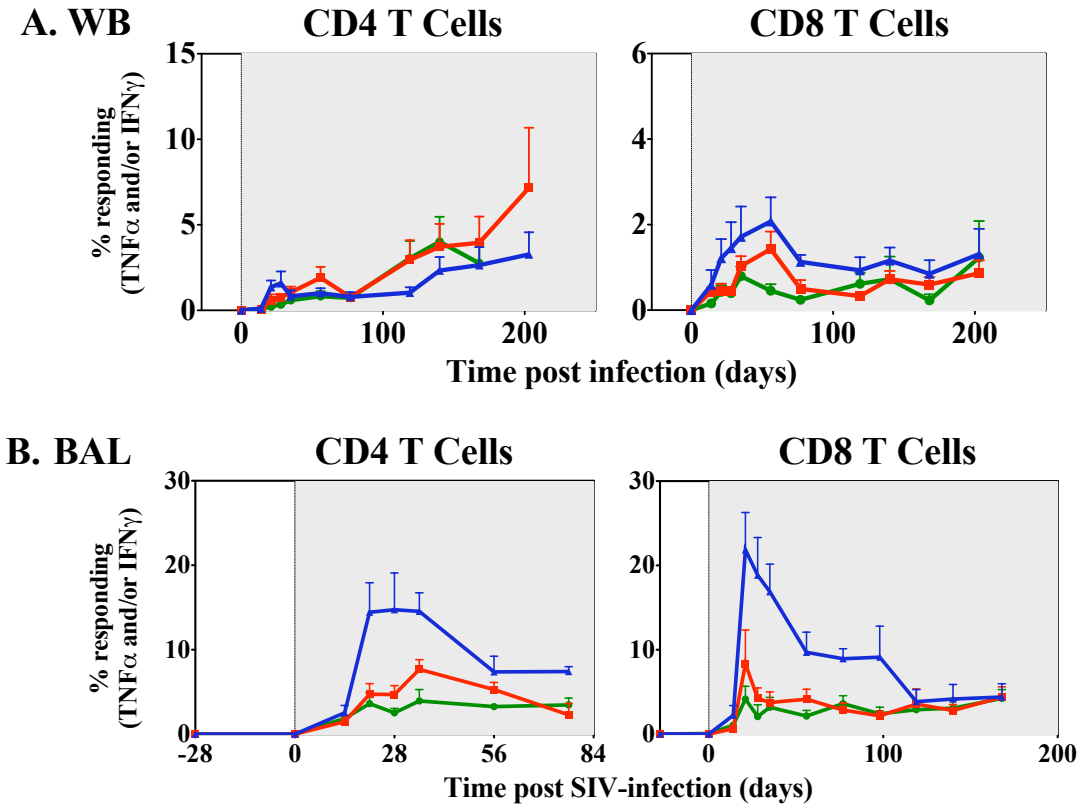

Figure 4-17 – IL-15 signaling blockade during acute SIV infection reduces SIV-specific T cell responses in BAL – Percent of CD4 and CD8 T cells responding to stimulation with SIV proteome by production of TNFa and/or IFNg measured by ICS from WB (A) and BAL (B). Anti-IL-15 Ab 3X (green, N=7), anti-IL-15 Ab 8X (red, N=8), or IgG1 control Ab (blue, N=8).

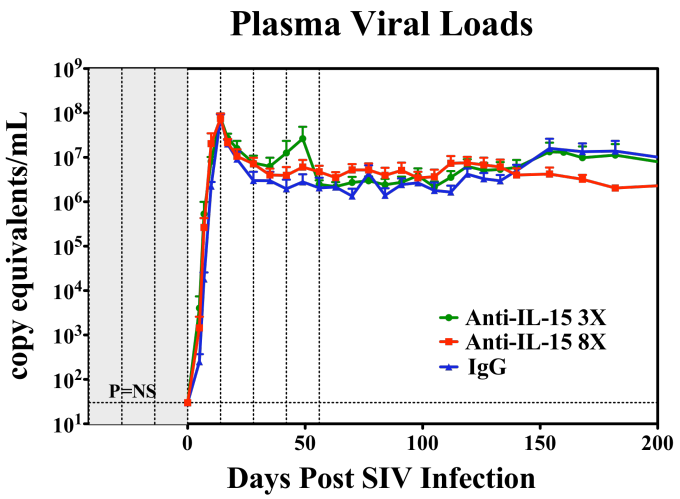

Figure 4-18 – Peak and plateau-phase SIV viral loads are not changed in RM after anti-IL-15 Ab treatment during acute SIV infection - Plasma viral loads of infected RM following anti-IL-15 Ab 3X (green, N=7), anti-IL-15 Ab 8X (red, N=8), or IgG1 control Ab (blue, N=8) administration during acute SIV infection. Gray vertical lines indicate days antibody was administered to RM. p=NS (Not Significant) - Statistical analysis was evaluated using repeated measures ANOVA with Tukey-Kramer adjustment to control for multiple comparisons.

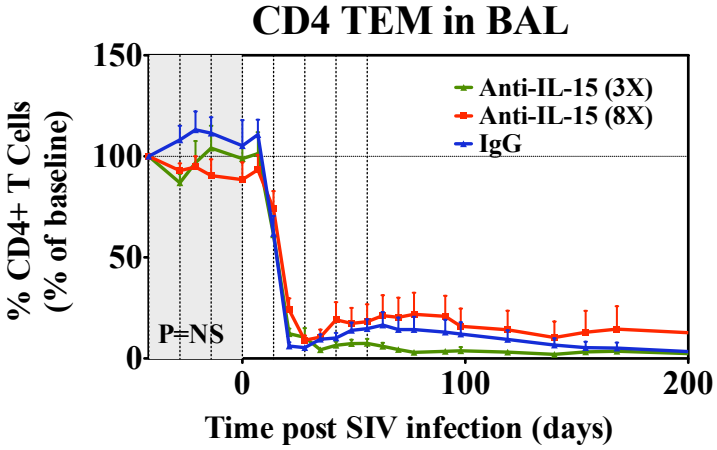

Figure 4-19 – Anti-IL-15 Ab treatment does not change CD4 depletion in the BAL during acute SIV-infection – Graph shows the percentage of CD4+ T cells in BAL graphed as percent of baseline. Anti-IL-15 Ab 3X (green, N=7), anti-IL-15 Ab 8X (red, N=8), or IgG1 control Ab (blue, N=8). Gray, vertical lines indicate days antibody was administered to RM. p=NS (Not Significant) - Statistical analysis was evaluated using repeated measures ANOVA with Tukey-Kramer adjustment to control for multiple comparisons.

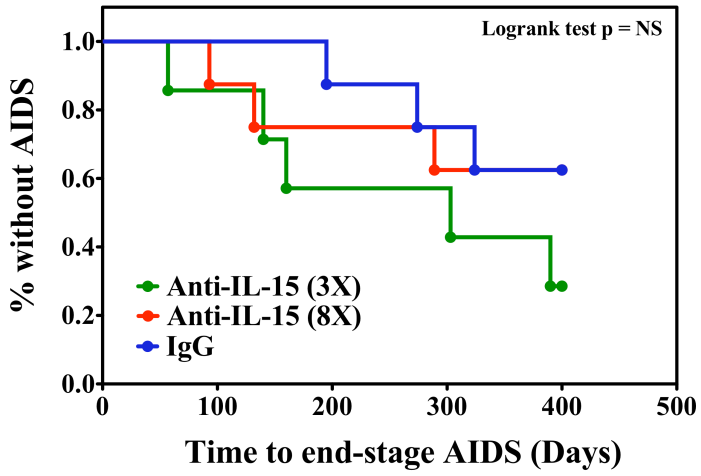

Figure 4-20 – Survival of rhesus macaques is not significantly altered following anti-IL-15 Ab treatment during acute SIV-infection – Graph shows Kaplan-Meier plot of time to end-stage AIDS following SIV-infection**.** Anti-IL-15 Ab 3X (green, N=7), anti-IL-15 Ab 8X (red, N=8), or IgG1 control Ab (blue, N=8).

Discussion

Anti-IL-15 Ab administration to SIV-infected RM

During pathogenic HIV/SIV infection and the resulting chronic immune activation, significantly increased IL-15 levels have been measured, potentially implicating increased IL-15 in driving depletion of CD4 T cell populations and pathogenesis (111, 135, 139, 140). Indeed, our measurements of IL-15 demonstrated increased IL-15 levels in both plasma and tissues of SIV-infected RM, confirming a dysregulation of this homeostatic cytokine during SIV-infection of RM. Of note, we also observed that sort-purified CD4 T cells from SIV-infected RM displayed a significantly delayed proliferation response when cultured with both γc chain cytokines IL-15 and IL-7 *in vitro*. Likely, the delayed proliferative responses of CD4 T cells from SIV-infected RM to γc cytokines *in vitro* is a result of high, chronic immune activation during SIV infection that has already induced high proliferation of these cells *in vivo*. Anti-IL-15 antibody administration, however, did not significantly alter T cell depletion, viral loads, or disease outcome compared to control treated RM during either acute or chronic phase SIV-infection. Moreover, during chronic SIV-infection, we found that levels of other homeostatic cytokines measured in the plasma did not change in response to anti-IL-15 Ab administration, suggesting that increased IL-15 is not affecting changes in other cytokines. Thus IL-15 by itself is not a key factor either driving or protecting from pathogenesis.

Anti-IL-15 Ab administration almost completely depleted NK cells of RM during chronic SIV-infection. Surprisingly, NK cell depletion during chronic SIV-infection of

RM did not change CD4 T cell depletion, viral loads or disease outcome. These data indicating that NK cells do not play a major role protecting against SIV disease are supported by a recently published study in which JAK3 inhibitor was administered to chronically SIV-infected RM. The JAK3 inhibitor resulted in NK cell depletion, but these RMs exhibited only an extremely modest, transient increase in viral loads, an effect that was not even observed in all 6 of the RM animals examined (128). It is therefore possible that during chronic SIV-infection, NK cells do not play a dominant role protecting against opportunistic infection and NK cells are not driving SIV pathogenesis. However, anti-IL-15 Ab was only administered for a short time during chronic SIV-infection, and thus may not have been adequate time to observe disruptions of NK cell protection against opportunistic infections during SIV-infection.

In our studies during acute phase SIV-infection, we began anti-IL-15 Ab administration six weeks prior to SIV inoculation. This led to NK cell depletion prior to SIV-infection and NK cell depletion was maintained throughout acute SIV-infection after either the 3- or 8-dose regimen of anti-IL-15 Ab. Interestingly, an absence of NK cells during acute SIV infection did not change peak or plateau-phase viral loads, CD4 T cell depletion, or long-term survival of RM. Our studies do not preclude a role for NK cells in preventing natural infection where a single infected cell is thought to lead to systemic infection, as our system used a high-titer dose of SIV that ensured infection of all animals. Nonetheless, after the initial take of infection, our study shows that NK cells are not a primary force in either controlling or driving pathogenesis during acute SIV-infection.

Anti-IL-15 Ab treatment of RM during SIV-infection led not only to drastic changes in NK cell populations, but also to significant changes in T cell population dynamics as well. Following anti-IL-15 Ab administration during SIV-infection, CD4 and CD8 TEM cell populations were initially depleted. CD4 and CD8 TEM cell populations were induced to proliferate, which was associated with a rise in TEM cell absolute numbers back towards pre-treatment levels. Increased TEM proliferation was sustained throughout anti-IL-15 Ab treatment during both chronic and acute-phase SIV-infection. Surprisingly, increased proliferation did not cause an increase in depletion of CD4 TEM cells or an increase in viral loads due to increased numbers of viral target cells. Moreover, disease outcome remained unchanged in anti-IL-15 Ab compared to IgG1 control Ab treated RM during both acute- and chronic-phase SIV infection. One caveat is that anti-IL-15 Ab administration was only maintained for a short period of time, so it is possible that if we sustained the IL-15 signaling blockade longer, the system would have eventually collapsed.

We monitored SIV-specific CD4 and CD8 T cell responses during both chronic and acute phase SIV-infection to understand how an IL-15 signal blockade would change antigen specific T cell responses during SIV-infection. IL-15 has been shown to increase the production of SIV-specific CD4 and CD8 T cell responses; however, during chronic SIV-infection, anti-IL-15 Ab administration caused no changes to SIV-specific CD4 or CD8 T cell responses compared to IgG control Ab administration. We did observe, however, anti-IL-15 Ab treatment led to decreases in SIV-specific CD4 and CD8 T cell responses in the whole blood during acute SIV-infection. Additionally, we observed a

significant decrease in SIV-specific CD4 and CD8 T cell responses in the BAL following anti-IL-15 Ab administration during acute SIV-infection. Thus, our data support that production and maintenance of SIV-specific CD4 and CD8 T cell responses during acute SIV-infection are dependent on IL-15 signals in RM (104, 106-108). Our studies in healthy RM indicated that CD4 and CD8 TEM absolute numbers can be supported by a homeostatic factor other than IL-15, likely IL-7. Thus, our data suggests that IL-7 is not able to maintain TEM function and antigen specific responses to the same extent that IL-7 is able to support absolute numbers and TEM homeostasis.

Although previous studies showed that increased levels of IL-15 during SIV infection correlated to increased plasma viral loads and worse disease outcome, we observed that blockade of IL-15 signaling during acute SIV infection did not change either peak- or plateau-phase plasma SIV viral loads (111). Moreover, we did not see a change in disease progression following administration of anti-IL-15 Ab either during acute or chronic phase SIV-infection. Our data strongly suggest that although a correlation of plasma IL-15 levels and SIV plasma viral loads may exist, there is likely no causal effect of increased plasma IL-15 resulting in higher SIV viral loads. This supports previous data that showed that CD8 T cell depletion led a spike of IL-15 and rapid disease progression during SIV infection, but when IL-15 was neutralized rapid progression was not stopped. Rather, rapid progression was caused by a lack in CD8 T cell protection during infection (154).

Taken all together, our data shows that increased IL-15 levels during SIV infection do not play a primary role driving SIV disease progression and CD4 T cell homeostatic failure and depletion.

Chapter 5 – Discussion and Conclusions

To characterize the role of IL-15 *in vivo,* we used the approach of administering a rhesusized anti-IL-15 Ab to healthy RM to understand how an IL-15 signal blockade would affect lymphocyte homeostasis in a healthy immune system. Antibody treatment was well tolerated by all RM, with no adverse side effects observed after multiple dosing. Moreover, *in vivo* anti-IL-15 Ab administration to RM effectively neutralized IL-15 signaling, causing a significant decrease in STAT5 phosphorylation in tissues as was verified by phosflow and immunostaining assays. As was observed previously in rhesus macaques and humans, anti-IL-15 Ab administration was safe (130, 131). Thus, our studies support the use of anti-IL-15 Ab in vivo in RM, where it may have parallels to dosing in humans.

IL-15 and NK cells

NK cells have been shown to be reliant on IL-15 in vivo in multiple species and accumulating data suggested that RM NK cells were regulated by IL-15 as well. The unique role of IL-15 maintaining RM NK cell homeostasis was first revealed in our studies investigating γc cytokine signaling. Whereas nearly all NK cells responded to exogenous doses of IL-15 by inducing STAT5 phosphorylation, most NK cell subsets did not induce STAT5 phosphorylation in response to doses of another γc cytokine, IL-7. Only the CD56+ CD16- NK cells were able to respond to high concentrations of IL-7 by phosphorylating STAT5. Our *in vitro* data, therefore, suggested that rhesus NK cells were also reliant on IL-15 mediated signaling *in vivo*, similar to mice (130). Indeed, we

found that anti-IL-15 Ab administration to healthy RM caused a significant depletion of NK cells in the WB and tissues of RM, which persisted over the course of antibody treatment. Notably, after ceasing anti-IL-15 Ab dosing, NK cells did not begin to rebound until close to ten weeks. The fact that NK cells did not replenish in RM for nearly ten weeks supports that IL-15 is necessary not only for NK cell survival, but also for early NK cell generation and development (87). Our data confirmed in rhesus macaques what previous studies have shown in other species; IL-15 mediated signaling is mandatory for NK cell generation and maintenance *in vivo* (99, 101, 122, 123, 130). RM NK cell subsets were all dependent on IL-15, but the CD16+ CD56- NK cell population was most sensitive to IL-15 mediated signaling, an observation made in previous macaque studies (114). Interestingly, we found that the CD16- CD56+ NK cell subset, which was the only subset responsive to IL-7, was the least depleted NK cell subset, suggesting that this population may receive homeostatic signals from IL-7 in the absence of IL-15. Remarkably, two separate studies administering anti-IL-15 Ab to humans did not cause NK cell depletion. Although the data is surprising, it is likely that human NK cells have evolved to be reliant on other γc cytokine signaling for maintenance *in vivo*, as XSCID humans are NK cell deficient. The ability of anti-IL15 Ab to practically eliminate NK cells throughout the peripheral blood and tissues of RM make it a valuable tool to test the various roles of NK cell function in health and disease.

We next used the anti-IL-15 Ab to investigate the function of NK cells during SIV-infection. Anti-IL-15 Ab administration almost completely depleted NK cells of RM during chronic SIV-infection. Surprisingly, NK cell depletion during chronic SIV-

infection of RM did not change CD4 T cell depletion, viral loads or disease outcome. These data indicating that NK cells do not play a major role protecting against SIV disease are supported by a recently published study in which JAK3 inhibitor was administered to chronically SIV-infected RM. The JAK3 inhibitor resulted in NK cell depletion, but these RMs exhibited only an extremely modest, transient increase in viral loads, an effect that was not even observed in all 6 of the RM animals examined (128). It is therefore possible that during chronic SIV-infection, NK cells do not play a dominant role protecting against opportunistic infection and NK cells are not driving SIV pathogenesis. However, anti-IL-15 Ab was only administered for a short time during chronic SIV-infection, and thus may not have been adequate time to observe disruptions of NK cell protection against opportunistic infections during SIV-infection.

In our studies during acute phases SIV-infection, we began anti-IL-15 Ab administration six weeks prior to SIV inoculation. This led to NK cell depletion prior to SIV-infection and NK cell depletion was maintained throughout acute SIV-infection after either the 3- or 8-dose regimen of anti-IL-15 Ab. Interestingly, an absence of NK cells during acute SIV infection did not change peak or plateau-phase viral loads, CD4 T cell depletion, or long-term survival of RM. Our studies do not preclude a role for NK cells in preventing natural infection where a single infected cell is thought to lead to systemic infection, as our system used a high-titer dose of SIV that ensured infection of all animals. Nonetheless, after the initial take of infection, our study shows that NK cells are not a primary force in either controlling or exacerbating pathogenesis during acute SIV infection.

IL-15 and T cells

IL-15 has been documented to regulate T cell populations in vivo and our studies investigating IL-15 regulation of RM lymphocytes revealed a primary role for IL-15 in T cell homeostasis as well. We started our experiments with in vitro studies, and first determined the ability of IL-15 and IL-7 to signal distinct T cell subsets. We observed that both IL-15 and IL-7 were able to signal all T cell subsets via STAT5 phosphorylation, though to varying degrees. Although there were slight differences in the abilities of IL-15 and IL-7 to signal CD4 versus CD8 T cells, overall both CD4 and CD8 T cells exhibited similar patterns of STAT5 phosphorylation in response to doses of IL-15 and IL-7. The similar *in vitro* response of CD4 and CD8 T cells to IL-15 supports the accumulating data that IL-15 is imperative not only to CD8 T cell homeostasis, but also to CD4 T cell homeostasis as well (25, 32, 60, 110).

Regardless of CD4 or CD8 expression, IL-15 and IL-7 had differing abilities to induce phosphorylation of STAT5 in memory versus naïve T cells. Whereas effector memory phenotype subsets TEM and TTM were highly responsive to IL-15, TEM and TTM subsets were considerably less responsive to IL-7. This *in vitro* data potentially suggested that *in vivo* TEM and TTM populations were regulated primarily by IL-15 and to a lesser extent by IL-7. In contrast, TN and TCM subsets demonstrated a distinct phenotype, being highly responsive to IL-7 but only slightly responsive to IL-15. The result that TN and TCM cell subsets were more sensitive to IL-7 supports abundant data in the literature, which show that TN and TCM subsets' homeostasis are primarily regulated by IL-7 *in vivo* (in addition to MHC interactions in the case of TN) (57-59, 157,

158). However, the observation that TN and TCM are able to induce STAT5 phosphorylation in response to IL-15, suggested that IL-15 was potentially involved in the regulation of these T cell subsets as well.

To understand how IL-15- and IL-7-induced STAT5 phosphorylation affected downstream changes in different T cell subsets, we next cultured sort-purified T cell populations *in vitro* with either IL-15 or IL-7. Notably, we observed that IL-15 induced the proliferation and differentiation of both TN and TCM to TEM *in vitro* when cultured with monocytes. In contrast, culture of either TN or TCM with IL-7 and monocytes led to only modest enhancement of T cell proliferation. Thus, IL-15 may regulate the homeostasis of TN and TCM populations by driving their differentiation to effector phenotype cells. Although not generally ascribed as a main function of IL-15, the ability of IL-15 to drive differentiation of effector memory T cells has been previously reported in the literature (25, 110).

Anti-IL-15 Ab treatment of healthy rhesus macaques revealed several aspects of TM homeostasis. Our *in vitro* data showed that IL-15 can drive the proliferation and differentiation of TN and TCM to TEM, an observation which has been reported in the literature (25, 110). Thus, in the absence of IL-15 mediated signaling, we may have expected an increase in TN or TCM absolute numbers as fewer of these cells were induced to differentiate to TEM. However, our data administering anti-IL-15 Ab to RM showed no change to TN or TCM absolute numbers or Ki-67 expression in WB over the course of treatment. Thus, TN and TCM differentiation to TEM may be an *in vitro* artifact caused by physiologically irrelevant high doses of cytokine. We did observe an

initial decline in TEM absolute numbers following anti-IL-15 Ab treatment, which may in part be due to decreased production of TEM from recently differentiated TN and TCM. It is therefore possible that IL-15 is inducing some TEM differentiation from TN and TCM *in vivo*. It is more likely, however, the decline in TEM absolute numbers is caused by decreased viability of TEM. Interestingly, following anti-IL-15 Ab administration during acute SIV-infection, we did observe a long-term decline of CD4 and CD8 TN absolute numbers. Thus, IL-15 may indeed have a role in TN homeostasis that has not previously been characterized.

Interestingly, anti-IL-15 Ab treatment of healthy rhesus macaques revealed a unique facet of TEM homeostasis. In the absence of IL-15 signaling, TEM numbers initially declined to approximately 30-40% of baseline levels. Strikingly, after two weeks of anti-IL-15 Ab dosing, TEM exhibited a burst of proliferation that corresponded with an increase in cell absolute numbers back to pre-treatment levels in WB. Our data suggest that TEM proliferation represents a homeostatic response to declining absolute numbers rather than the anti-IL-15 Ab exhibiting an activating role *in vivo*. Previous studies have reported that although some antibodies against γc cytokines displayed blocking effects *in vitro*, the same antibodies became activating *in vivo* and amplified cytokine mediated signaling (159-164). Notably, in cases where an antibody against a γc cytokine demonstrated *in vivo* cytokine signal amplification, all observed *in vivo* effects were activating with no blocking effects. Our anti-IL-15 Ab, in contrast, showed blocking effects *in vivo,* such as decreased phospho-STAT5 levels, NK cell depletion, and T cell depletion, thus confirming our anti-IL-15 Ab caused an IL-15 signal blockade

in vivo. We also considered that T cells maybe indirectly induced to proliferate in response to anti-IL-15 Ab forming immune complexes that stimulate Fc receptors. To test this possibility we administered the same anti-IL-15 Ab with a mutated Fc receptor-binding site and observed this had no effect on antibody mediated IL-15 signal blockade, T cell or NK cell dynamics. We thus concluded that the TEM proliferation observed two weeks following anti-IL-15 Ab treatment was not an artifact of the antibody dosing itself, but rather indicated a separate homeostatic event.

We considered that, during anti-IL-15 Ab administration, a homeostatic factor other than IL-15 maybe inducing TEM proliferation as a backup system to maintain population numbers *in vivo* in the absence of IL-15 signaling. Measurements of plasma cytokine levels revealed no changes in other known immune-modulating cytokines including IL-7, TNFa, and IL-12. Interestingly, despite the fact that IL-7 levels were not changed in the plasma of anti-IL-15 Ab compared to IgG control Ab treated RM, our data suggest that IL-7 could be involved in the observed homeostatic TEM proliferation. Our phosflow data revealed that a significantly increased percent of both CD4 and CD8 TEM were able to induce STAT5 phosphorylation in response to IL-7 *ex vivo* after anti-IL-15 Ab treatment compared to control Ab treatment. Confirming this observation *in vivo*, when anti-IL-15 Ab treated RM were dosed with IL-7, CD4 and CD8 TEM absolute numbers significantly increased compared to IgG control Ab treated RM dosed with IL-7. Interestingly, a previous study in RM showed that *in vivo* JAK3 inhibition caused CD8 and CD4 T cell depletion, but T cell numbers only rebounded after cessation of inhibitor dosing (129). This study suggests that a separate JAK3 mediated signaling event,

potentially IL-7 signaling, may be involved in the proliferation and accumulation of CD4 and CD8 TEM cells after IL-15 signal blockade in our system. Taken together and in line with our *in vitro* signaling data, it is likely that TEM are able to receive homeostatic signals from both IL-15 and IL-7 *in vivo* that help maintain TEM numbers despite immune system perturbations.

We further characterized the anti-IL-15 Ab induced TEM proliferation by identifying where in the RM TEM were proliferating. To that end, we dosed RM with BrdU at the peak of anti-IL-15 Ab induced TEM proliferation and immediatedly harvested tissues to monitor BrdU incorporation, and thus proliferation of TEM throughout the body. We observed significantly increased proliferation of TEM in WB, LN, kidney, lung, and liver, but we did not observe increased TEM BrdU incorporation in mucosal sites such as the BAL, colon, jejunum, ileum, or vaginal mucosa. This restriction of the homeostatic TEM proliferation to select tissues and organs further implicates that IL-7 is involved in the TEM homeostatic proliferative response. Although stromal fibroblastic reticular cells in lymphoid organs have been observed as primary producers of IL-7 (165, 166), IL-7 expression has also been detected in liver and kidney tissue as well (167). Thus, TEM proliferation was observed primarily in sites known to produce IL-7.

Because TEM proliferation was widespread in the body, we used immunostaining to visualize multiple tissues throughout the body to help identify any systemic phenotypic effects that were associated anti-IL-15 Ab compared to IgG1 control Ab treatment in RM. Interestingly, after anti-IL-15 Ab administration, we observed a significant increase of

active caspase-3 staining in tissues of RM compared to IgG control Ab dosing. Active caspase-3 has been shown to be a cellular mediator of apoptosis, likely indicating that cell death is increased in multiple RM tissues after IL-15 signal blockade (168).

An increase in active caspase-3 expression, indicating widespread cellular apoptosis was initially surprising because we observed the induction of TEM proliferation and rebound of absolute numbers in WB suggesting that the TEM population was receiving homeostatic signals that were supporting their renewal after depletion following IL-15 signal blockade. However, despite accumulation of TEM absolute numbers toward baseline levels in WB, TEM continued to proliferate throughout anti-IL-15 Ab administration potentially suggesting the population numbers were unstable. Furthermore, TEM remained relatively depleted in some tissues such as the colon following anti-IL-15 Ab treatment and TEM homeostatic proliferation. In an effort to understand these observations, we used microarray to analyze TEM expression profiles at the peak of their proliferative response to anti-IL-15 Ab compared to IgG control Ab administration. We observed an upregulation of activation and cell cycling genes indicating the cells had been induced to proliferate. Interestingly, there was also an increase in mitochondrial dysfunction genes associated with a deficit in cell energy. Our data thus suggests that TEM are becoming activated and entering into cell cycle, but once into cell cycle the TEM do not have adequate energy to complete replication and become pre-apoptotic; taken together, this data indicate that TEM are turning over at an increased rate.

Overall, our *in vitro* data suggest that RM IL-15 is involved in the homeostasis of both CD4 and CD8 TM cells. Interestingly, our data demonstrate that T cell dependence on IL-15 varies with the differentiation status of the TM cell subset. From our experiments administering anti-IL-15 Ab to RM, we confirmed that *in vivo*, IL-15 primarily functions to maintain effector memory T cell homeostasis. In the absence of IL-15 mediated signaling in RM, another homeostatic factor, likely IL-7, maintained TEM numbers but TEM exhibited a high-turnover homeostasis. Based on our own observations and data in the scientific literature, we propose a model whereby both IL-15 and IL-7 share regulation of TM homeostasis, though to varying degrees depending on the differentiation status of the TM subset (Figure 5-1). Whereas IL-7 primarily supports TCM homeostasis, IL-15 primarily supports TEM homeostasis and drives TEM differentiation from TCM. However, it is likely that both TCM and TEM are able to receive homeostatic signals from both IL-15 and IL-7, *in vivo*, to help maintain TM homeostasis despite immune system perturbations.

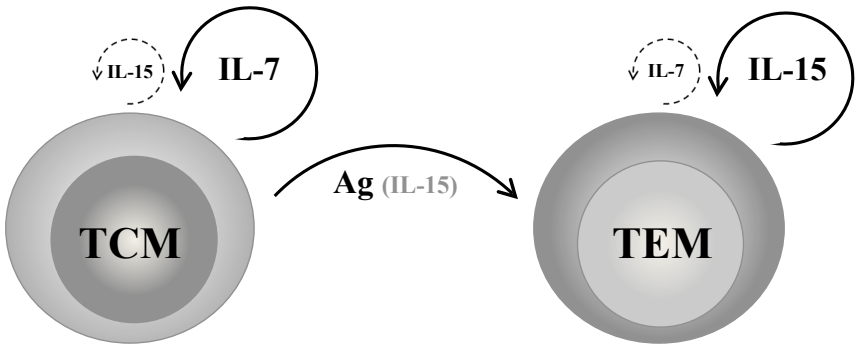

Figure 5-1 – Proposed model of TM homeostasis shared by both IL-15 and IL-7 - IL-15 and IL-7 share regulation of TM homeostasis, though to varying degrees depending on the differentiation status of the TM subset. Whereas IL-7 primarily supports TCM homeostasis, IL-15 primarily supports TEM homeostasis and drives TEM differentiation from TCM. However, it is likely that both TCM and TEM are able to receive homeostatic signals from both IL-15 and IL-7, *in vivo*, to help maintain TM homeostasis despite immune system perturbations.

We next used the anti-IL-15 Ab to understand how IL-15 affects T cell homeostasis during SIV-infection. Following anti-IL-15 Ab administration during SIV-infection, CD4 and CD8 TEM cell populations were initially depleted. CD4 and CD8 TEM cell populations were induced to proliferate which was associated with a rise in TEM absolute numbers back to pre-treatment levels. Increased proliferation was sustained throughout anti-IL-15 Ab treatment during both chronic and acute-phase SIV-infection. Surprisingly, increased proliferation did not cause an increase in depletion of CD4 T cells or an increase in viral loads due to increased numbers of viral target cells. Moreover, disease outcome remained unchanged in anti-IL-15 Ab compared to IgG1 control Ab treated RM during both acute- and chronic-phase SIV infection.

We monitored SIV-specific CD4 and CD8 T cell responses during both chronic and acute phase SIV-infection to understand how an IL-15 signal blockade would change antigen specific T cell responses during SIV-infection. IL-15 has been shown to increase the production of SIV-specific CD4 and CD8 T cell responses; however, during chronic SIV-infection, anti-IL-15 Ab administration caused no changes to SIV-specific CD4 or CD8 T cell responses compared to IgG control Ab administration. We did observe, however, anti-IL-15 Ab treatment led to decreases in SIV-specific CD4 and CD8 T cell responses in the whole blood during acute SIV-infection. Additionally, we observed a significant decrease in SIV-specific CD4 and CD8 T cell responses in the BAL following anti-IL-15 Ab administration during acute SIV-infection. Thus, our data support that production and maintenance of SIV-specific CD4 and CD8 T cell responses during acute SIV-infection are dependent on IL-15 signals in RM (104, 106-108). Our studies in

healthy RM indicate that CD4 and CD8 TEM absolute numbers can be supported by a homeostatic factor other than IL-15, likely IL-7. Thus, our data suggests that IL-7 is not able to maintain TEM function and antigen specific responses to the same extent that IL-7 is able to support absolute numbers and TEM homeostasis.

IL-15 and SIV pathogenesis

During pathogenic HIV/SIV infection and the resulting chronic immune activation, significantly increased IL-15 levels have been measured, potentially implicating increased IL-15 in driving depletion of CD4 T cell populations and pathogenesis (111, 135, 139, 140). Indeed, our measurements of IL-15 demonstrated increased IL-15 levels in both plasma and tissues of SIV-infected RM, confirming a dysregulation of this homeostatic cytokine during SIV-infection of RM. Of note, we also observed that sort-purified CD4 T cells from SIV-infected RM displayed a significantly delayed proliferation response when cultured with both γc chain cytokines IL-15 and IL-7. Anti-IL-15 antibody administration, however, did not significantly alter T cell depletion, viral loads, or disease outcome compared to control treated RM during either acute or chronic phase SIV-infection. Moreover, during chronic SIV-infection, we found that levels of other homeostatic cytokines measured in the plasma did not change in response to anti-IL-15 Ab administration, suggesting that increased IL-15 is not affecting changes in other cytokines. Thus IL-15 by itself is not a key factor either driving or protecting from pathogenesis. Rather it is likely IL-15 levels are dysregulated as a result of chronic immune activation, but not a primary driver of chronic immune activation.

Although previous studies showed that increased levels of IL-15 during SIV infection correlated to increased plasma viral loads and worse disease outcome, we observed that blockade of IL-15 signaling during acute SIV infection did not change either peak- or plateau-phase plasma SIV viral loads (111). Moreover, we did not see a change in disease progression following administration of anti-IL-15 Ab either during acute or chronic phase SIV-infection. Our data strongly suggest that although a correlation of plasma IL-15 levels and SIV plasma viral loads may exist, there is likely no causal effect of increased plasma IL-15 resulting in higher SIV viral loads. This supports previous data that showed that CD8 T cell depletion led a spike of IL-15 and rapic disease progression during SIV infection, but when IL-15 was neutralized rapid progression was not stopped. Rather, rapid progression was caused by a lack in CD8 T cell protection during infection (154). Taken all together, our data shows that increased IL-15 levels during SIV infection do not play a primary role driving SIV disease progression and CD4 T cell homeostatic failure and depletion.

References

1. WHO. Global Health Observatory Data Repository. 2011.
2. (UNAIDS) JUNPoHA. Report on the global HIV/AIDS epidemic 2008 2008 Contract No.: Document Number|.
3. Rodger AJ, Fox Z, Lundgren JD, Kuller LH, Boesecke C, Gey D, et al. Activation and coagulation biomarkers are independent predictors of the development of opportunistic disease in patients with HIV infection. J Infect Dis. 2009;200(6):973-83. PMCID: 2892757.
4. Silvestri G. AIDS pathogenesis: a tale of two monkeys. J Med Primatol. 2008;37 Suppl 2:6-12.
5. Pantaleo G, Graziosi C, Demarest JF, Butini L, Montroni M, Fox CH, et al. HIV infection is active and progressive in lymphoid tissue during the clinically latent stage of disease. Nature. 1993;362(6418):355-8.
6. Wei X, Ghosh SK, Taylor ME, Johnson VA, Emini EA, Deutsch P, et al. Viral dynamics in human immunodeficiency virus type 1 infection. Nature. 1995;373(6510):117-22.
7. Embretson J, Zupancic M, Ribas JL, Burke A, Racz P, Tenner-Racz K, et al. Massive covert infection of helper T lymphocytes and macrophages by HIV during the incubation period of AIDS. Nature. 1993;362(6418):359-62.
8. Mellors JW, Rinaldo CR, Jr., Gupta P, White RM, Todd JA, Kingsley LA. Prognosis in HIV-1 infection predicted by the quantity of virus in plasma. Science. 1996;272(5265):1167-70.
9. Lyles RH, Munoz A, Yamashita TE, Bazmi H, Detels R, Rinaldo CR, et al. Natural history of human immunodeficiency virus type 1 viremia after seroconversion and proximal to AIDS in a large cohort of homosexual men. Multicenter AIDS Cohort Study. J Infect Dis. 2000;181(3):872-80.
10. Giorgi JV, Hultin LE, McKeating JA, Johnson TD, Owens B, Jacobson LP, et al. Shorter survival in advanced human immunodeficiency virus type 1 infection is more closely associated with T lymphocyte activation than with plasma virus burden or virus chemokine coreceptor usage. J Infect Dis. 1999;179(4):859-70.
11. Deeks SG, Kitchen CM, Liu L, Guo H, Gascon R, Narvaez AB, et al. Immune activation set point during early HIV infection predicts subsequent CD4+ T-cell changes independent of viral load. Blood. 2004;104(4):942-7.
12. Hazenberg MD, Otto SA, van Benthem BH, Roos MT, Coutinho RA, Lange JM, et al. Persistent immune activation in HIV-1 infection is associated with progression to AIDS. AIDS. 2003;17(13):1881-8.
13. Brenchley JM, Price DA, Schacker TW, Asher TE, Silvestri G, Rao S, et al. Microbial translocation is a cause of systemic immune activation in chronic HIV infection. Nat Med. 2006;12(12):1365-71.
14. Valentine LE, Watkins DI. Relevance of studying T cell responses in SIV-infected rhesus macaques. Trends Microbiol. 2008;16(12):605-11.
15. Grossman Z, Picker LJ. Pathogenic mechanisms in simian immunodeficiency virus infection. Curr Opin HIV AIDS. 2008;3(3):380-6.

16. Hirsch VM, Lifson JD. Simian immunodeficiency virus infection of monkeys as a model system for the study of AIDS pathogenesis, treatment, and prevention. Adv Pharmacol. 2000;49:437-77.
17. Letvin NL, King NW. Immunologic and pathologic manifestations of the infection of rhesus monkeys with simian immunodeficiency virus of macaques. J Acquir Immune Defic Syndr. 1990;3(11):1023-40.
18. Estes JD. Role of collagen deposition in lymphatic tissues and immune reconstruction during HIV-1 and SIV infections. Curr HIV/AIDS Rep. 2009;6(1):29-35.
19. Sestak K. Chronic diarrhea and AIDS: insights into studies with non-human primates. Curr HIV Res. 2005;3(3):199-205.
20. Brown CR, Czapiga M, Kabat J, Dang Q, Ourmanov I, Nishimura Y, et al. Unique pathology in simian immunodeficiency virus-infected rapid progressor macaques is consistent with a pathogenesis distinct from that of classical AIDS. J Virol. 2007;81(11):5594-606. PMCID: 1900277.
21. Bassing CH, Swat W, Alt FW. The mechanism and regulation of chromosomal V(D)J recombination. Cell. 2002;109 Suppl:S45-55.
22. Sadofsky MJ. The RAG proteins in V(D)J recombination: more than just a nuclease. Nucleic Acids Res. 2001;29(7):1399-409. PMCID: 31291.
23. Mombaerts P, Iacomini J, Johnson RS, Herrup K, Tonegawa S, Papaioannou VE. RAG-1-deficient mice have no mature B and T lymphocytes. Cell. 1992;68(5):869-77.
24. Pitcher CJ, Hagen SI, Walker JM, Lum R, Mitchell BL, Maino VC, et al. Development and homeostasis of T cell memory in rhesus macaque. J Immunol. 2002;168(1):29-43.
25. Picker LJ, Reed-Inderbitzin EF, Hagen SI, Edgar JB, Hansen SG, Legasse A, et al. IL-15 induces CD4 effector memory T cell production and tissue emigration in nonhuman primates. J Clin Invest. 2006;116(6):1514-24. PMCID: 1459071.
26. Sallusto F, Geginat J, Lanzavecchia A. Central memory and effector memory T cell subsets: function, generation, and maintenance. Annu Rev Immunol. 2004;22:745-63.
27. Lanzavecchia A, Sallusto F. Dynamics of T lymphocyte responses: intermediates, effectors, and memory cells. Science. 2000;290(5489):92-7.
28. Esser MT, Marchese RD, Kierstead LS, Tussey LG, Wang F, Chirmule N, et al. Memory T cells and vaccines. Vaccine. 2003;21(5-6):419-30.
29. Lanzavecchia A, Sallusto F. Understanding the generation and function of memory T cell subsets. Curr Opin Immunol. 2005;17(3):326-32.
30. Willinger T, Freeman T, Hasegawa H, McMichael AJ, Callan MF. Molecular signatures distinguish human central memory from effector memory CD8 T cell subsets. J Immunol. 2005;175(9):5895-903.
31. Picker LJ, Hagen SI, Lum R, Reed-Inderbitzin EF, Daly LM, Sylwester AW, et al. Insufficient production and tissue delivery of CD4+ memory T cells in rapidly progressive simian immunodeficiency virus infection. J Exp Med. 2004;200(10):1299-314. PMCID: 2211921.
32. Okoye A, Meier-Schellersheim M, Brenchley JM, Hagen SI, Walker JM, Rohankhedkar M, et al. Progressive CD4+ central memory T cell decline results in CD4+

effector memory insufficiency and overt disease in chronic SIV infection. J Exp Med. 2007;204(9):2171-85. PMCID: 2118701.
33. Takeda S, Rodewald HR, Arakawa H, Bluethmann H, Shimizu T. MHC class II molecules are not required for survival of newly generated CD4+ T cells, but affect their long-term life span. Immunity. 1996;5(3):217-28.
34. Swain SL, Hu H, Huston G. Class II-independent generation of CD4 memory T cells from effectors. Science. 1999;286(5443):1381-3.
35. Murali-Krishna K, Lau LL, Sambhara S, Lemonnier F, Altman J, Ahmed R. Persistence of memory CD8 T cells in MHC class I-deficient mice. Science. 1999;286(5443):1377-81.
36. Leignadier J, Hardy MP, Cloutier M, Rooney J, Labrecque N. Memory T-lymphocyte survival does not require T-cell receptor expression. Proc Natl Acad Sci U S A. 2008;105(51):20440-5. PMCID: 2629296.
37. Martin B, Becourt C, Bienvenu B, Lucas B. Self-recognition is crucial for maintaining the peripheral CD4+ T-cell pool in a nonlymphopenic environment. Blood. 2006;108(1):270-7.
38. Takada K, Jameson SC. Self-class I MHC molecules support survival of naive CD8 T cells, but depress their functional sensitivity through regulation of CD8 expression levels. J Exp Med. 2009;206(10):2253-69. PMCID: 2757867.
39. Nakajima H, Shores EW, Noguchi M, Leonard WJ. The common cytokine receptor gamma chain plays an essential role in regulating lymphoid homeostasis. J Exp Med. 1997;185(2):189-95. PMCID: 2196113.
40. DiSanto JP, Muller W, Guy-Grand D, Fischer A, Rajewsky K. Lymphoid development in mice with a targeted deletion of the interleukin 2 receptor gamma chain. Proc Natl Acad Sci U S A. 1995;92(2):377-81. PMCID: 42743.
41. Cao X, Shores EW, Hu-Li J, Anver MR, Kelsall BL, Russell SM, et al. Defective lymphoid development in mice lacking expression of the common cytokine receptor gamma chain. Immunity. 1995;2(3):223-38.
42. Noguchi M, Yi H, Rosenblatt HM, Filipovich AH, Adelstein S, Modi WS, et al. Interleukin-2 receptor gamma chain mutation results in X-linked severe combined immunodeficiency in humans. Cell. 1993;73(1):147-57.
43. Kondo M, Takeshita T, Ishii N, Nakamura M, Watanabe S, Arai K, et al. Sharing of the interleukin-2 (IL-2) receptor gamma chain between receptors for IL-2 and IL-4. Science. 1993;262(5141):1874-7.
44. Russell SM, Keegan AD, Harada N, Nakamura Y, Noguchi M, Leland P, et al. Interleukin-2 receptor gamma chain: a functional component of the interleukin-4 receptor. Science. 1993;262(5141):1880-3.
45. Noguchi M, Nakamura Y, Russell SM, Ziegler SF, Tsang M, Cao X, et al. Interleukin-2 receptor gamma chain: a functional component of the interleukin-7 receptor. Science. 1993;262(5141):1877-80.
46. Kondo M, Takeshita T, Higuchi M, Nakamura M, Sudo T, Nishikawa S, et al. Functional participation of the IL-2 receptor gamma chain in IL-7 receptor complexes. Science. 1994;263(5152):1453-4.

47. Russell SM, Johnston JA, Noguchi M, Kawamura M, Bacon CM, Friedmann M, et al. Interaction of IL-2R beta and gamma c chains with Jak1 and Jak3: implications for XSCID and XCID. Science. 1994;266(5187):1042-5.
48. Kimura Y, Takeshita T, Kondo M, Ishii N, Nakamura M, Van Snick J, et al. Sharing of the IL-2 receptor gamma chain with the functional IL-9 receptor complex. Int Immunol. 1995;7(1):115-20.
49. Asao H, Okuyama C, Kumaki S, Ishii N, Tsuchiya S, Foster D, et al. Cutting edge: the common gamma-chain is an indispensable subunit of the IL-21 receptor complex. J Immunol. 2001;167(1):1-5.
50. Surh CD, Sprent J. Homeostasis of naive and memory T cells. Immunity. 2008;29(6):848-62.
51. Ma A, Koka R, Burkett P. Diverse functions of IL-2, IL-15, and IL-7 in lymphoid homeostasis. Annu Rev Immunol. 2006;24:657-79.
52. Boyman O, Purton JF, Surh CD, Sprent J. Cytokines and T-cell homeostasis. Curr Opin Immunol. 2007;19(3):320-6.
53. Boyman O, Krieg C, Homann D, Sprent J. Homeostatic maintenance of T cells and natural killer cells. Cell Mol Life Sci. 2012;69(10):1597-608.
54. Fry TJ, Moniuszko M, Creekmore S, Donohue SJ, Douek DC, Giardina S, et al. IL-7 therapy dramatically alters peripheral T-cell homeostasis in normal and SIV-infected nonhuman primates. Blood. 2003;101(6):2294-9.
55. Moniuszko M, Fry T, Tsai WP, Morre M, Assouline B, Cortez P, et al. Recombinant interleukin-7 induces proliferation of naive macaque CD4+ and CD8+ T cells in vivo. J Virol. 2004;78(18):9740-9. PMCID: 515001.
56. Prlic M, Lefrancois L, Jameson SC. Multiple choices: regulation of memory CD8 T cell generation and homeostasis by interleukin (IL)-7 and IL-15. J Exp Med. 2002;195(12):F49-52. PMCID: 2193558.
57. Kondrack RM, Harbertson J, Tan JT, McBreen ME, Surh CD, Bradley LM. Interleukin 7 regulates the survival and generation of memory CD4 cells. J Exp Med. 2003;198(12):1797-806. PMCID: 2194153.
58. Lenz DC, Kurz SK, Lemmens E, Schoenberger SP, Sprent J, Oldstone MB, et al. IL-7 regulates basal homeostatic proliferation of antiviral CD4+T cell memory. Proc Natl Acad Sci U S A. 2004;101(25):9357-62. PMCID: 438981.
59. Seddon B, Tomlinson P, Zamoyska R. Interleukin 7 and T cell receptor signals regulate homeostasis of CD4 memory cells. Nat Immunol. 2003;4(7):680-6.
60. Purton JF, Tan JT, Rubinstein MP, Kim DM, Sprent J, Surh CD. Antiviral CD4+ memory T cells are IL-15 dependent. J Exp Med. 2007;204(4):951-61. PMCID: 2118539.
61. Ohteki T, Suzue K, Maki C, Ota T, Koyasu S. Critical role of IL-15-IL-15R for antigen-presenting cell functions in the innate immune response. Nat Immunol. 2001;2(12):1138-43.
62. Ohteki T. Critical role for IL-15 in innate immunity. Curr Mol Med. 2002;2(4):371-80.
63. Pelletier M, Ratthe C, Girard D. Mechanisms involved in interleukin-15-induced suppression of human neutrophil apoptosis: role of the anti-apoptotic Mcl-1 protein and

several kinases including Janus kinase-2, p38 mitogen-activated protein kinase and extracellular signal-regulated kinases-1/2. FEBS Lett. 2002;532(1-2):164-70.
64. Ottonello L, Frumento G, Arduino N, Bertolotto M, Dapino P, Mancini M, et al. Differential regulation of spontaneous and immune complex-induced neutrophil apoptosis by proinflammatory cytokines. Role of oxidants, Bax and caspase-3. J Leukoc Biol. 2002;72(1):125-32.
65. Kennedy MK, Park LS. Characterization of interleukin-15 (IL-15) and the IL-15 receptor complex. J Clin Immunol. 1996;16(3):134-43.
66. Armitage RJ, Macduff BM, Eisenman J, Paxton R, Grabstein KH. IL-15 has stimulatory activity for the induction of B cell proliferation and differentiation. J Immunol. 1995;154(2):483-90.
67. Bulfone-Paus S, Ungureanu D, Pohl T, Lindner G, Paus R, Ruckert R, et al. Interleukin-15 protects from lethal apoptosis in vivo. Nat Med. 1997;3(10):1124-8.
68. Musso T, Calosso L, Zucca M, Millesimo M, Puliti M, Bulfone-Paus S, et al. Interleukin-15 activates proinflammatory and antimicrobial functions in polymorphonuclear cells. Infect Immun. 1998;66(6):2640-7. PMCID: 108250.
69. Badolato R, Ponzi AN, Millesimo M, Notarangelo LD, Musso T. Interleukin-15 (IL-15) induces IL-8 and monocyte chemotactic protein 1 production in human monocytes. Blood. 1997;90(7):2804-9.
70. Jinushi M, Takehara T, Tatsumi T, Kanto T, Groh V, Spies T, et al. Autocrine/paracrine IL-15 that is required for type I IFN-mediated dendritic cell expression of MHC class I-related chain A and B is impaired in hepatitis C virus infection. J Immunol. 2003;171(10):5423-9.
71. Dubois SP, Waldmann TA, Muller JR. Survival adjustment of mature dendritic cells by IL-15. Proc Natl Acad Sci U S A. 2005;102(24):8662-7. PMCID: 1150852.
72. Mrozek E, Anderson P, Caligiuri MA. Role of interleukin-15 in the development of human CD56+ natural killer cells from CD34+ hematopoietic progenitor cells. Blood. 1996;87(7):2632-40.
73. Carson WE, Ross ME, Baiocchi RA, Marien MJ, Boiani N, Grabstein K, et al. Endogenous production of interleukin 15 by activated human monocytes is critical for optimal production of interferon-gamma by natural killer cells in vitro. J Clin Invest. 1995;96(6):2578-82. PMCID: 185961.
74. Carson WE, Giri JG, Lindemann MJ, Linett ML, Ahdieh M, Paxton R, et al. Interleukin (IL) 15 is a novel cytokine that activates human natural killer cells via components of the IL-2 receptor. J Exp Med. 1994;180(4):1395-403. PMCID: 2191697.
75. Giri JG, Kumaki S, Ahdieh M, Friend DJ, Loomis A, Shanebeck K, et al. Identification and cloning of a novel IL-15 binding protein that is structurally related to the alpha chain of the IL-2 receptor. EMBO J. 1995;14(15):3654-63. PMCID: 394440.
76. Grabstein KH, Eisenman J, Shanebeck K, Rauch C, Srinivasan S, Fung V, et al. Cloning of a T cell growth factor that interacts with the beta chain of the interleukin-2 receptor. Science. 1994;264(5161):965-8.
77. Giri JG, Ahdieh M, Eisenman J, Shanebeck K, Grabstein K, Kumaki S, et al. Utilization of the beta and gamma chains of the IL-2 receptor by the novel cytokine IL-15. EMBO J. 1994;13(12):2822-30. PMCID: 395163.

78. Johnston JA, Bacon CM, Finbloom DS, Rees RC, Kaplan D, Shibuya K, et al. Tyrosine phosphorylation and activation of STAT5, STAT3, and Janus kinases by interleukins 2 and 15. Proc Natl Acad Sci U S A. 1995;92(19):8705-9. PMCID: 41035.
79. Huntington ND, Puthalakath H, Gunn P, Naik E, Michalak EM, Smyth MJ, et al. Interleukin 15-mediated survival of natural killer cells is determined by interactions among Bim, Noxa and Mcl-1. Nat Immunol. 2007;8(8):856-63. PMCID: 2951739.
80. Hildeman D, Jorgensen T, Kappler J, Marrack P. Apoptosis and the homeostatic control of immune responses. Curr Opin Immunol. 2007;19(5):516-21.
81. Rochman Y, Spolski R, Leonard WJ. New insights into the regulation of T cells by gamma(c) family cytokines. Nat Rev Immunol. 2009;9(7):480-90. PMCID: 2814538.
82. Minagawa M, Watanabe H, Miyaji C, Tomiyama K, Shimura H, Ito A, et al. Enforced expression of Bcl-2 restores the number of NK cells, but does not rescue the impaired development of NKT cells or intraepithelial lymphocytes, in IL-2/IL-15 receptor beta-chain-deficient mice. J Immunol. 2002;169(8):4153-60.
83. Nakazato K, Yamada H, Yajima T, Kagimoto Y, Kuwano H, Yoshikai Y. Enforced expression of Bcl-2 partially restores cell numbers but not functions of TCRgammadelta intestinal intraepithelial T lymphocytes in IL-15-deficient mice. J Immunol. 2007;178(2):757-64.
84. Miyazaki T, Liu ZJ, Kawahara A, Minami Y, Yamada K, Tsujimoto Y, et al. Three distinct IL-2 signaling pathways mediated by bcl-2, c-myc, and lck cooperate in hematopoietic cell proliferation. Cell. 1995;81(2):223-31.
85. Koka R, Burkett PR, Chien M, Chai S, Chan F, Lodolce JP, et al. Interleukin (IL)-15R[alpha]-deficient natural killer cells survive in normal but not IL-15R[alpha]-deficient mice. J Exp Med. 2003;197(8):977-84. PMCID: 2193874.
86. Burkett PR, Koka R, Chien M, Chai S, Boone DL, Ma A. Coordinate expression and trans presentation of interleukin (IL)-15Ralpha and IL-15 supports natural killer cell and memory CD8+ T cell homeostasis. J Exp Med. 2004;200(7):825-34. PMCID: 2213280.
87. Castillo EF, Stonier SW, Frasca L, Schluns KS. Dendritic cells support the in vivo development and maintenance of NK cells via IL-15 trans-presentation. J Immunol. 2009;183(8):4948-56.
88. Dubois S, Mariner J, Waldmann TA, Tagaya Y. IL-15Ralpha recycles and presents IL-15 In trans to neighboring cells. Immunity. 2002;17(5):537-47.
89. Castillo EF, Schluns KS. Regulating the immune system via IL-15 transpresentation. Cytokine.59(3):479-90. PMCID: 3422378.
90. Prlic M, Blazar BR, Farrar MA, Jameson SC. In vivo survival and homeostatic proliferation of natural killer cells. J Exp Med. 2003;197(8):967-76. PMCID: 2193876.
91. Mortier E, Advincula R, Kim L, Chmura S, Barrera J, Reizis B, et al. Macrophage- and dendritic-cell-derived interleukin-15 receptor alpha supports homeostasis of distinct CD8+ T cell subsets. Immunity. 2009;31(5):811-22.
92. Musso T, Calosso L, Zucca M, Millesimo M, Ravarino D, Giovarelli M, et al. Human monocytes constitutively express membrane-bound, biologically active, and interferon-gamma-upregulated interleukin-15. Blood. 1999;93(10):3531-9.

93. Mortier E, Woo T, Advincula R, Gozalo S, Ma A. IL-15Ralpha chaperones IL-15 to stable dendritic cell membrane complexes that activate NK cells via trans presentation. J Exp Med. 2008;205(5):1213-25. PMCID: 2373851.
94. Lucas M, Schachterle W, Oberle K, Aichele P, Diefenbach A. Dendritic cells prime natural killer cells by trans-presenting interleukin 15. Immunity. 2007;26(4):503-17. PMCID: 2084390.
95. Mortier E, Bernard J, Plet A, Jacques Y. Natural, proteolytic release of a soluble form of human IL-15 receptor alpha-chain that behaves as a specific, high affinity IL-15 antagonist. J Immunol. 2004;173(3):1681-8.
96. Bergamaschi C, Bear J, Rosati M, Beach RK, Alicea C, Sowder R, et al. Circulating IL-15 exists as heterodimeric complex with soluble IL-15Ralpha in human and mouse serum. Blood.120(1):e1-8. PMCID: 3390963.
97. Schluns KS, Lefrancois L. Cytokine control of memory T-cell development and survival. Nat Rev Immunol. 2003;3(4):269-79.
98. Dubois S, Shou W, Haneline LS, Fleischer S, Waldmann TA, Muller JR. Distinct pathways involving the FK506-binding proteins 12 and 12.6 underlie IL-2-versus IL-15-mediated proliferation of T cells. Proc Natl Acad Sci U S A. 2003;100(24):14169-74. PMCID: 283564.
99. Lodolce JP, Boone DL, Chai S, Swain RE, Dassopoulos T, Trettin S, et al. IL-15 receptor maintains lymphoid homeostasis by supporting lymphocyte homing and proliferation. Immunity. 1998;9(5):669-76.
100. Wherry EJ, Becker TC, Boone D, Kaja MK, Ma A, Ahmed R. Homeostatic proliferation but not the generation of virus specific memory CD8 T cells is impaired in the absence of IL-15 or IL-15Ralpha. Adv Exp Med Biol. 2002;512:165-75.
101. Kennedy MK, Glaccum M, Brown SN, Butz EA, Viney JL, Embers M, et al. Reversible defects in natural killer and memory CD8 T cell lineages in interleukin 15-deficient mice. J Exp Med. 2000;191(5):771-80. PMCID: 2195858.
102. Zhang X, Sun S, Hwang I, Tough DF, Sprent J. Potent and selective stimulation of memory-phenotype CD8+ T cells in vivo by IL-15. Immunity. 1998;8(5):591-9.
103. Becker TC, Wherry EJ, Boone D, Murali-Krishna K, Antia R, Ma A, et al. Interleukin 15 is required for proliferative renewal of virus-specific memory CD8 T cells. J Exp Med. 2002;195(12):1541-8. PMCID: 2193552.
104. Schluns KS, Williams K, Ma A, Zheng XX, Lefrancois L. Cutting edge: requirement for IL-15 in the generation of primary and memory antigen-specific CD8 T cells. J Immunol. 2002;168(10):4827-31.
105. Boyer JD, Robinson TM, Kutzler MA, Vansant G, Hokey DA, Kumar S, et al. Protection against simian/human immunodeficiency virus (SHIV) 89.6P in macaques after coimmunization with SHIV antigen and IL-15 plasmid. Proc Natl Acad Sci U S A. 2007;104(47):18648-53. PMCID: 2141831.
106. Saito K, Yajima T, Kumabe S, Doi T, Yamada H, Sad S, et al. Impaired protection against Mycobacterium bovis bacillus Calmette-Guerin infection in IL-15-deficient mice. J Immunol. 2006;176(4):2496-504.

107. Bhadra R, Guan H, Khan IA. Absence of both IL-7 and IL-15 severely impairs the development of CD8 T cell response against Toxoplasma gondii. PLoS One.5(5):e10842. PMCID: 2877110.
108. Tripathi P, Kurtulus S, Wojciechowski S, Sholl A, Hoebe K, Morris SC, et al. STAT5 is critical to maintain effector CD8+ T cell responses. J Immunol.185(4):2116-24. PMCID: 2991082.
109. Kaech SM, Hemby S, Kersh E, Ahmed R. Molecular and functional profiling of memory CD8 T cell differentiation. Cell. 2002;111(6):837-51.
110. Geginat J, Sallusto F, Lanzavecchia A. Cytokine-driven proliferation and differentiation of human naive, central memory, and effector memory CD4(+) T cells. J Exp Med. 2001;194(12):1711-9. PMCID: 2193568.
111. Eberly MD, Kader M, Hassan W, Rogers KA, Zhou J, Mueller YM, et al. Increased IL-15 production is associated with higher susceptibility of memory CD4 T cells to simian immunodeficiency virus during acute infection. J Immunol. 2009;182(3):1439-48. PMCID: 2662754.
112. Mueller YM, Do DH, Altork SR, Artlett CM, Gracely EJ, Katsetos CD, et al. IL-15 treatment during acute simian immunodeficiency virus (SIV) infection increases viral set point and accelerates disease progression despite the induction of stronger SIV-specific CD8+ T cell responses. J Immunol. 2008;180(1):350-60.
113. McKinlay A, Radford K, Kato M, Field K, Gardiner D, Khalil D, et al. Blood monocytes, myeloid dendritic cells and the cytokines interleukin (IL)-7 and IL-15 maintain human CD4+ T memory cells with mixed helper/regulatory function. Immunology. 2007;120(3):392-403. PMCID: 2265893.
114. Lugli E, Goldman CK, Perera LP, Smedley J, Pung R, Yovandich JL, et al. Transient and persistent effects of IL-15 on lymphocyte homeostasis in nonhuman primates. Blood.116(17):3238-48. PMCID: 2995354.
115. Sneller MC, Kopp WC, Engelke KJ, Yovandich JL, Creekmore SP, Waldmann TA, et al. IL-15 administered by continuous infusion to rhesus macaques induces massive expansion of CD8+ T effector memory population in peripheral blood. Blood.118(26):6845-8. PMCID: 3245206.
116. Berger C, Berger M, Hackman RC, Gough M, Elliott C, Jensen MC, et al. Safety and immunologic effects of IL-15 administration in nonhuman primates. Blood. 2009;114(12):2417-26. PMCID: 2746471.
117. Berger C, Berger M, Beard BC, Kiem HP, Gooley TA, Riddell SR. Proliferation-linked apoptosis of adoptively transferred T cells after IL-15 administration in macaques. PLoS One.8(2):e56268. PMCID: 3572023.
118. Villinger F, Miller R, Mori K, Mayne AE, Bostik P, Sundstrom JB, et al. IL-15 is superior to IL-2 in the generation of long-lived antigen specific memory CD4 and CD8 T cells in rhesus macaques. Vaccine. 2004;22(25-26):3510-21.
119. Kanai T, Thomas EK, Yasutomi Y, Letvin NL. IL-15 stimulates the expansion of AIDS virus-specific CTL. J Immunol. 1996;157(8):3681-7.
120. Farag SS, Caligiuri MA. Human natural killer cell development and biology. Blood Rev. 2006;20(3):123-37.

121. Jamieson AM, Isnard P, Dorfman JR, Coles MC, Raulet DH. Turnover and proliferation of NK cells in steady state and lymphopenic conditions. J Immunol. 2004;172(2):864-70.
122. Cooper MA, Bush JE, Fehniger TA, VanDeusen JB, Waite RE, Liu Y, et al. In vivo evidence for a dependence on interleukin 15 for survival of natural killer cells. Blood. 2002;100(10):3633-8.
123. Ranson T, Vosshenrich CA, Corcuff E, Richard O, Muller W, Di Santo JP. IL-15 is an essential mediator of peripheral NK-cell homeostasis. Blood. 2003;101(12):4887-93.
124. Hochweller K, Striegler J, Hammerling GJ, Garbi N. A novel CD11c.DTR transgenic mouse for depletion of dendritic cells reveals their requirement for homeostatic proliferation of natural killer cells. Eur J Immunol. 2008;38(10):2776-83.
125. Koka R, Burkett P, Chien M, Chai S, Boone DL, Ma A. Cutting edge: murine dendritic cells require IL-15R alpha to prime NK cells. J Immunol. 2004;173(6):3594-8.
126. Kallies A, Carotta S, Huntington ND, Bernard NJ, Tarlinton DM, Smyth MJ, et al. A role for Blimp1 in the transcriptional network controlling natural killer cell maturation. Blood.117(6):1869-79.
127. Imada K, Bloom ET, Nakajima H, Horvath-Arcidiacono JA, Udy GB, Davey HW, et al. Stat5b is essential for natural killer cell-mediated proliferation and cytolytic activity. J Exp Med. 1998;188(11):2067-74. PMCID: 2212377.
128. Takahashi Y, Mayne AE, Khowawisetsut L, Pattanapanyasat K, Little D, Villinger F, et al. In Vivo Administration of a JAK3 Inhibitor to Chronically SIV Infected Rhesus Macaques Leads to NK Cell Depletion Associated with Transient Modest Increase in Viral Loads. PLoS One.8(7):e70992. PMCID: 3724739.
129. Conklyn M, Andresen C, Changelian P, Kudlacz E. The JAK3 inhibitor CP-690550 selectively reduces NK and CD8+ cell numbers in cynomolgus monkey blood following chronic oral dosing. J Leukoc Biol. 2004;76(6):1248-55.
130. Lebrec H, Horner MJ, Gorski KS, Tsuji W, Xia D, Pan WJ, et al. Homeostasis of Human NK Cells Is Not IL-15 Dependent. J Immunol.191(11):5551-8.
131. Baslund B, Tvede N, Danneskiold-Samsoe B, Larsson P, Panayi G, Petersen J, et al. Targeting interleukin-15 in patients with rheumatoid arthritis: a proof-of-concept study. Arthritis Rheum. 2005;52(9):2686-92.
132. Russell SM, Tayebi N, Nakajima H, Riedy MC, Roberts JL, Aman MJ, et al. Mutation of Jak3 in a patient with SCID: essential role of Jak3 in lymphoid development. Science. 1995;270(5237):797-800.
133. Macchi P, Villa A, Giliani S, Sacco MG, Frattini A, Porta F, et al. Mutations of Jak-3 gene in patients with autosomal severe combined immune deficiency (SCID). Nature. 1995;377(6544):65-8.
134. Henningsson L, Jirholt P, Bogestal YR, Eneljung T, Adiels M, Lindholm C, et al. Interleukin 15 mediates joint destruction in Staphylococcus aureus arthritis. J Infect Dis.206(5):687-96.
135. Roberts L, Passmore JA, Williamson C, Little F, Bebell LM, Mlisana K, et al. Plasma cytokine levels during acute HIV-1 infection predict HIV disease progression. AIDS.24(6):819-31. PMCID: 3001189.

136. Abadie V, Discepolo V, Jabri B. Intraepithelial lymphocytes in celiac disease immunopathology. Semin Immunopathol.34(4):551-66.
137. Zdrenghea MT, Mallia P, Johnston SL. Immunological pathways in virus-induced COPD exacerbations: a role for IL-15. Eur J Clin Invest.42(9):1010-5.
138. Waldmann TA, Conlon KC, Stewart DM, Worthy TA, Janik JE, Fleisher TA, et al. Phase 1 trial of IL-15 trans presentation blockade using humanized Mik-Beta-1 mAb in patients with T-cell large granular lymphocytic leukemia. Blood.121(3):476-84. PMCID: 3548167.
139. Caufour P, Le Grand R, Cheret A, Neildez O, Thiebot H, Theodoro F, et al. Longitudinal analysis of CD8(+) T-cell phenotype and IL-7, IL-15 and IL-16 mRNA expression in different tissues during primary simian immunodeficiency virus infection. Microbes Infect. 2001;3(3):181-91.
140. Stacey AR, Norris PJ, Qin L, Haygreen EA, Taylor E, Heitman J, et al. Induction of a striking systemic cytokine cascade prior to peak viremia in acute human immunodeficiency virus type 1 infection, in contrast to more modest and delayed responses in acute hepatitis B and C virus infections. J Virol. 2009;83(8):3719-33. PMCID: 2663284.
141. Mueller YM, Petrovas C, Bojczuk PM, Dimitriou ID, Beer B, Silvera P, et al. Interleukin-15 increases effector memory CD8+ t cells and NK Cells in simian immunodeficiency virus-infected macaques. J Virol. 2005;79(8):4877-85. PMCID: 1069542.
142. Calarota SA, Otero M, Hermanstyne K, Lewis M, Rosati M, Felber BK, et al. Use of interleukin 15 to enhance interferon-gamma production by antigen-specific stimulated lymphocytes from rhesus macaques. J Immunol Methods. 2003;279(1-2):55-67.
143. Neeson P, Boyer J, Kumar S, Lewis MG, Mattias L, Veazey R, et al. A DNA prime-oral Listeria boost vaccine in rhesus macaques induces a SIV-specific CD8 T cell mucosal response characterized by high levels of alpha4beta7 integrin and an effector memory phenotype. Virology. 2006;354(2):299-315. PMCID: 1635491.
144. Halwani R, Boyer JD, Yassine-Diab B, Haddad EK, Robinson TM, Kumar S, et al. Therapeutic vaccination with simian immunodeficiency virus (SIV)-DNA + IL-12 or IL-15 induces distinct CD8 memory subsets in SIV-infected macaques. J Immunol. 2008;180(12):7969-79.
145. Demberg T, Boyer JD, Malkevich N, Patterson LJ, Venzon D, Summers EL, et al. Sequential priming with simian immunodeficiency virus (SIV) DNA vaccines, with or without encoded cytokines, and a replicating adenovirus-SIV recombinant followed by protein boosting does not control a pathogenic SIVmac251 mucosal challenge. J Virol. 2008;82(21):10911-21. PMCID: 2573219.
146. Yin J, Dai A, Kutzler MA, Shen A, Lecureux J, Lewis MG, et al. Sustained suppression of SHIV89.6P replication in macaques by vaccine-induced CD8+ memory T cells. AIDS. 2008;22(14):1739-48.
147. Dubie RA, Maksaereekul S, Shacklett BL, Lemongello D, Cole KS, Villinger F, et al. Co-immunization with IL-15 enhances cellular immune responses induced by a vif-deleted simian immunodeficiency virus proviral DNA vaccine and confers partial

protection against vaginal challenge with SIVmac251. Virology. 2009;386(1):109-21. PMCID: 3640844.
148. Soloff AC, Liu X, Gao W, Day RD, Gambotto A, Barratt-Boyes SM. Adenovirus 5- and 35-based immunotherapy enhances the strength but not breadth or quality of immunity during chronic SIV infection. Eur J Immunol. 2009;39(9):2437-49.
149. Yin J, Dai A, Laddy DJ, Yan J, Arango T, Khan AS, et al. High dose of plasmid IL-15 inhibits immune responses in an influenza non-human primates immunogenicity model. Virology. 2009;393(1):49-55.
150. Manrique M, Kozlowski PA, Wang SW, Wilson RL, Micewicz E, Montefiori DC, et al. Nasal DNA-MVA SIV vaccination provides more significant protection from progression to AIDS than a similar intramuscular vaccination. Mucosal Immunol. 2009;2(6):536-50.
151. Sui Y, Zhu Q, Gagnon S, Dzutsev A, Terabe M, Vaccari M, et al. Innate and adaptive immune correlates of vaccine and adjuvant-induced control of mucosal transmission of SIV in macaques. Proc Natl Acad Sci U S A.107(21):9843-8. PMCID: 2906837.
152. Valentin A, von Gegerfelt A, Rosati M, Miteloudis G, Alicea C, Bergamaschi C, et al. Repeated DNA therapeutic vaccination of chronically SIV-infected macaques provides additional virological benefit. Vaccine.28(8):1962-74. PMCID: 2830913.
153. Lugli E, Mueller YM, Lewis MG, Villinger F, Katsikis PD, Roederer M. IL-15 delays suppression and fails to promote immune reconstitution in virally suppressed chronically SIV-infected macaques. Blood.118(9):2520-9. PMCID: 3167360.
154. Okoye A, Park H, Rohankhedkar M, Coyne-Johnson L, Lum R, Walker JM, et al. Profound CD4+/CCR5+ T cell expansion is induced by CD8+ lymphocyte depletion but does not account for accelerated SIV pathogenesis. J Exp Med. 2009;206(7):1575-88. PMCID: 2715089.
155. Walker JM, Maecker HT, Maino VC, Picker LJ. Multicolor flow cytometric analysis in SIV-infected rhesus macaque. Methods Cell Biol. 2004;75:535-57.
156. Alves NL, Hooibrink B, Arosa FA, van Lier RA. IL-15 induces antigen-independent expansion and differentiation of human naive CD8+ T cells in vitro. Blood. 2003;102(7):2541-6.
157. Rathmell JC, Farkash EA, Gao W, Thompson CB. IL-7 enhances the survival and maintains the size of naive T cells. J Immunol. 2001;167(12):6869-76.
158. Schluns KS, Kieper WC, Jameson SC, Lefrancois L. Interleukin-7 mediates the homeostasis of naive and memory CD8 T cells in vivo. Nat Immunol. 2000;1(5):426-32.
159. Boyman O, Kovar M, Rubinstein MP, Surh CD, Sprent J. Selective stimulation of T cell subsets with antibody-cytokine immune complexes. Science. 2006;311(5769):1924-7.
160. Stancovski I, Hurwitz E, Leitner O, Ullrich A, Yarden Y, Sela M. Mechanistic aspects of the opposing effects of monoclonal antibodies to the ERBB2 receptor on tumor growth. Proc Natl Acad Sci U S A. 1991;88(19):8691-5. PMCID: 52575.
161. Finch DK, Midha A, Buchanan CL, Cochrane D, Craggs RI, Cruwys S, et al. Identification of a potent anti-IL-15 antibody with opposing mechanisms of action in vitro and in vivo. Br J Pharmacol.162(2):480-90. PMCID: 3031067.

162. Boyman O, Ramsey C, Kim DM, Sprent J, Surh CD. IL-7/anti-IL-7 mAb complexes restore T cell development and induce homeostatic T Cell expansion without lymphopenia. J Immunol. 2008;180(11):7265-75.
163. Rubinstein MP, Kovar M, Purton JF, Cho JH, Boyman O, Surh CD, et al. Converting IL-15 to a superagonist by binding to soluble IL-15R{alpha}. Proc Natl Acad Sci U S A. 2006;103(24):9166-71. PMCID: 1482584.
164. Chertova E, Bergamaschi C, Chertov O, Sowder R, Bear J, Roser JD, et al. Characterization and favorable in vivo properties of heterodimeric soluble IL-15.IL-15Ralpha cytokine compared to IL-15 monomer. J Biol Chem.288(25):18093-103. PMCID: 3689953.
165. Jiang Q, Li WQ, Aiello FB, Mazzucchelli R, Asefa B, Khaled AR, et al. Cell biology of IL-7, a key lymphotrophin. Cytokine Growth Factor Rev. 2005;16(4-5):513-33.
166. Link A, Vogt TK, Favre S, Britschgi MR, Acha-Orbea H, Hinz B, et al. Fibroblastic reticular cells in lymph nodes regulate the homeostasis of naive T cells. Nat Immunol. 2007;8(11):1255-65.
167. Sawa Y, Arima Y, Ogura H, Kitabayashi C, Jiang JJ, Fukushima T, et al. Hepatic interleukin-7 expression regulates T cell responses. Immunity. 2009;30(3):447-57.
168. Cohen GM. Caspases: the executioners of apoptosis. Biochem J. 1997;326 (Pt 1):1-16. PMCID: 1218630.
169. Cline AN, Bess JW, Piatak M, Jr., Lifson JD. Highly sensitive SIV plasma viral load assay: practical considerations, realistic performance expectations, and application to reverse engineering of vaccines for AIDS. J Med Primatol. 2005;34(5-6):303-12.